Spring 2022

The kanarra fold-thrust system -- The leading edge of the sevier fold-thrust belt, southwest Utah

William Joseph Michael Chandonia

THE KANARRA FOLD-THRUST SYSTEM—THE LEADING EDGE OF THE SEVIER FOLD-THRUST BELT, SOUTHWEST UTAH

by

WILLIAM JOSEPH MICHAEL CHANDONIA

A DISSERTATION

Presented to the Graduate Faculty of the

MISSOURI UNIVERSITY OF SCIENCE AND TECHNOLOGY

In Partial Fulfillment of the Requirements for the Degree

DOCTOR OF PHILOSOPHY

in

GEOLOGY & GEOPHYSICS

2022

Approved by:

John P. Hogan, Advisor
Andreas Eckert
Jonathan Obrist-Farner
Klaus Woelk
Wan Yang

PUBLICATION DISSERTATION OPTION

This dissertation consists of the following article, formatted in the style used by the Missouri University of Science and Technology.

Paper I: Pages 3-108 have been submitted to *Geology of the Intermountain West*.

ABSTRACT

The Jurassic to Eocene Sevier fold-thrust belt is the subject of continued scientific curiosity in tectonics, stratigraphy, and industry. Understanding its development in southwest Utah is hindered in part due to the multiple origins proposed for the Kanarra anticline, a major leading edge structure—a drag fold along the Hurricane fault, Laramide monocline, Sevier fault propagation fold, or a combination of these—which have confused its tectonic significance and regional context. This confusion results from the structural complexity of its exposed eastern limb, as well as displacement and burial of its crest and western limb beneath Neogene sediments and volcanics along the Hurricane fault. New, detailed bedrock geologic mapping of the central portion of the fold near Kanarraville, Utah and geologic cross sections restored to Cretaceous time (i.e., pre-Basin and Range extension) demonstrate the formation of a composite anticline- syncline pair and fold accommodation thrust faulting are linked in the development of this Sevier structure. A previously unrecognized thrust, the Red Rock Trail thrust, formed due to fold tightening as a "break thrust" in a favorable position to link with the basal detachment. The traditional "Kanarra anticline" is more appropriately termed the "Kanarra fold-thrust system" considering the formation of the Red Rock Trail thrust and other thrusts on the fold. The east verging Red Rock Trail thrust locally presents as a distinctive cataclasite zone in the Navajo Sandstone, which is thrust over the Jurassic Carmel and younger Cretaceous strata. Traceable from Kanarraville to Parowan Gap, this thrust is the leading edge of the Sevier fold-thrust belt in southwest Utah. Stratigraphic relationships constrain the development of the Kanarra fold-thrust system to the Late Cretaceous to Early Eocene (~80 to 50 Ma). Thus the Red Rock Trail thrust records eastward advancement of the Sevier deformation front from the Iron Springs thrust (~100 Ma, coinciding with magmatic flare-ups in the Cordilleran arc and indicating close correspondence between arc-related processes and foreland deformation.

ACKNOWLEDGMENTS

Foremost, I would like to sincerely thank Dr. John P. Hogan for his support and continued mentorship throughout my graduate studies at Missouri University of Science and Technology. I am grateful for Dr. Andreas Eckert's suggestions, expertise in numerical approaches to geology, and emphasis on the importance of fundamental geological concepts, which assisted in my professional development and improved my figure drafting skills. Dr. Jonathan Obrist-Farner's deep knowledge of stratigraphy helped advance my stratigraphic skillset, and our collaborative discussions in the field on the lithology and fossils of the Permian-Lower Triassic section aided my structural interpretations along the Kanarra fold-thrust system. Dr. Klaus Woelk's unique perspective and constructive questions broadened the discussion and helped me think critically on the structural model of the area. Dr. Wan Yang's passion for paleogeology and expert knowledge elevated our discussions about the global significance of this project and the context of the Kanarra fold-thrust system within Utah's regional geologic history. I am thankful for the collaboration and constructive feedback of my colleagues and field assistants at this university. My utmost thanks to the Geosciences and Geological and Petroleum Engineering department for their financial support and the privilege of being a graduate teaching assistant. Through the years, it was a pleasure to teach and lead many early career geologists and engineers.

The unconditional support and love from my family and friends enriched this part of my life and made my achievements possible. I cherish their enduring presence and encouragement, and the many happy memories we share of this time in Missouri.

This work is also dedicated to my late father, Charles Dale Chandonia, who is my inspiration and shared my passion of Geology.

TABLE OF CONTENTS

Page

LIST OF ILLUSTRATIONS

Figure Page

PAPER I

LIST OF TABLES

1. INTRODUCTION

The leading edges of fold-thrust belts are of considerable academic and industrial interest due to their preservation of evidence which enhances our understanding the geologic history of the continents, as well as their capacity for generating resource reservoirs for water, hydrocarbons, and minerals In particular, understanding the geologic history of the world's mountain belts (orogens) aids geologists in predicting the distribution and concentration of these resources for the betterment of society, as well as unlocking the sequence of past geologic events and their temporo-spatial distribution.

The North American Cordillera is a world-class example of subduction-dominated orogeny, and has generated hydrocarbon fields and gold-silver deposits across the American West. At the furthest eastern extent of the North American Cordillera, spanning from Canada to Mexico, is the Jurassic- to Eocene-age Sevier fold-thrust belt. The Sevier fold-thrust belt has been dissected and extended by later Basin and Range tectonism. It has been further obscured by extension-induced magamatic processes, including basaltic and andesitic lava flows as well as laccolith-generated megalandslides. These later events have clouded the true temporo-spatial relationship and location of the leading edge of the fold-thrust belt, particularly in southwest Utah. Here, the degree to which the leading edge has been dissected and mantled by later processes has led many to mischaracterize or disregard the quintessential leading edge structures in the area, and thus misplace the Sevier fold-thrust belt leading edge. These include the Kanarra fold-thrust system, which hosts a hitherto unrecognized, regional-scale leading edge thrust, the Red Rock Trail thrust.

This work seeks to constrain the regional tectonic significance and relationships between leading edge features in southwest Utah, the Sevier fold-thrust belt proper, and the development of the leading edges of fold-thrust belts globally. Specifically, this project investigates the following: 1) how fold and thrust belts advance at the leading edge; 2) what the role of folding and faulting is in defining the structural architecture of the leading edge; and 3) where the leading edge of the Sevier fold-thrust belt is located in southwest Utah. I address these questions from a field-based perspective locally in southwest Utah, unraveling the presence and nature of fold accommodation faults which comprise the Kanarra fold-thrust system, the relationship between these thrusts and their effects on folding and advancement of the leading edge at Kanarrville, Cedar City, and Parowan Gap, and the relationship between the traditional Kanarra and Pintura anticlines. Counterintuitively, this is possible by the presence and activity of a major Basin and Range normal fault, the Hurricane fault, which has uplifted and exposed the Kanarra fold-thrust system to erosion and cross-strike stream dissection. The ideal exposure of this structure allows for detailed geologic mapping through creek beds across the strike of exposed layers, remote mapping procedures, and construction of cross sections along the fold from Kanarraville to Cedar City. The results of this work indicate the Kanarra fold-thrust system and Virgin anticline comprise a set of folds at the leading edge of the Sevier fold-thrust belt, folds which dominated the Sevier mountain front towards the end of Cretaceous time.

PAPER

I. THE KANARRA FOLD-THRUST-SYSTEM: THE LEADING EDGE OF THE SEVIER FOLD-AND-THRUST BELT, SOUTHWESTERN UTAH

W. J. M. Chandonia
Department of Geosciences and Geological and Petroleum Engineering
Missouri University of Science and Technology
Rolla, Missouri 65409–0050
Tel: 573–341–4616
Email: wjcmf9@mst.edu

ABSTRACT

The multiple origins proposed for the Kanarra anticline in southwest Utah as a drag-fold along the Hurricane fault, a Laramide monocline, a Sevier fault-propagation fold, or a combination of these processes serve to muddy its tectonic significance. This in part reflects the structural complexity of the exposed half of the fold that evolves from open and upright to overturned and tight, is cross-cut by multiple faults, is subsequently dismembered by the Hurricane fault, and its western half buried along with the hanging wall of the Hurricane fault beneath Tertiary and younger sediments and volcanics. We present the results of new, detailed bedrock geologic mapping of the central portion of the fold near Kanarraville, Utah as well as a geologic cross-section restored to Cretaceous time (i.e., pre-Basin and Range extension). Our work demonstrates that formation of a compound anticline-syncline pair and thrust faulting are inextricably linked in the development of this structure during the Sevier orogeny. We identify a previously unrecognized thrust, the Red Rock Trail thrust, as a late out-of-the-syncline thrust that was in a favorable orientation and position to link with the thrust ramp of the basal decollement to form a “break thrust”. We rename the traditional “Kanarra anticline” as the Kanarra fold-thrust system to acknowledge the close spatial and temporal association of folding and thrusting and the relationship of this structure to the Sevier fold-thrust belt. The east verging Red Rock Trail thrust is locally well recognized by the development of a distinctive cataclasite in the Navajo Sandstone that is thrust over the Jurassic Carmel and younger Cretaceous formations and can be traced from Kanarraville to Parowan Gap Utah as the leading edge of the Sevier fold-thrust belt in southwest Utah. Stratigraphic relationships in the southern and northern portion of the Kanarra fold-thrust system constrain the development of this structure to the late Cretaceous to early Eocene (~80 to 50 Ma). Movement along the Iron Springs thrust at ~100 Ma (Quick et al., 2020), and then eastward advancement of the Sevier Deformation front to the Red Rock Trail thrust at ~80 to 50 Ma coincided with well documented magmatic flare-ups in the Cordilleran arc in the hinterland of the Sevier fold-thrust belt consistent with a close correspondence between arc related processes and foreland deformation.

Keywords: fold-thrust, fold-thrust belt leading edge, Sevier fold-thrust belt

1. INTRODUCTION

The Sevier fold-thrust belt (Armstrong, 1968; Burchfiel and Davis, 1972) is an integral component of the Cordilleran orogenic belt that affected western North America from the late Jurassic (~165 Ma) to the Eocene (~50 Ma) (Herring and Greene, 2016; Yonkee and Weil, 2015). Magmatism, deformation, and accompanying sedimentation during this time was in response to plate convergence, concomitant subduction of the oceanic Farallon plate along the western edge of the North America plate, and accretion of various outboard terranes (DeCelles, 2004; DeCelles and Graham, 2015; DeCelles et al., 2009; Ducea et al., 2015; Lageson et al., 2001) Across the Cordilleran retro-arc several prominent, east-directed “thin-skinned” thrusts, folded and imbricated Proterozoic to Mesozoic miogeoclinal sediments, resulting in at least 350 km of shortening at the latitude of central to northern Utah

(DeCelles, 2004; Herring and Greene, 2016). Significant advancement in the understanding of the structural style, spatial progression, and effect on foreland sedimentation during collisional orogenesis have come from extensive investigation of the Sevier fold-thrust belt in northern and central Utah (Chidsey et al., 2007; Constenius, 1996; Constenius et al., 2003; DeCelles, 2004; DeCelles and Coogan, 2006; Herring and Greene, 2016; Pujols et al., 2020) as well as in Nevada (Di Fiori et al., 2021; Giallorenzo et al., 2018; Long, 2015). However, the temporal and spatial evolution of deformation associated with the Sevier fold-thrust belt varies considerably along strike (e.g., see Figure 1 of Quick et al. (2020)). In central to northern Utah, at the latitude of the Salt Lake Salient (~41°N), the Sevier fold-thrust belt remained active longer (ca. 100 My), over a wider deformation belt (~500 km), and propagated further inland (e.g., 56 Ma Hogsback thrust). In contrast, in the southern portion of the fold-and thrust belt, at the latitude of Las Vegas recess (~36°N), thin-skinned deformation was of shorter duration (ca. 50 My) and formed a narrower deformation belt (~100 km wide). Quick et al. (2020) attributed this along strike spatial and temporal variation in the advancement of the Sevier deformation front to "structural inheritance"; the location of the buried western edge of Precambrian continental crust least affected by extension (i.e., the hinge line) as well as the location of prominent extensional basement structures (e.g., transform faults). The sinuous trace defined by the multiple salients and recesses of the retro-arc Sevier fold-and-thrust belt reflects the form of the rifted Precambrian North American continental margin and the prominent role reactivated extensional structures in the basement had on the eastward advancement of the Sevier deformation front (Paulsen and Marshak, 1999; Picha and Gibson, 1985; Quick et al., 2020).

The location and timing of arrival of the Sevier deformation front in southwestern Utah, the region linking the northern and southern portions of the fold-thrust belt (Figure 1), remains a subject of debate (Biek et al. (2010), p. 29, 31). This is due, in part, to the complexity of the bedrock and surficial geology of southwest Utah. Here contractional structures associated with the Sevier orogeny are variably dissected by Cenozoic "Basin and

Range” extensional faulting (e.g., the Hurricane fault), obscured by intrusion of Tertiary laccoliths (e.g., the Pine Valley and/or Three Peaks laccolith), covered by Miocene to Holocene basalt flows, or buried by significant landslides (Biek, 2003a,b; Biek and Hayden, 2016; Biek et al., 2010; Hurlow and Biek, 2003; Knudsen, 2014a; Quick et al., 2020). Biek et al. (2010) defined the leading edge of the Sevier fold-thrust belt in southwestern Utah by the location of the Square Top Mountain thrust (their easternmost significant thrust) and the Virgin, Pintura, and Kanarra anticlines (Figure 1). They link the Square Top Mountain thrust with the Keystone-Muddy Mountain-Tule Spring thrust system in southeast Nevada and have its northern extension associated with the Blue Mountain-Iron Springs Gap-Canyon Range thrust system (see Biek et al. (2010), Figure 5, p. 6). Arrival of the leading edge of the Sevier fold-thrust belt in southwest Utah is thus constrained by the emergence of the Square Top Mountain thrust and the erosional beveling of the Pintura anticline and is broadly thought to be between the Late Cretaceous to early Tertiary (Biek et al. (2010) p. 27, 31). Recently Quick and others, (2020) constrained emergence of the Iron Spring thrust to latest Albian–earliest Cenomanian (~100 Ma); an age considerably earlier than previously proposed but similar in age to the ~99 Ma Keystone thrust (Fleck and Carr, 1990). The discrepancy in the timing of arrival and location of the leading edge of the Sevier fold-thrust belt in southwest Utah highlights the uncertainty associated with Sevier deformation in southwest Utah; we suggest this, in part, stems from long-lived uncertainty associated with the nature of the Kanarra anticline as traditionally defined (Armstrong, 1968; Averitt, 1962; Biek, 2007a; Biek et al., 2010; Gregory and Williams, 1947; Threet, 1963a,b). The Kanarra anticline is coincident with the trace of the Cordilleran hinge line in southwest Utah, extending from near Toquerville to Cedar City for ~53 km (Figure 2). The development of the Kanarra anticline has been contentious since it was first described by Dutton (1880), who did not recognize the fold as a separate feature from the Hurricane fault.

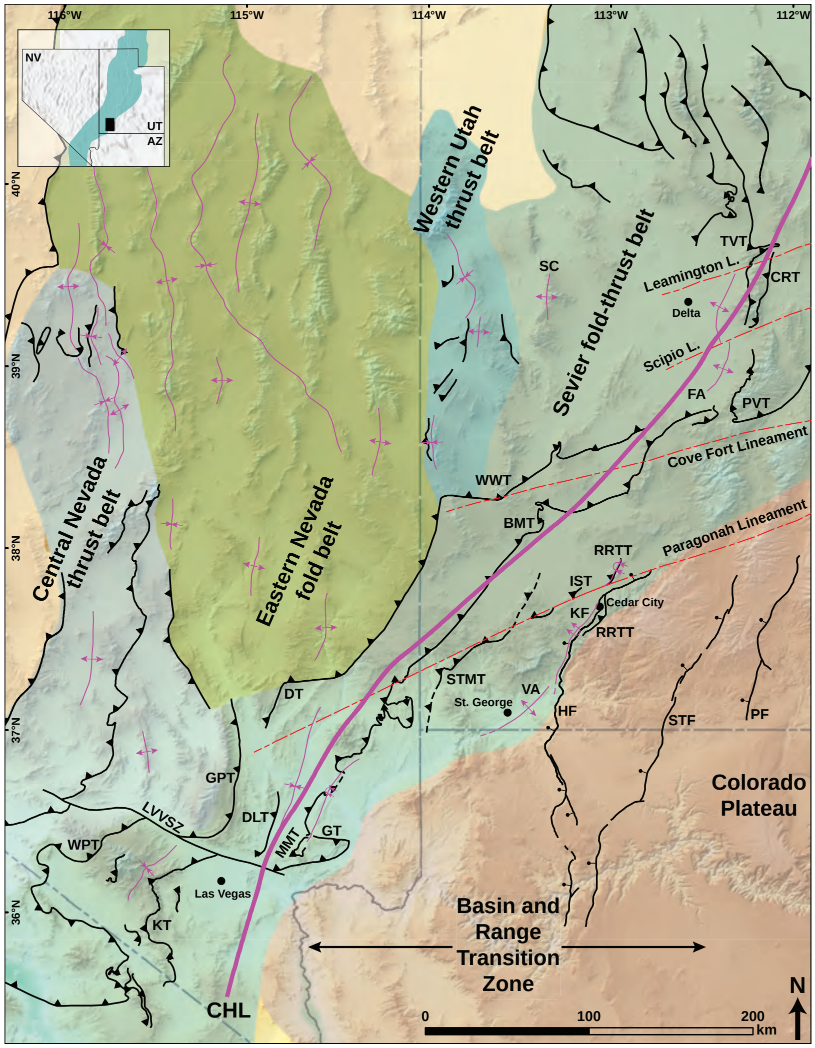

Figure 1. Regional overview map showing the Sevier frontal fold-thrust belt in relation to Cordilleran hinterland deformation belts and the craton. Included are Proterozoic rift-related lineaments and Basin and Range structures. Fold abbreviations: SC—Sevier Culmination; FA—Fillmore Arch; VA—Virgin Anticline; KF—Kanarra fold. Thrust abbreviations: WPT—Wheeler Pass thrust; KT—Keystone thrust; GPT—Gass Peak thrust; DLT—Dry Lake thrust; MMT—Muddy Mountains thrust; GT—Glendale thrust; DT—Delamar thrust; STMT—Square Top Mountain thrust; IST—Iron Springs thrust; WWT—Wah Wah thrust; BMT—Blue Mountain thrust; PVT—Pavant thrust; CRT—Canyon Range thrust; TVT—Tintic Valley thrust. Basin and Range structures: LVVSZ—Las Vegas Valley Shear Zone; HF—Hurricane fault; STF—Sevier-Toroweap fault; PF—Paunsaugunt fault. After Quick et al. (2020), compiled from Biek et al. (2015); Giallorenzo et al. (2018); Herring and Greene (2016); Long (2012, 2015); Page et al. (2005); Picha and Gibson (1985); Stokes et al. (1963); Wernicke et al. (1988); Willis (1999); Wyld et al. (2003); Yonkee and Weil (2015). DEM visualization from the USGS National Map 3D Elevation Program (3DEP).

Over time, the traditional Kanarra anticline has alternately been interpreted as forming during Mesozoic reverse faulting along the Hurricane fault (e.g., Lovejoy (1978)), a Laramide monocline (i.e., thick-skinned fault propagation fold, see Enriquez St. Pierre and Johnson (2021), Figures 1 and 2), and as a Sevier-age thin-skinned fault propagation fold (see Grant et al. (1994)) modified by rotation of the footwall of the Hurricane fault during Basin and Range extension (Stewart and Taylor, 1996). The ambiguity in the strain significance of the Kanarra anticline reflects complications due to dismemberment of the anticline by the Hurricane Fault (i.e., the west dipping limb may be buried beneath younger sediments of Cedar Valley), off-set of the axial trace of the fold (i.e., along the Proterozoic Paunsagaunt Lineament), as well as burial by prominent landslides Biek et al. (2015); Picha and Gibson (1985); Threet (1963a,b). Current consensus recognizes the Kanarra anticline as a contractional fault propagation fold formed during the Sevier Orogeny (see Biek et al. (2010)) although alternative interpretations as a Laramide-age monocline persist (see Enriquez St. Pierre and Johnson (2021), Figure 1, 2).

The role of thrusting in the development of the Kanarra anticline is poorly understood. Grant et al. (1994) and Nowir and Grant (1995) show the Kanarra anticline near Kanarraville, Utah to be an asymmetric, overturned anticline, with imbricate thrust splays merging into a high-level detachment fault that soles along the base of the Permian Kaibab Formation (Nowir and Grant (1995) Figure 6, p. 201). Older "flank thrusts" are shown on both limbs of the fold; the flank thrust on the overturned eastern limb corresponds to the "Taylor Creek thrust system" of Kurie (1966) who interpreted it as a back thrust. The easternmost thrust fault is a "rollover-break thrust", a term assigned by Nowir and Grant (1995) (p. 200), which displaced the overturned limb of the anticline to the east and is shown to have breached the surface. Several of these thrusts, including the rollover-break thrust were inferred and necessary to produce a balanced cross-section through the Kanarra anticline (Nowir and Grant, 1995). However, in their cross section the "rollover-break thrust" is shown to have simultaneously both normal and reverse separation along its length (see Nowir and Grant (1995) Figure 6, p. 201). Previous geologic maps (e.g., Averitt (1967) and subsequent geologic maps (e.g., Biek and Hayden (2016) of the Kanarra anticline include the west-directed Taylor Creek thrust system but do not show the presence of a leading edge east-directed thrust. As a result, many publications show the Keystone-Muddy Mountain-Square Top Mountain-Iron Springs-Canyon Range thrusts as the leading edge of the Sevier orogeny in southwest Utah (e.g., Hintze (2005), Figure 66, p. 61).

Establishing the location of the leading edge of the Sevier fold-thrust belt in southwest Utah is critical to linking the spatial and temporal advancement of the Sevier deformation front along its strike length and interpretation of its effect on foreland sedimentation. We report the results of new detailed geologic mapping and structural cross sections of the traditional Kanarra anticline, near Kanarraville, Utah. Our work demonstrates that thrust faults and folding are inextricably linked in all stages of formation of the Kanarra anticline. Our geologic mapping identifies the previously speculated ('rollover-break thrust' of Nowir and Grant (1995)), but unrealized leading-edge thrust of the Sevier fold-thrust belt along the eastern overturned limb of this portion of the Kanarra anticline—our Red Rock Trail thrust. We characterize the complete profile of the folds associated with Sevier deformation in the late Cretaceous that places the "traditional Kanarra anticline" of previous work within the fuller context of the Kanarra anticline proper. Utilizing these results, we reexamine the northern portion of the Kanarra anticline near Cedar City, Utah at the Red Hill to demonstrate the regional continuity in the tectonic style and significance of this structure. We propose renaming this structure as the *Kanarra fold-thrust system* to clarify its tectonic significance as the easternmost leading edge of the Sevier fold-thrust belt in southwestern Utah.

2. GEOLOGICAL SETTING

In southwest Utah, the Colorado Plateau Province is dissected by several large normal faults which define the topographic expression of the transition zone into the Basin and Range Province (Figure 1). Each of the “High Plateaus” of the transition zone is one in a series of down-stepping blocks towards the Basin and Range Province. These steps are bounded by north-trending normal fault zones which are 100s of km long—some continuing southwards into Arizona and the Grand Canyon region. From east to west, these transition zone normal faults are the Paunsaugant, Sevier-Toroweap, and Hurricane faults (Biek et al. (2015)) The Markagunt Plateau is the westernmost of the High Plateaus. The Hurricane Cliffs and Hurricane fault lie just east of the Cordilleran hinge line and mark the western edge of the Markagunt Plateau and the Basin and Range transition zone (Figure 1). Stratigraphic separation on the Hurricane fault is estimated to be up to 2500 meters (>8200 feet) just north of St. George, near Toquerville (Stewart and Taylor, 1996).

2.1. THE TRADITIONAL KANARRA ANTICLINE

Cropping out along the Hurricane Cliffs between St. George and Cedar City are late Paleozoic to Cretaceous sediments that have been uplifted, dissected, and well exposed in the rugged topography of the footwall of the Hurricane fault. North of St. George, from the town of Toquerville to Cedar City, these strata were deformed into the Kanarra fold (Gregory and Williams (1947)) during the Sevier orogeny (Figure 1, Figure 2) Here, the eastern limb of the Kanarra anticline trends north-northeast for over 50 km and is well

exposed along its length in several across-strike, incised stream valleys in the footwall of the Hurricane fault (Averitt, 1962; Biek, 2007a; Gregory and Williams, 1947). Consequently, part of the traditional Kanarra anticline hinge and the entire western limb of the fold have been displaced downward along with the hanging wall of the Hurricane fault and are buried beneath the sediment fill in the Cedar Valley half-graben. The hinge

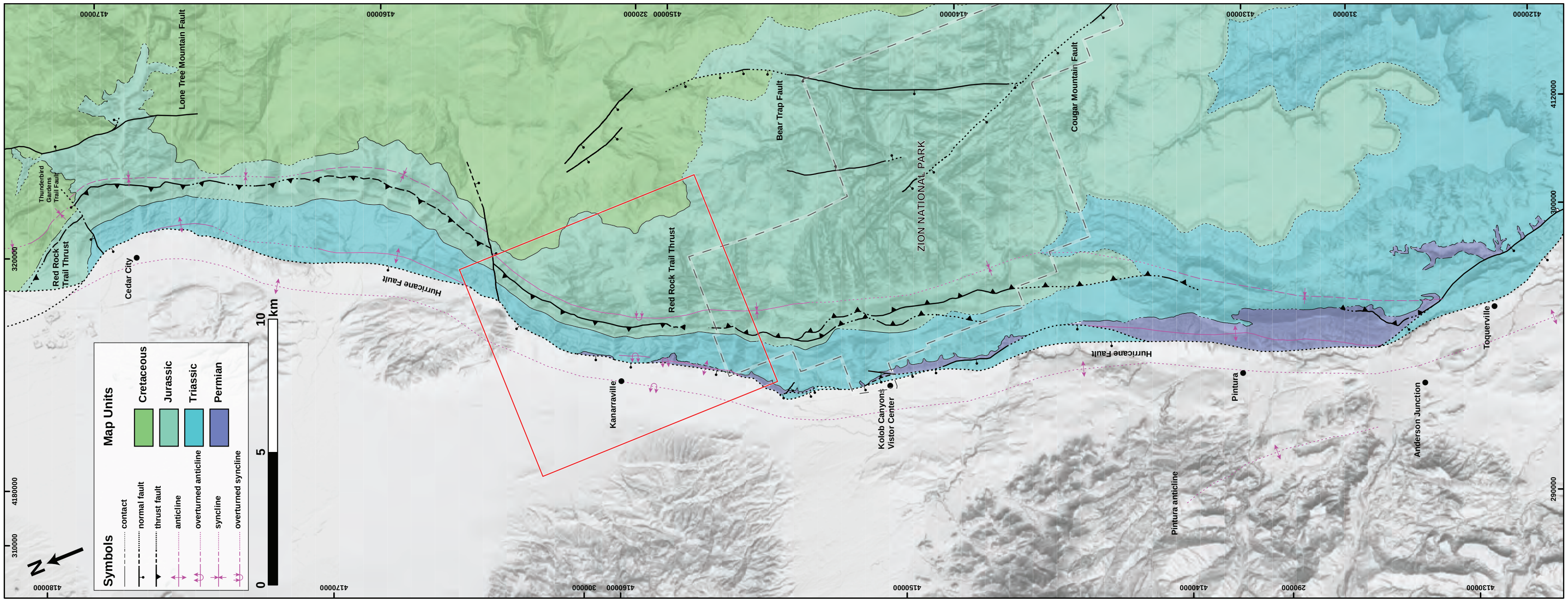

Figure 2. Simplified map of the Kanarra fold-thrust system (1:110000-scale). Major unit divisions and structural features shown. The map is rotated 22°NW to afford a vertical view of the entire structure. The leading anticline axial trace is marked where exposed. The Kanarra fold-thrust system hinge zone, dropped down along the Hurricane fault, is shown as a concealed anticlinal axial trace in Cedar Valley. Compiled from the study area geologic map (red rectangle) as well as Averitt (1962); Averitt and Threet (1973); Biek (2007a,b); Biek and Hayden (2016); Biek et al. (2010, 2015); Hurlow and Biek (2003); Knudsen (2014a); Rowley et al. (2006) Zion National Park boundaries are from the USGS National Map vector GIS datasets for Iron and Washington counties. The DEM visualization is a mosaic from 3DEP elevation data by the USGS and LIDAR collected for southern Utah by the Utah Geospatial Resource Center and Utah Division of Emergency Management.

zone of the traditional Kanarra anticline is discontinuously exposed along its entire length and is locally displaced along faults such as the Murie Creek fault (Figure 2). Beginning at Shurtz Creek, the Kanarra anticline plunges northwards and develops a distinct closure just past Cedar City along the Red Hill (Averitt, 1962). The fold is likely a doubly plunging anticline; however, the presumed southern closure of the fold has been sheared away along the Hurricane fault near Toquerville.

The portion of the Kanarra anticline exposed in the footwall of the Hurricane fault is comprised of approximately ten contiguous structural domains which smoothly transition into each other (Figure 2). Each domain is approximately 2 to 13 kilometers in length and differs from its neighbors by a combination of variation in bedding facing direction, bedding strike direction, fold axis plunge, or exposed structural level. These domains form large, smoothly curved sections (i.e., salients and recesses) in map view (Figure 2). Along most of its length, the Kanarra fold is upright, excepting local displacement by fold accommodation faults such as that seen in the hanging wall of Hurlow and Biek's (2003) "Taylor Creek fault". The deepest structural levels of the fold crop out near its southern terminus between Pintura and Toquerville.

The structural domains near Kanarraville, the approximate center of the structure, represent some of the deepest structural levels exposed along the Hurricane Cliffs. This section of the Kanara anticline hosts the greatest structural complexity in terms of folding and faulting (see (Biek and Hayden, 2016; Nowir and Grant, 1995). Here, bedding abruptly overturns along a 10 kilometer section of the fold and is displaced and repeated along multiple faults. Understanding the spatial and temporal evolution of the central portion the Kanarra anticline, the structurally most complex portion of the fold, through detailed geologic mapping is critical to resolving its tectonic significance to the evolution of the Sevier orogeny in southwest Utah. The detailed 1:15000-scale geologic map and 1:10000-scale structural map of the central portion of the Kanarra anticline are presented in Figure 3 and Figure 4, respectively.

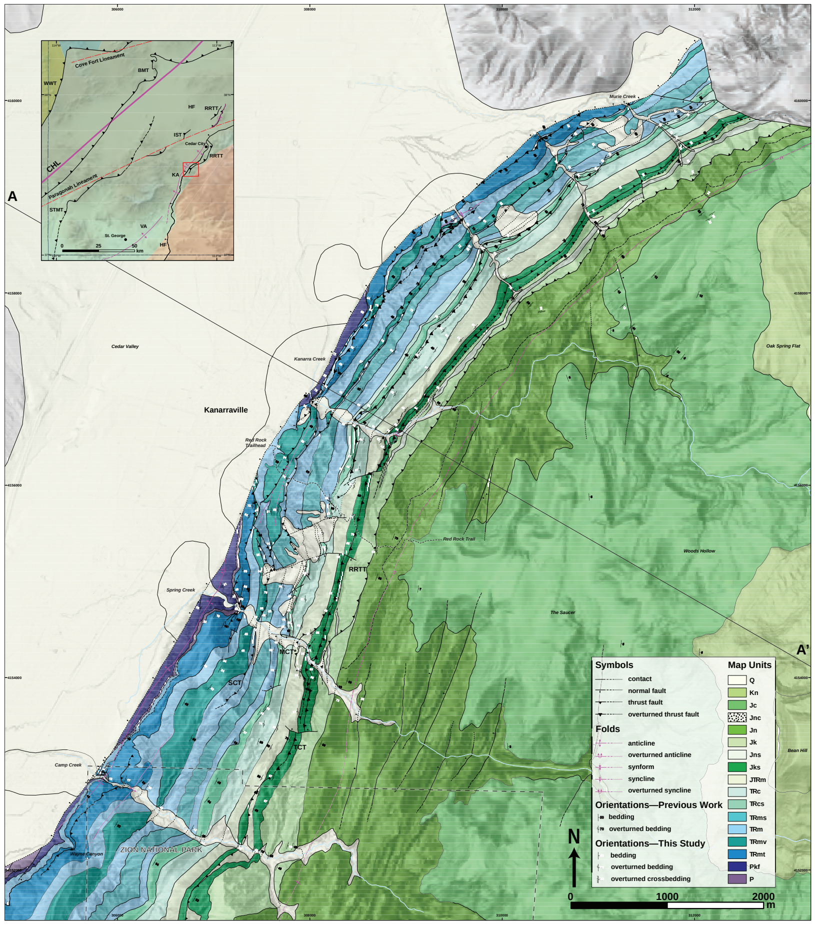

Figure 3. Geologic map of the Kanarra fold-thrust system (1:15000-scale). Map based on across- and along-strike field mapping between Camp Creek and Murie Creek, from the Hurricane fault scarp to the Carmel formation along the Markagunt Plateau. See reffig12 for field stop locations highlighted in this study. Contacts mapped in the field are further constrained using a combination of Google Earth, LIDAR data, previous mapping, and Rick Allmendinger's GMDE program (Allmendinger, 2020; Averitt, 1962, 1967; Biek and Hayden, 2016). Structure abbreviations: SCT—Spring Creek thrust; KCT—Kanarra Creek thrust; HCT—Hicks Creek thrust; TCT—Taylor Creek thrust; RRTT—Red Rock Trail thrust. Contacts on the plateau, north of Murie creek, and beyond Wayne Canyon are after Averitt (1962) and Biek and Hayden (2016). Orientation measurements referenced from previous mappers are labelled in white. Landscape feature labels, boundaries, and streams are from the USGS National Map vector GIS datasets for Iron and Washington counties. The DEM visualization is generated from LIDAR elevation data for southern Utah collected by the Utah Geospatial Resource Center and Utah Division of Emergency Management in 2020.

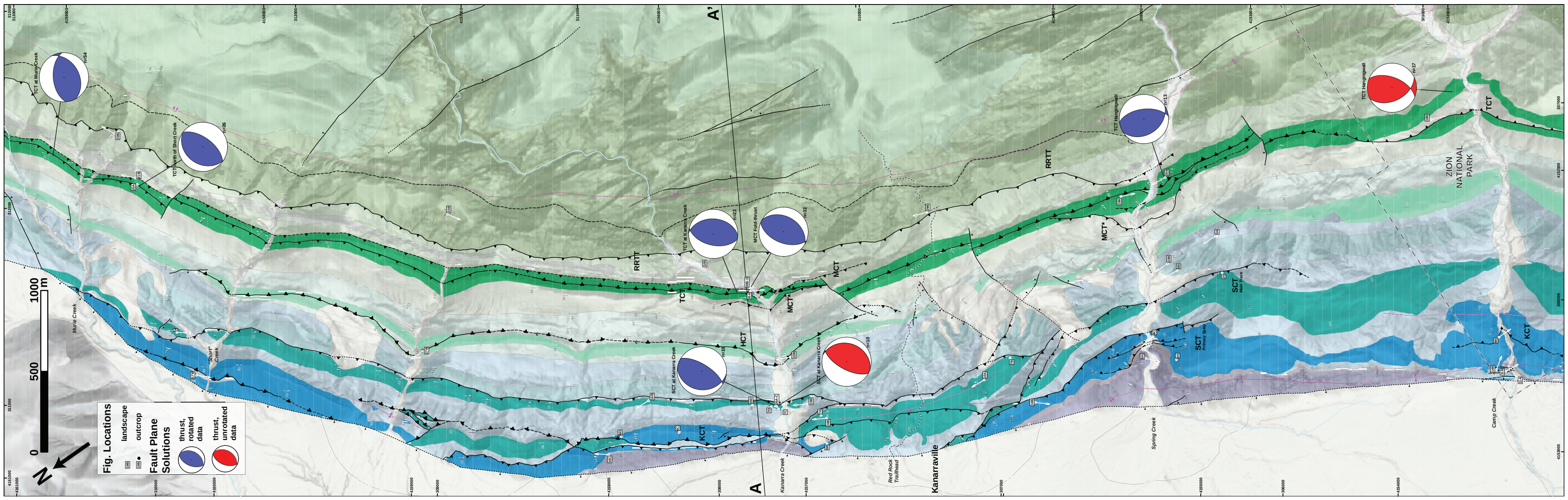

Figure 4. Structural map with fault plane solutions and figure locations (1:10000-scale). Landscape field photos are represented by an arrow showing the view direction bearing. The map is rotated 35°NW to afford a vertical view of the Kanarra fold-thrust system at this scale. Stratigraphic contacts and orientations are de-emphasized, excepting thin, competent layers which host the major fold accommodation faults mapped along the fold limb. Fault plane solution diagrams include the number of measurements at a location; solutions with rotated data are blue and unrotated are red. For further details see reftab3 and the text. For fault abbreviations, see Figure 3. Landscape feature labels, boundaries, and streams are from the USGS National Map vector GIS datasets for Iron and Washington counties. The DEM visualization is generated from LIDAR elevation data for southern Utah collected by the Utah Geospatial Resource Center and Utah Division of Emergency Management in 2020. Fault plane solutions generated in Allmendinger's FaultKin program. (Allmendinger et al., 2012; Marrett and Allmendinger, 1990).

3. METHODS

3.1. GEOLOGIC MAP

Field mapping using topographic maps and aerial imagery was conducted during the summers of 2016-2019. Field data were collected and backed up in real time with FieldMove™(2017-2018) (e.g., Muir (2015)) and StraboSpot (Walker et al. (2019)). Across-strike and along-strike traverses at Camp Creek, Spring Creek, Kanarra Creek, "Short" Creek, Murie Creek, and along Kanarra Mountain Road (Figure 3) were employed to efficiently cover ground. The location of contacts mapped in the field (particularly difficult and concealed contacts) were refined using a combination of GMDE (Allmendinger (2020)), Google Earth, recent LIDAR data, and previous work (Averitt, 1962, 1967; Biek and Hayden, 2016)). GMDE (see Allmendinger (2020)) was also used to estimate unit thickness, test structural interpretations, as well as map projections of contacts, faults, and axial traces at a regional scale (as opposed to outcrop-scale) for the 1:15000-scale geologic map and 1:10000-scale structural map (Figure 3 and Figure 4). The 1:110000-scale map of the Kanarra anticline (Figure 2) was produced from field observations, previous 7.5-minute quadrangles (Averitt, 1962, 1967; Averitt and Threet, 1973; Biek, 2007a,b; Biek and Hayden, 2016; Hurlow and Biek, 2003; Knudsen, 2014a) 2016), and three 30x60 quadrangles (Biek et al., 2010, 2015; Rowley et al., 2006) Each map plate was compiled in ArcMap and finalized using Adobe Illustrator.

3.2. GEOLOGIC CROSS SECTION

The geologic cross-sections are constructed using field measurements, published unit thicknesses, and unit thicknesses based upon current mapping using the Move™software by Petroleum Experts. The kinked, parallel fold model employed in the cross sections reflects the structural style observed in the field. The cross section through the study area is based on the geologic map (Figure 3). The cross section through the Red Hill is based on unpublished mapping by the authors and previous work (Averitt and Threet (1973); Knudsen (2014a)), and it employs the same kinked, parallel fold model as the cross section from the central portion of the fold.

The structural style of the Kanarra anticline is a composite of fold-thrust structures including forced and buckle folding Butler et al. (2020). These fold styles are well-exposed and well-developed within the Timpoweap Member and Fossil Mountain Member of the Kaibab Formation (Figure 3 and Figure 5), but are observed in several other units as well. The fold shapes and position of fold accommodation faults (e.g., Cloos (1961, 1964); Mitra (2002a)) within the layering suggest a component of buckling before faulting. Each fold is comprised of smooth-hinged "kinks" formed by kink panels of varying size and number (Figure 5; see also Faill (1973); Faill and Wells (1974), Figure 61, p. 143; also p. 138 to 150).

Map-scale views of folded layers show smooth-hinged kinks in the field and are also manifested in the structural domains of the Kanarra anticline (Figure 2). In the field, the southern cliff face at the mouth of Spring Creek hosts a large, outcrop-scale composite fold-thrust structure and buckle fold train within the Fossil Mountain Member (Figure 5A). At the western end of this train is a break-thrust fold (Figure 5A inset; see also Willis (1893), Plate 33, p.~228; Fischer et al. (1992)). This *family* of folds and faults (*c.f.* Dahlstrom (1969a)) mimics the structural style of the Kanarra anticline and informs our kinked break-thrust fold model used in cross section.

3.3. SHEAR FRACTURE MEASUREMENTS

Shear fracture sets within competent strata along the Kanarra fold are associated with major fold accommodation faults and are found along their mapped traces. Elsewhere, these shear fractures are commonly called "mesoscale" or "outcrop scale" faults, but for clarity we restrict the term "fault" to the scale of the map and "shear fracture" or "slickenside" to

Figure 5. Spring Creek canyon fold-thrust structure outcrop. A) View south on a composite fold-thrust structure within the Fossil Mountain Member of the Kaibab. Inset: Close-up of the "leading" fold, a semi-fractal model of the Kanarra fold. B) View south above the entrance to Camp Creek. Folds within the Timpoweap Member are cut by antithetic thrusts in the hangingwall of the Kanarra Creek thrust. C) View north onto the leading anticline of the Kanarra fold-thrust system from the Spring Creek Canyon trail.

the scale of the outcrop. Exposure and accessibility of shear fractures are limited by their preservation in highly fractured rock, the commonly high density of vegetation, and the rugged topography of the resistant ridges along which they are found.

Exposed shear fractures commonly erode so the rock on one side is "missing", allowing measurement of the fracture and lineation (e.g., slickenlines) on the fracture surface. For each shear fracture, the strike, dip, and rake of slickenlines are measured and recorded. For consistency, rakes are always measured down from right hand rule strike along the fracture plane, and slip sense interpreted separately. Slip sense, or movement of the missing piece relative to the fracture plane, is interpreted based on R-type and P-type fracture steps (common in sandstones) or mineral fibers (common in carbonates) on the fracture surface (Allmendinger et al. (1989); Petit (1987)) sense is also constrained, when possible, by offset of marker beds, drag-folds, and oblique exposures of shear fracture sets. These shear fractures are analyzed using FaultKin and Stereonet (Allmendinger et al. (2012)) to produce a fault plane solution which can be used to estimate the aggregate, map-scale orientation and slip sense of the fault plane at several locations on the fold limb. Using the average bedding orientation at each shear fracture set location, we rotate the fault plane solutions model so that local bedding fits the average orientation of bedding at Camp Creek where the Kanarra fold is upright and open. This allows for direct comparison of fault plane solutions along the length of the fold. We undertake these analyses primarily to document the presence and deformation history of early-formed thrusts as the fold evolves from a gentle, open fold in the southern portion of the map area to a steep, tight, overturned fold in the northern portion of the map area in an approximate "temporal-progression" of structural development and strain accumulation during folding.

4. STRATIGRAPHY

Deposition of Paleozoic miogeoclinal sediments along the passive margin of the western coast of Laurentia was strongly controlled by subsidence from post-rift lithospheric cooling and structural lineaments formed during rifting. During this time, cyclical deposition generated a zone of westward-thickening marine-marginal marine strata beginning at the craton edge, known as the Cordilleran hingeline (see Figure 1; (Picha and Gibson, 1985; Stokes, 1976; Wernicke et al., 1988)). Thick packages of competent strata—locally including the Cambrian Bonanza King Formation, Upper Cambrian Nopah Dolomite, Mississippian Redwall Limestone, and Permian Queantoweap Sandstone—were deposited during this period (Biek et al., 2010; Hintze, 1986, 2005; Hurlow and Biek, 2003). While these units are unexposed in the map area, their presence and contribution to the mechanical response of the stratigraphic package are important to the development of the Kanarra fold-thrust system. The ages, names, rock type, thicknesses, and patterns of formations cropping out in the map area or included in the cross-sections are shown in Table 1 and Table 2.

Table 1. Unit thicknesses at Kanarra Creek, all values in meters.

Unit	Formation	Member	T_{min}	T_{max}	Sources	This Study
Kw	Wahweap	—	—	—	Averitt (1962)	—
Kst	Straight Cliffs	—	—	—	Averitt (1962)	188
Kn	Naturita	—	—	45(+)	Biek and Hayden (2016)	258*
Kcm	Cedar Mountain	—	—	8	Biek and Hayden (2016)	—
Jcw	Carmel	Windsor	45	60	Biek and Hayden (2016)	—
Jcp	Carmel	Pariah River	37	45	Biek and Hayden (2016)	—
Jcx	Carmel	Crystal Creek	60	75	Biek and Hayden (2016)	—
Jcc	Carmel	Coop Creek	150	165	Biek and Hayden (2016)	—

Table 1. Unit thicknesses at Kanarra Creek, all values in meters. (cont.)

Unit	Formation	Member	T_{min}	T_{max}	Sources	This Study
Jtm	Temple Cap	—	1	9	Biek and Hayden (2016)	—
Jcu	Carmel, Temple Cap	—	248	294	Biek and Hayden (2016)	404**
Jn	Navajo Sandstone	—	550	600	Biek and Hayden (2016)	634
Jkc	Kayenta	Cedar City Tongue	200	300	Biek and Hayden (2016)	60
Jns	Navajo Sandstone	Shurtz Tongue	0	30	Biek and Hayden (2016)	25
Jkm	Kayenta	Main Body	120	150	Biek and Hayden (2016)	120
Jks	Kayenta	Springdale Sandstone	30	45	Biek and Hayden (2016)	52
JTRm	Moenave	Dinosaur Canyon	90	150	Biek and Hayden (2016)	129
TRcu	Chinle	Petrified Forest	90	120	Biek and Hayden (2016)	122
TRcs	Chinle	Shinarump Conglomerate	30	60	Biek and Hayden (2016)	41
TRcl	Chinle	Lower	—	—	Knudsen (2014a)	36
TRmu	Moenkopi	Upper Red	60	75	Biek and Hayden (2016)	93
TRms	Moenkopi	Shnabkaib	120	150	Biek and Hayden (2016)	130
TRmm	Moenkopi	Middle Red	120	150	Biek and Hayden (2016)	135
TRmv	Moenkopi	Virgin	45	60	Biek and Hayden (2016)	64
TRml	Moenkopi	Lower Red	—	75	Biek and Hayden (2016)	86
TRmt	Moenkopi	Timpoweap	—	37	Biek and Hayden (2016)	68
TRmr	Moenkopi	Rock Canyon Conglomerate	0	27	Biek and Hayden (2016)	18
Pkh	Kaibab	Harrisburg	—	30	Biek and Hayden (2016)	12
Pkf	Kaibab	Fossil Mountain	—	60(+)	Biek and Hayden (2016)	70***
Ptw	Toroweap	Woods Ranch	37	76	Hurlow and Biek (2003)	83
Ptbs	Toroweap	Brady Canyon–Seligman	76	87	Hurlow and Biek (2003)	53

Table 1. Unit thicknesses at Kanarra Creek, all values in meters. (cont.)

Unit	Formation	Member	T_{min}	T_{max}	Sources	This Study
Pqu	Queantoweap Sandstone	Upper	400	500	Hurlow and Biek (2003)	407
Pql	Queantoewap Sandstone	Lower	37	245	Hurlow and Biek (2003)	241
Pp	Pakoon Dolomite	—	—	75(+)	Hurlow and Biek (2003)	90
Pec	Callville Limestone	—	—	85	Hurlow and Biek (2003)	85
Mr	Redwall Limestone	—	—	370	Biek et al. (2010)	370
Dmp	Muddy Peak Dolomite	Pinnacle Unit	—	49	Hintze (1986)	49
Dms	Muddy Peak Dolomite	Slope Forming Unit	—	158	Hintze (1986)	159
Cnd	Nopah Dolomite	—	114	396	Steed (1980), Hintze (1986)	114
Cbk	Bonanza King	—	762		Hintze (1986)	762
Cba	Bright Angel Shale	—	75	100	Biek et al. (2010)	90
Ct	Tapeats Sandstone	—	—	400	Biek et al. (2010)	400

* Due to inaccessibility and the thinness of Kcm, we do not divide the Kcm and Kn at Kanarraville

** Similarly, due to poor contact visibility and accessbility we do not divide the Carmel and Temple Cap Formations

*** Beyond Pkf, none of the following strata are exposed at Kanarraville

Table 2. Unit thicknesses at the Red Hill, all values in meters.

Unit	Formation	Member	T_{min}	T_{max}	Sources	This Study
Kw	Wahweap	—	—	300	Knudsen (2014a)	300
Kst	Straight Cliffs	—	702	707	Knudsen (2014a)	417
Kn	Naturita	—	—	290	Knudsen (2014a)	290

Table 2. Unit thicknesses at the Red Hill, all values in meters. (cont.)

Unit	Formation	Member	T_{min}	T_{max}	Sources	This Study
Kcm	Cedar Mountain	—	15	18	Knudsen (2014a)	18
Jcw	Carmel	Windsor	75	90	Knudsen (2014a)	90
Jcpl	Carmel	Pariah River	11	15	Knudsen (2014a)	15
Jcpg	Carmel	Pariah River	—	37	Knudsen (2014a)	37
Jcx	Carmel	Crystal Creek	—	90	Knudsen (2014a)	90
Jcc	Carmel	Coop Creek	—	193	Knudsen (2014a)	193
Jtm	Temple Cap	—	—	37	Knudsen (2014a)	37
Jn	Navajo Sandstone	—	—	325	Knudsen (2014a)	417
Jkc	Kayenta	Cedar City Tongue	—	130	Knudsen (2014a)	124
Jns	Navajo Sandstone	Shurtz Tongue	—	90	Knudsen (2014a)	139
Jkm	Kayenta	Main Body	—	88	Knudsen (2014a)	68
Jks	Kayenta	Springdale Sandstone	—	40	Knudsen (2014a)	67
JTRm	Moenave	Dinosaur Canyon	—	90	Knudsen (2014a)	76
TRcu	Chinle	Petrified Forest	—	90	Knudsen (2014a)	77
TRcs	Chinle	Shinarump Conglomerate	9	15	Knudsen (2014a)	30
TRcl	Chinle	Lower	—	60	Knudsen (2014a)	50
TRmu	Moenkopi	Upper Red	—	120	Knudsen (2014a)	95
TRms	Moenkopi	Shnabkaib	—	98	Knudsen (2014a)	108
TRmm	Moenkopi	Middle Red	—	128	Knudsen (2014a)	128
TRmv	Moenkopi	Virgin	—	40	Knudsen (2014a)	49
TRml	Moenkopi	Lower Red	—	75	Knudsen (2014a)	75
TRmt	Moenkopi	Timpoweap	—	37	Knudsen (2014a)	37 *

Table 2. Unit thicknesses at the Red Hill, all values in meters. (cont.)

Unit	Formation	Member	T_{min}	T_{max}	Sources	This Study
TRmr	Moenkopi	Rock Canyon Conglomerate	0	27	Biek and Hayden (2016)	18
Pkh	Kaibab	Harrisburg	—	30	Biek and Hayden (2016)	12
Pkf	Kaibab	Fossil Mountain	—	60(+)	Biek and Hayden (2016)	70
Ptw	Toroweap	Woods Ranch	37	76	Hurlow and Biek (2003)	83
Ptbs	Toroweap	Brady Canyon–Seligman	76	87	Hurlow and Biek (2003)	53
Pqu	Queantoweap Sandstone	Upper	400	500	Hurlow and Biek (2003)	407
Pql	Queantoewap Sandstone	Lower	37	245	Hurlow and Biek (2003)	241
Pp	Pakoon Dolomite	—	—	75(+)	Hurlow and Biek (2003)	90
Pec	Callville Limestone	—	—	85	Hurlow and Biek (2003)	85
Mr	Redwall Limestone	—	—	370	Biek et al. (2010)	370
Dmp	Muddy Peak Dolomite	Pinnacle Unit	—	49	Hintze (1986)	49
Dms	Muddy Peak Dolomite	Slope Forming Unit	—	158	Hintze (1986)	159
Cnd	Nopah Dolomite	—	114	396	Steed (1980), Hintze (1986)	114
Cbk	Bonanza King	—	762		Hintze (1986)	762
Cba	Bright Angel Shale	—	75	100	Biek et al. (2010)	90
Ct	Tapeats Sandstone	—	—	400	Biek et al. (2010)	400

* Beyond TRmt, none of the following strata are exposed at the Red Hill

Towards the end of the Permian, basin conditions began to change significantly Biek et al. (2010); Hintze (1986, 2005). A dwindling pattern of shorter and shorter cycles, marked by thinner strata, followed deposition of the Queantoweap Sandstone. During the beginning of the Tertiary, base level fell, and an unconformity (i.e., the TR-1 unconformity) surface developed on exposed, previously submarine sediments Pipiringos and O'Sullivan (1978). In the field area, the absence of large portions of the incompetent Harrisburg Member of the Permian Kaibab Formation marks the presence of this major unconformity Hintze (1986). Locally, the Rock Canyon Conglomerate Member, or the Timpoweap Member, of the Lower Triassic Moenkopi Formation rests unconformably on the Harrisburg Member and, in places, the Fossil Mountain Member of the Permian Kaibab Formation (Figure 3). Following the Rock Canyon Conglomerate Member, the final cycles of the passive margin sequence deposition are recorded in the Moenkopi Formation (Figures 3 to 5). Higher frequency, relatively short-lived cycles led to deposition of thin, competent limestones and sandstones interbedded with thicker, incompetent mudstones and siltstones. These incompetent layers are also known as the Triassic redbeds: the Lower Red, Middle Red, Shnabkaib, and Upper Red Members. The major competent layers within this package are found in the Timpoweap and Virgin Members, though both primarily consist of incompetent siltstones and shales.

A switch to terrestrial (i.e., fluvial and lacustrine) depositional environments beginning in the late Triassic and into the early Jurassic, led to deposition of thin, competent layers of sandstones and conglomerates interbedded within relatively thicker mudstones and siltstones. Significant thin, competent strata within this package include the Shinarump Conglomerate Member of the Upper Triassic Chinle Formation, the Dinosaur Canyon Member of the Upper Triassic-Lower Jurassic Moenave Formation, the Springdale Sandstone Member of the Lower Jurassic Kayenta Formation, and the Shurtz Tongue of the Lower Jurassic Navajo Sandstone. This package is capped by the last thick, competent layer deposited in the stratigraphic section, the Navajo Sandstone.

Each of these competent units became ridge-formers upon uplift and exposure of the Kanarra fold-thrust system. The geologic map of the area (Figure 3), as well as the aerial photo terrain view (Figure 6), show their spatial distribution and topographic expression. Unconformably overlying the Navajo Sandstone are the Middle Jurassic Temple Cap and Carmel Formations, consisting of interbedded competent layers of limestone and/or sandstone and incompetent layers of mudstone and gypsum (e.g., Sprinkel et al. (2011)). In the northeast portion of the map area, dips on the Carmel Formation as high as 39°are observed (Figure 3). The Carmel Formation is the youngest unit in the map area affected by the formation of the development of the Kanarra fold-thrust system. The upper portion of the Carmel Formation was partially removed by erosion during the Cretaceous, and is unconformably overlain by thin, dispersed orogenic Cedar Mountain Formation (Biek et al. (2010)). The sub-Cretaceous unconformity is capped everywhere by the Cretaceous Naturita Formation and the Straight Cliffs Formations. In the map area, the Jurassic Carmel Formation and Cretaceous strata crop out as gentle, vegetated slope formers and subhorizontal ledges at the top of the Hurricane Cliffs (Figure 3).

4.1. DISTINGUISHING THE TIMPOWEAP MEMBER FROM THE VIRGIN MEMBER

Correlating and grouping Mesozoic and Cenozoic stratigraphic packages across the Great Basin and the Colorado Plateau is an ongoing endeavor, and our understanding of depositional environment and lithology improves as updates are made. Name and grouping changes have been suggested for several units in the past two decades (e.g., Carpenter (2014); Hautmann et al. (2013); Hofmann et al. (2013, 2014); Lucas and Tanner (2006); Lucas et al. (2007)). Some have stuck, but not all suggested changes are reflected in current maps. For this reason, and because an in-depth stratigraphic analysis is beyond our scope, this paper follows the convention of using member and formation names based upon recent local mapping ((Biek and Hayden, 2016; Knudsen, 2014a)). Nevertheless, the detailed

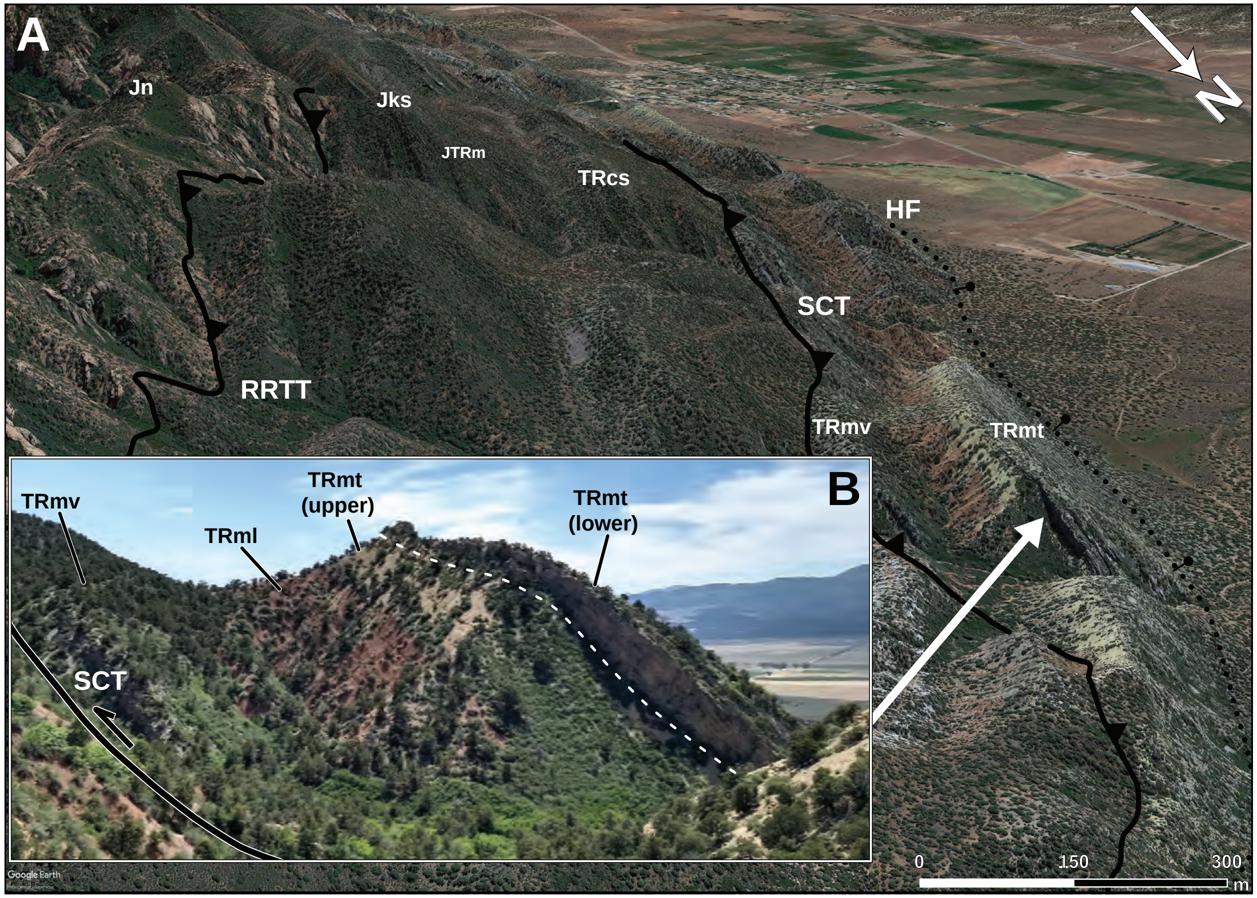

Figure 6. The Triassic-Jurassic section at Short Creek. A) View southwest into Short Creek onto overturned stratigraphy along the Kanarra fold. Here, the Timpoweap Member forms the first of several ridges rising from the east above Cedar Valley. Google Earth 3D terrain view basemap, supplemented with Landsat/Copernicus imagery. B) Field photo looking onto the Timpoweap ridge. In the background, the contact with the Lower Red Member, the shale grades vertically into a deep purple-gray color.

characteristics of certain units—particularly the Timpoweap and Virgin Members of the Moenkopi Formation—are critical to unravelling the complex structural relationships along the eastern limb of the Kanarra anticline, particularly the relative timing of early- versus late-forming thrust faults in the development of the Kanarra fold-thrust system.

In southwest Utah, Moenkopi strata up to the Shnabkaib Member represent a series of intertonguing lithosomes ((Hofmann et al., 2013; Lucas et al., 2007), Figure 2). They are part of a cyclic stratigraphic pattern which reflects sequential transgressions and regressions along the Cordilleran hingeline during the Triassic. Though the exact sequence boundaries may lie within lithostratigraphic units, the shallow marine-sabkha units generally represent transgressive packages which correlate to units elsewhere part of the Thaynes Formation (or Thaynes Group), whereas the redbeds represent regressive packages (Lucas et al., 2007). The shallow marine lithosomes, particularly the Timpoweap and the Virgin Members of the Lower Triassic Moenkopi Formation, have similar lithologies and fossil distributions. This can make them difficult to distinguish in the field, especially in complexly faulted areas where they are juxtaposed and overturned. For accurate discernment between the Timpoweap and Virgin Members, careful consideration must be given to their topographic expression (i.e., "fingerprint", Figure 6 and Figure 7), distribution of lithologies, and characteristic local fossil associations.

4.1.1. The Timpoweap Member. The topographic signature of the Timpoweap Member is distinct from that of the Virgin Member (Figure 6 and Figure 7. The unit can be divided approximately in half; a lower and upper parts. The lower part forms a thick (over 20 meters) ledge, whereas the upper part forms a slope. Unlike the Virgin Member, thin resistant rock layers or "fins" are largely absent in the Timpoweap Member. The ledge is a thick-bedded, gray to buff tan limestone, whereas the slope is an incompetent, yellow micritic shale (Figure 6 and Figure 7).

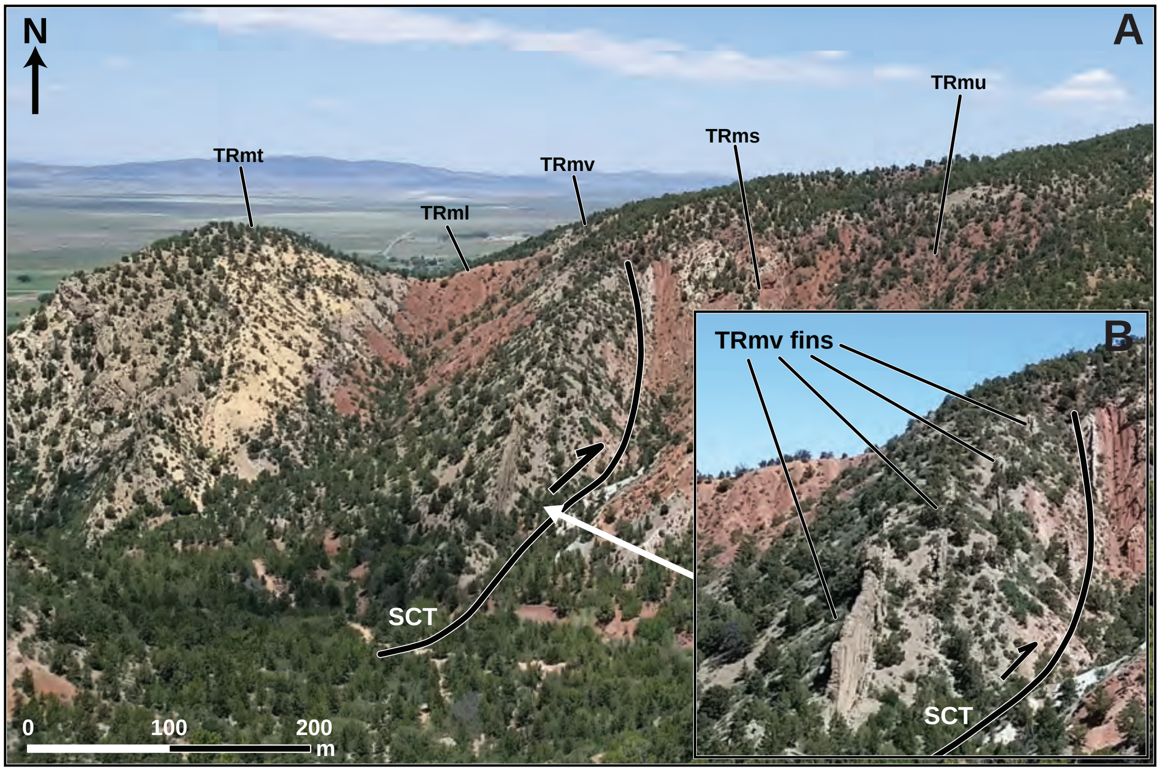

Figure 7. The Lower Moenkopi Formation in Spring Creek. A) View north across Spring Creek onto Lower Moenkopi Formation units. The hill to the west is cored by the Fossil Mountain Member of the Permian Kaibab Formation (not pictured here). Within tens of meters, upright Timpoweap Member capping the hill transitions to steep, overturned Virgin Member. Here, the differences in color and topographic fingerprint between the Timpoweap Member and Virgin Member are distinct. The upper yellow shale of the Timpoweap Member on the hilltop is underlain by the gray-yellow ledgeforming lower unit. The yellow shale grades into the purple-gray mudstone near the contact with the the Lower Red Member. To the east, vertical to overturned gray limestone and tan sandstone fins interbedded with gray-purple mudstone form a ridge of Virgin Member. The Spring Creek thrust displaces this ridge eastward, truncating the Middle Red Member. Inset (B) emphasizes the alternating competent fins and mudstone in the Virgin Member.

Where the Rock Canyon Conglomerate Member is present, the conglomeratic facies grades upward into the ledgeforming Timpoweap, so that the lowermost limestone beds may contain isolated, thin, pebble conglomerate lenses. Some limestone beds in the ledgeforming Timpoweap are sand-rich; others appear sandy on their weathered faces, particularly the buff tan beds, yet most of these are a recrystallized Dunham mudstone. Fresh faces on the buff tan beds reveal a deep gray, crystalline limestone. This contrasts markedly with thick, tan beds in the Virgin Member which are quartz arenite. A thin, discontinuous, dark brown, sand-bearing limestone outcrops within the yellow slope-forming shale, and commonly hosts shell beds. At the top of the unit, the yellow micritic shale abruptly darkens to a deep purple gray before the contact with the lower red member. This purple-gray layer can lead to confusion between the Timpoweap and Virgin Members, at it resembles the purple mudstones in the Virgin Member, and is not always present in the Timpoweap Member, particularly at thrust contacts. However, the purple-gray layer is distinctly part of the Timpoweap (*c.f.* Lucas et al. (2007)) and only appears near its upper contact.

In the field area, fossils in the Timpoweap Member are scarce, particularly in comparison to the abundant fossiliferous outcrops in the Virgin Limestone Member. The fossil assemblages of the Timpoweap Member and the Virgin Limestone Member contain genera that are common to both members. However, there are "key fossils" intrinsic to the Timpoweap Member that enable it to be distinguished from the Virgin Member (Lucas et al. (2007); Figure 8 of this paper). These characteristic Timpoweap Member fossils occur within shell beds or the traces of shell beds, which hinders easy identification. Ammonites (Figure 8A, Figure 8C) were rare and poorly preserved are exclusive to the Timpoweap Member. The discovery of *Wasatchites* (Figure 8C) on the ridge north of Kanarra Creek also confirm this unit as the Timpoweap Member.

4.1.2. The Virgin Member. The most distinct map to outcrop-scale characteristic of the Virgin Member is its topographic signature (Figure 7). The unit consists of several thin, competent, weathering-resistant fins set within a package of much thicker (tens of

Figure 8. Fossils used in the field to distinguish the Timpoweap Member. A and C) Ammonites of differing levels of preservation. The ammonite in (A) is entirely replaced by calcite and was found in a limestone ledge within the Timpoweap Member at Spring Creek. The partial ammonite in (C) was found in a sand-bearing, recrystallized limestone bed along the ridge capped by Timpoweap north of Kanarra Creek. Though the level of preservation makes interpretation dificult, from the shell decorations and size, (A) appears to be *Anasibirites* and (C) appears to be *Wasachites* (e.g., Lucas et al. (2007)). Ammonites are known to occur in the Virgin Member (**?**, but none were found in the Kanarraville area. B and D) Specimens of *Eumorphotis* (*c.f.* Figure 6 of Hautmann et al. (2013); Figure 11 of Hofmann et al. (2014)), a bivalve genus dominantly found in the Timpoweap Member in the field area.

meters) incompetent rock. The fins are all similar in thickness, typically 1-4 meters, although fins up to 8 meters are reported (see Knudsen (2014a)). The competent fins tend to be gray or tan, and together they form resistant ridges interbedded within the incompetent rock layers. Where the fins are steeply dipping, they stand high above the intervening incompetent strata (Figure 7). The fins are comprised of medium to very thick-bedded limestone or tan, fine-grained quartz arenite. Locally fins can contain both lithologies, and where they do there is a sharp contact from sandstone into limestone. The incompetent intervals contain variegated mudstone and siltstones varying in color from gray, to brown, to purple. Within the field area, the Virgin Member is dominantly composed of sandstone, siltstone, or mudstone and minor limestone, with the incompetent strata comprising over two-thirds of the total thickness. Where depositional contacts are preserved, the top of the Virgin Limestone Member is marked by a sharp transition into a double layer of gypsum at the base of the Middle Red Member.

In the field area, the Virgin Member is distinguished from the Timpoweap Member by the presence of the following "key fossils"; the trace fossil *Thalassinoides* and two major body fossil types: the brachiopod *Rhychonella* and two types of crinoids (Figure 9). The trace fossil *Thalassinoides* was found only within the Virgin Limestone, along the bottom of a very thick-bedded tan quartz arenite ledge which commonly outcrops near the top of the unit (Figure 9A). The trace fossil is preserved as interweaving casts of tunnels with triple junctions and is interpreted as *Thalassinoides* (*c.f.* Figure 16A of Hofmann et al. (2013)); this trace fossil was found at Kanarra Creek where the Virgin Member is overturned. In addition, the brachiopod *Rhychonella* is common only to the Virgin Limestone (Figure 9C), where it is restricted to the limestone layers. While the brachiopod is most similar to *Rhychonella* from the Thaynes Formation (see Perry and Chatterton (1979), Figure 13), its size and plications also resemble *Piarorhynchella* (*c.f.* Figure 9C1 of Hofmann et al. (2013)) and *Lissorhynchia* ((Wang et al., 2017)). The brachiopds commmonly form thin shell beds, and complete, individual shell fossils can be found near outcrops where they erode out of the limestone fins (Figure 9C). They are small, with their long axes typically less than 2 cm long, and contain rounded, relatively wide, plications which greatly increase

Figure 9. Fossils used in the field to distinguish the Virgin Member. A) Interweaving bioturbations reminiscent of *Thalassinoides* at base of overturned, thick-bedded sandstone ledge near the entrance to Kanarra Creek. B) Pentagonal crinoids in gray limestone of the Virgin Member just north of Spring Creek. C) Brachiopod shell bed and well-preserved specimen (inset) found at Kanarra Creek. D) Star-shaped and pentagonal crinoids within tan, fine-grained sandstone in the Virgin Member—Triassic crinoids of either type are exclusive to the Virgin Member in the study area.

in amplitude at the shell midpoint. Two types of five-sided crinoid stem plates were also found exclusively in the limestone or sandstone layers of the Virgin Limestone Member. One resembles a five-sided star (Figure 9D), while the other has more rounded corners, straighter sides, and more closely resembles a pentagon (Figure 9B). These types of crinoid are entirely unique to the Virgin Member and, along with the brachiopods, were used as marker fossils while in the field.

5. STRUCTURE

The complexity of structural elements, folds, and faults of the Kanarra fold-thrust system reflects the protracted, multi-phase geologic history of an area that straddles several major long-lived lithospheric boundaries: The Cordilleran hinge line, the leading edge of the Sevier fold-and-thrust belt, and the boundary between the Basin and Range Province and the Colorado Plateau Province (Figure 1). Resolving the tectonic significance of the Kanarra fold-thrust system in the context of this extended geologic history requires understanding the inextricable temporal and spatial relationship of contractional faults (i.e., thrusts) to the development of the Kanarra anticline. This relationship is best preserved in the central portion of the Kanarra fold-thrust system (Figure 2) and is best understood using the detailed geologic map of this area (Figure 3 and Figure 4) and a structural cross-section through the Kanarra fold-thrust system *prior* to its dismemberment by the Hurricane fault during Basin and Range extension (Figure 10). This cross-section shows the full profile of the restored Kanarra fold-thrust system at the time of the Sevier orogeny. The compound nature of the Kanarra anticline, consisting of an eastern leading anticline (i.e., the traditional Kanarra anticline of previous literature), a broad sub-horizontal hinge zone, and the trailing western anticline are clearly identifiable within this cross-section.

We discuss the nature of the Kanarra anticline, which is a paired anticline-syncline structure first (see Figure 10, followed by the associated “early” and “late” fold accommodation faults Butler et al. (2020); Cawood and Bond (2020); Cloos (1964); Mitra (2002a) and their role in the formation of the Kanarra anticline-syncline pair, as well as the development of the previously unrecognized, easternmost, leading edge thrust fault (i.e., the Red Rock Trail thrust) associated with the Sevier orogeny in southwest Utah (Figure 2). We call this structural assemblage the Kanarra fold-thrust system to 1) emphasize these structures are genetically related and tied to the Sevier orogeny and 2) remove the ambiguity in the tectonic significance of the “Kanarra anticline” that continues to persist in the literature (e.g., see Enriquez St. Pierre and Johnson (2021), Figure 1 and 2). Finally, the location in the field area where extensional faults associated with the Hurricane fault zone are best exposed is presented.

5.1. THE KANARRA ANTICLINE-SYNCLINE PAIR

The western trailing limb of the Kanarra anticline was severed and buried, along with the hanging wall of the Hurricane fault in Cedar Valley, beneath a thick mantle of alluvium shed off the Hurricane Cliffs (Figure 2 and Figure 3. Field observations and aerial imagery indicate the style of the Kanarra folds is overall “kink-like”. Field exposure of sparse, isolated remnants of the hinge zone along the strike of the leading anticline (Figure 10) exhibit this kink style of folding. In cross-section, the Kanarra anticline-syncline pair can be represented with a series of kink panels; collectively these kink panels contribute to defining the overall form of the anticline and the syncline.

The Kanarra anticline has a compound geometric form (Figure 10). The fold form has many of the characteristics of idealized fault propagation folds that develop in the hanging wall of blind thrust faults (e.g., Davis et al. (2011); Mitra (2002b), p. 414–428). The anticline is defined by a long, shallowly dipping westward, trailing limb, a relatively flat hinge zone, and a shorter leading limb that is steeply dipping west and overturned. Overall, the folded layers form an asymmetric, east verging, over-turned anticline (Figure 10). The overturned leading anticlinal limb verges eastward along with a tight, east-verging syncline. The leading anticline is defined by five kink panels with an overall rounded form characteristic of buckle folds, (see the Navajo Sandstone in Figure 10, and buckling Fischer et al. (1992); Willis (1893) may have contributed to the initial stages of folding of these strata. The trailing limb of the Kanarra anticline includes an early fold accommodation fault

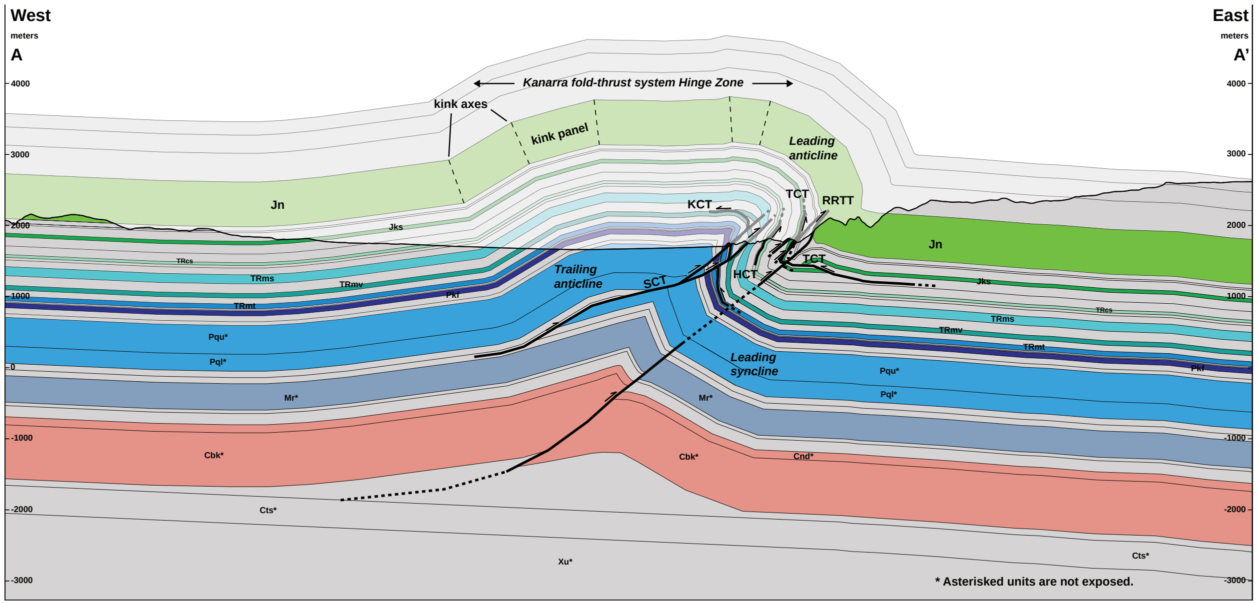

Figure 10. Cross section of the Kanarra fold-thrust system at Kanarra Creek. The restored Sevier structure is shown circa 80 Ma, based on field mapping along Kanarra Creek. Kink axes and components of the hinge zone are annotated for reference. Eroded geology is faded out. The pre-extension trailing limb and fold crest are constrained by the tilted, subhorizontal regional along the Hurricane cliffs and the shape of the closely-related Pintura anticline (Hurlow and Biek (2003)). No strata below the Fossil Mountain member of the Kaibab formation (Pkf) are exposed at the location of the cross section; unexposed layer thickness and presence are constrained by local data sources (see Table 1; Biek et al. (2010); Hintze (1986); Hurlow and Biek (2003); Van Kooten (1988)). Unexposed, thick, competent layers (Cbk-Cnd, Mr, Pq) are colored according to age; exposed ridge-former colors correspond to the map. Present-day topography is included to emphasize the ridge-formers, but is not representative of the Cretaceous erosion surface. Structure west of the Hurricane Cliffs, within the present-day Cedar Valley graben, does not represent present-day bedrock geology. Unexposed structure constrained by surface control, fold style, and assumption of buckle folding before break-thrust faulting. Structure abbreviations: SCT—Spring Creek thrust; KCT—Kanarra Creek thrust; HCT—Hicks Creek thrust; TCT—Taylor Creek thrust; RRTT—Red Rock Trail thrust.

which has merged with the later, exposed Spring Creek thrust (Figure 10; see later section for more detail). Displacement along the Spring Creek thrust forms a trailing or distal fault-bend fold (e.g., Davis et al. (2011) p. 409–413) in the hanging wall of the trailing limb of the Kanarra anticline. This fault-bend fold modifies the overall geometric form of the Kanarra anticline crest into a composite fold with a “trailing anticline” and a “leading anticline” ((Figure 10).

5.1.1. Axial Trace of the Leading Anticline. The trailing anticline and hinge line of the Kanarra anticline are buried—only the leading anticline of the fold crops out and is discussed here. In the field, locations where the hinge zone of the leading anticline, along which shallow, west-dipping strata rotate into the eastern leading limb of the anticline, are sparsely exposed (e.g., Figure 11). These remnants of the hinge zone are used to define the discontinuous trace of the *leading* anticline axial surface along the length of the fold (Figure 2). In previous literature the leading anticline was known as the Kanarra anticline, or because of the discontinuous, dissected, nature of the hinge zone along the strike of the fold, locally assigned other names (e.g., Hintze (2005), Squaw Creek anticline, p. 175). In the central portion of the Kanarra fold-thrust system, there are three locations where the hinge zone is well-exposed: 1) Camp Creek, 2) Spring Creek, and 3) just south of Kanarra Creek (Figure 2 Figure 3).

5.1.2. Axial Trace at Camp Creek. At Camp Creek, the leading anticline is upright and open. The axial trace is exposed in Lower Moenkopi units and the Fossil Mountain Member of the Kaibab Formation which crop out in the canyon at the mouth of Camp Creek. Fault splays of the Hurricane fault cut the hinge zone near the creek mouth (Figure 11); its axial trace is lost south of the creek where it has been sheared away (Figure 2 and Figure 3). Within the canyon, a steep axial surface separates consistently westward-dipping (~10-15°W) from east-dipping (~15°E) bedding in limestone of the Fossil Mountain Member. Here in the core of the hinge, multiple meter-scale kink panels in the limestone impart an

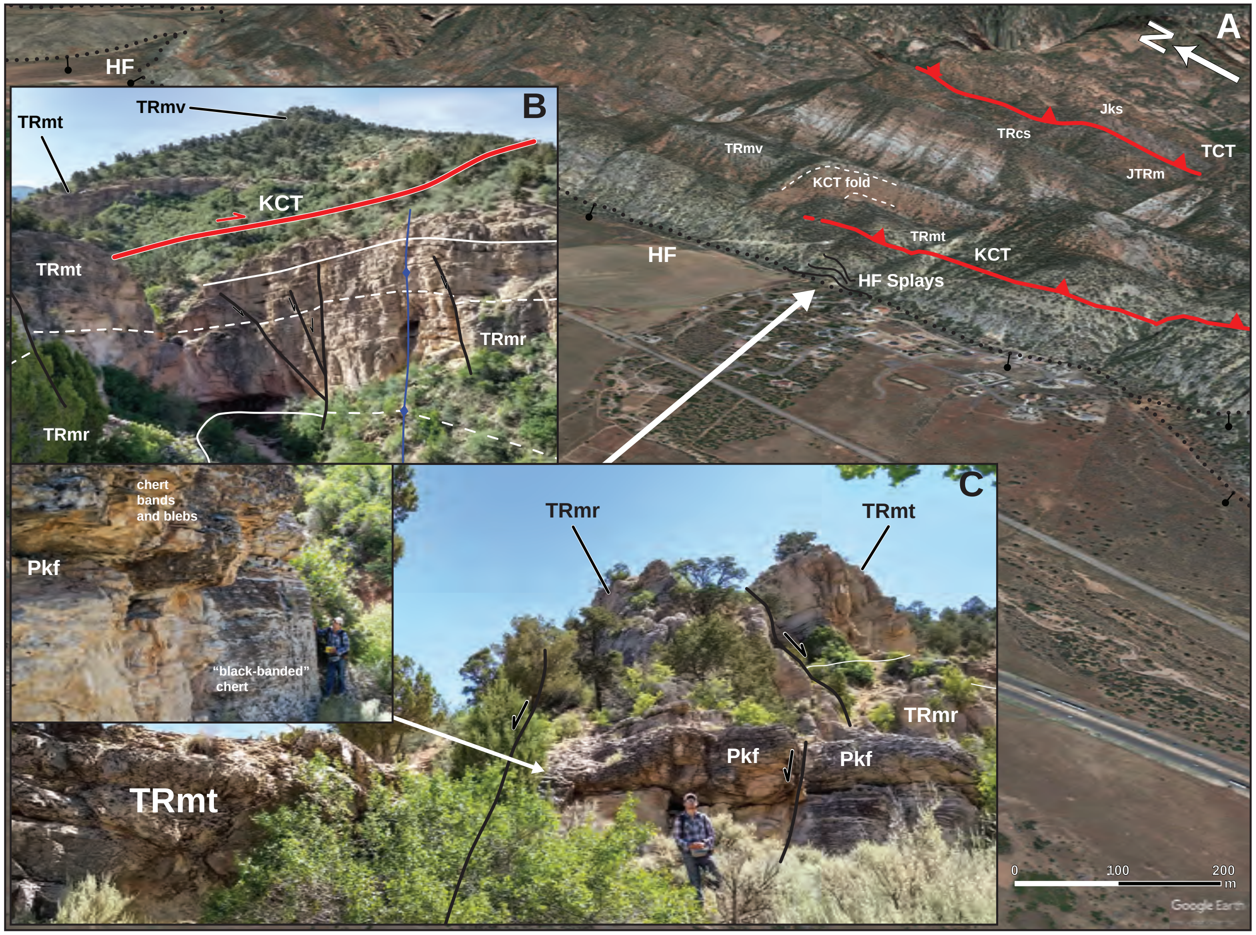

Figure 11. Leading anticline hinge zone and Hurricane fault zone near Camp Creek. A) Google Earth 3D terrain view with Landsat/Copernicus imagery of the leading anticline hinge zone. B) Low-displacement normal faults within the Hurricane fault zone at the creek mouth. C) Horst of Rock Canyon Conglomerate Member west of (B). Dylan Webb in foreground.

open, gentle flexure best seen at the bottom of the canyon (Figure 11B). The geometry of the leading anticline is reflected in the shape of the hinge, which is horizontal and open, with the enclosing strata forming a ~150°angle.

5.1.3. Axial Trace at Spring Creek. The hinge zone of the leading anticline is well exposed within a 60-meter-high canyon wall at the mouth of Spring Creek. The cliff face exposes the Fossil Mountain Member of the Kaibab Formation capped by the Timpoweap Member of the Moenkopi Formation. The hinge zone, while still appearing rounded, tightens considerably between Camp Creek and Spring Creek. At Spring Creek, the angle between strata forming the hinge zone has decreased from ~150°to ~65°(close). Here, the steep (~80°), west-dipping axial surface roughly parallels the trace of the Hurricane fault. East along Spring Creek, the transition from steeply dipping to overturned is readily shown by rotation of the primary bedding orientation in the Kiabab Formation to steep, vertical dips and by the steeply overturned, resistant "fins" in the Virgin Member of the Lower Triassic Moenkopi Formation (see Figure 3 and Figure 7).

5.1.4. Axial Trace near Kanarra Creek. Just north of Spring Creek, the hinge zone of the leading anticline is truncated by the Hurricane fault ~500 meters from the transition to overturned bedding in the Timpoweap Member (Figure 12A, Figure 12C). East of this truncation, several thrusts of the Spring Creek thrust system cut through the hinge zone, with the largest (the *primary splay*, see *Spring Creek thrust system*) displacing overturned Timpoweap Member onto shallow, west-dipping (~8°W), and presumably upright Virgin Member. A low ridge of the Virgin Limestone Member east of the thrust truncation hosts a close (~35°interlimb angle), gently inclined, overturned fold. On the east side of the low Virgin Member topographic ridge, part of the reclined fold nose is preserved (Figure 12), and the Middle Red Member double-gypsum layer is disharmonically folded into an "S-fold" on the eastern limb. Bedding taken west of the fold nose indicate a shallow-dipping (15-25°W), upright western limb, whereas bedding on its steeper (45-55°W) eastern limb is overturned.

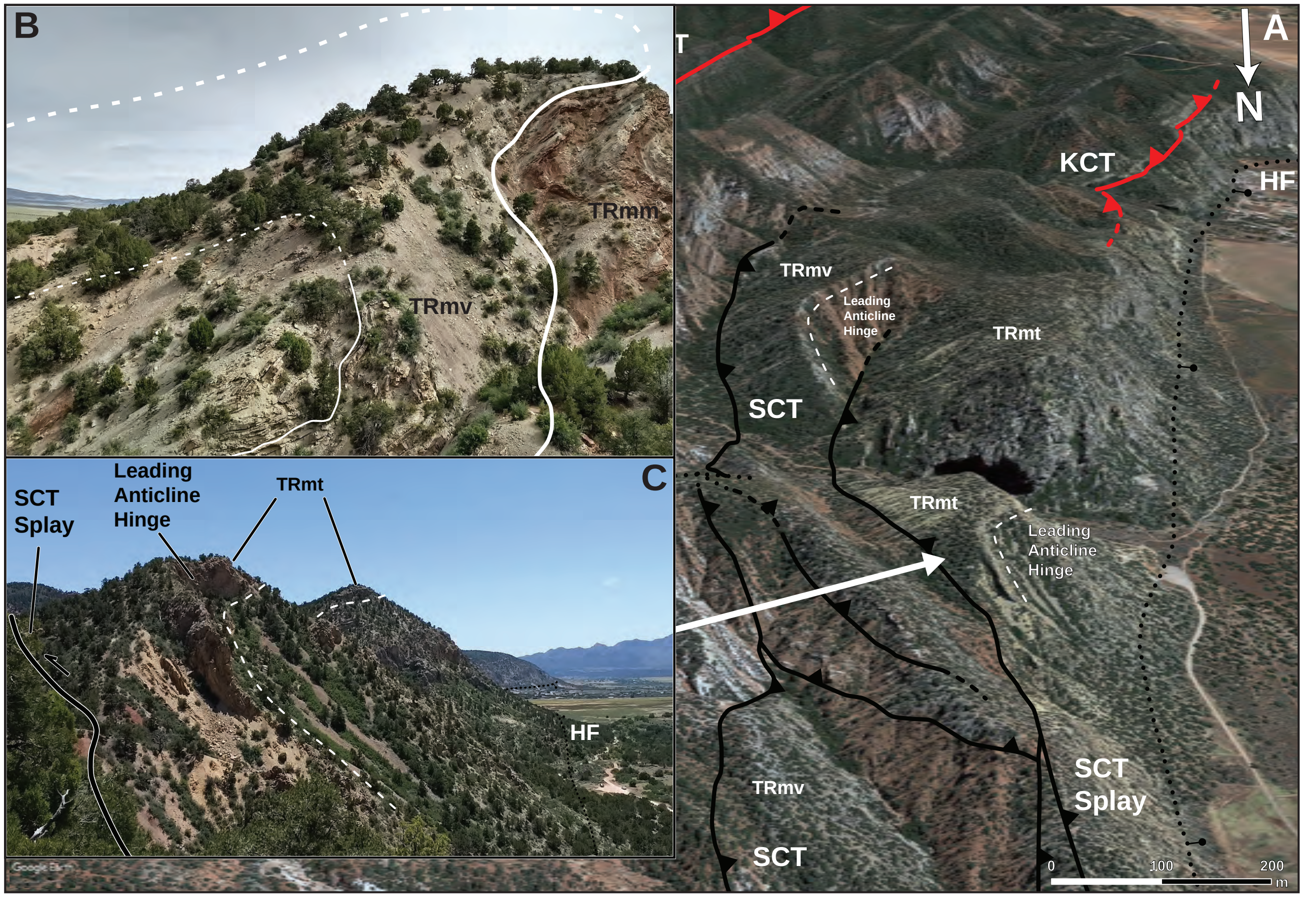

Figure 12. Leading anticline hinge zone near Kanarra Creek. A) Google Earth 3D terrain view with Landsat/Copernicus imagery looking south into Spring Creek where the Kanarra fold-thrust system overturns. B) Field photo looking south of upright (middle and background) and overturned (middleground) Timpoweap, outlined with dashed white lines. C) View to the north onto a tight, gently reclined, closure on the leading anticline hinge within the Virgin Member east of (B).

The axial trace of this fold can be mapped northwards for nearly the entire length of the low Virgin Member ridge (~1000 meters) until it peters out at Kanarra Creek, likely cut by the Spring Creek thrust. A small, later thrust (also ~1000 meters long), cuts through the western limb of this fold (Figure 3). This thrust likely formed to accommodate strain within the overtightened fold hinge. The entire structure is transported eastward along the *main trace* of the Spring Creek thrust just to the east of the ridge. We interpret the tightly folded Virgin Member here to be the northernmost remnant of the leading anticline hinge zone in the study area, cut and modified by transport along the Spring Creek thrust.

5.2. EARLY CONTRACTION FAULTS

The Kanarra anticline-syncline pair is faulted along its length (Figure 2). The greatest density of faults crops out in the central section where the limb is overturned (Figure 3). Typically, these faults (i.e., fault planes) are poorly exposed and inaccessible to direct observation. They are mappable through observations of truncation, folding, or attenuation of incompetent strata along competent ridge-formers. Where possible, striated, stepped shear fracture sets within competent units were measured in the field to determine the aggregate sense of slip of the larger thrust surfaces (see *Methods*, Marrett and Allmendinger (1990); Petit (1987). Most of these faults are contractional faults associated with the Sevier orogeny and the formation of the Kanarra fold-thrust system.

Contraction faults associated with the Kanarra anticline can be subdivided into "early" and "late" contraction faults relative to the evolution of the Kanarra anticline from an open upright fold to a tight overturned asymmetric anticline-syncline pair. Early contraction faults have the following attributes consistent with their inception as thrust faults at the earliest stages of folding. The strike of these faults is typically sub-parallel to parallel to bedding (Figure 3). The map-scale patterns of the fault traces through the topography constrains the dip on these faults to be typically 10-25°higher than bedding in their footwalls, consistent with early thrusts. Ridge-formers are commonly duplicated by these thrusts, doubling, or tripling the original thickness of these units. Statistical solutions of measurements of rake, displacement direction, and orientation of striated, stepped shear fracture populations along these duplications indicate thrust sense of slip (Table 3, Figure 4). Additionally, asymmetric folds, while not always present, indicate displacement consistent with thrusting (e.g., Figure 5 and Figure 12 In the central section of the Kanarra anticline, several early-formed contraction faults were folded and are overturned along with the eastern limb of the leading anticline (Figure 3, Figure 4, and Figure 10). These overturned thrusts have been previously misidentified as normal faults, presumably based upon the displacement along the thrust fault, indicating normal separation after rotation to overturned. we have identified these structures as folded thrusts.

These early thrusts occur at all scales, with the largest, the Taylor Creek thrust (Biek (2007a); Kurie (1966)) being many kilometers long (Figure 2). Due to dismemberment of the Kanarra anticline by the Hurricane Fault, these thrusts crop out only within the hinge zone of the leading anticline and the eastern limb of the Kanarra anticline. However, similar early contraction thrusts are present on the western limb of the closely associated Virgin anticline (e.g., at Silver Reef) and along its crest (Biek (2003a,b)). Because these faults tend to form on the limbs (flanks) of folds, we refer to these early-formed thrusts as flank thrusts (e.g., **?**), though they are known by other names (a type of "fold accommodation fault" or "wedge faults", *c.f.* Cloos (1961); Faill and Wells (1974); Mitra (2002a). We infer that flank thrusts were also present on the trailing limb of the Kanarra anticline (i.e., the Spring Creek thrust) and their presence is supported by our mapping and structural cross-section of the Kanarra fold-thrust system (Figure 3, Figure 4, and Figure 10). The significant flank thrusts within the central portion of the Kanarra fold-thrust system are discussed in the following sections.

5.2.1. Kanarra Creek Thrust System. The Kanarra Creek thrust is the westernmost exposed thrust in the map area (Figure 3). It is commonly associated with repetition of stratigraphic units lower in the section, typically the Timpoweap and Lower Red Members of the Moenkopi Formation, and crops out close to the hinge zone of the leading anticline of the Kanarra anticline. We infer its trace is discontinuous along the length of the Kanarra anticline due to the structural level of exposure and to its removal from view because of displacement of the hanging wall of the Hurricane fault.

The southernmost occurrence of the Kanarra Creek thrust in the map area is at Camp Creek (Figure 3, Figure 4). Here the leading anticline is upright and open. The Kanarra Creek thrust crops out along the hinge of the fold where it duplicates the ledge-forming limestone layer in the Timpoweap Member (Figure 13). The thrust has been affected by folding and dips shallowly eastward at ~20°(~10°greater than the strata in its footwall) and displaces strata in the hanging wall to the west. In the hanging wall of the thrust is an asymmetric (tops-to-the-west) fold within the Lower Red Member (*c.f.* Figure 11. Based on structural level and repetition of stratigraphic units, the Kanarra Creek thrust continues southwards along strike into Wayne Canyon (see Figure 3, Figure 4, and Figure 11; further south it may correlate to the thrust along the Black Ridge in the Pintura 7.5-minute Quadrangle (e.g., Biek et al. (2010); Hurlow and Biek (2003).

In Spring Creek, the Kanarra Creek thrust crops out along the hinge zone of the leading anticline (Figure 3, Figure 4). North of Spring Creek, portions of the fault and the hinge zone of the fold have been removed by the Hurricane fault. Continuing northward, remnants of the hinge zone of the leading anticline are complexly faulted by both early and late thrust faults (Figure 12). The intensity of deformation requires accurate identification of stratigraphic units and their spatial relationships to identify the location of the Kanarra Creek thrust (see *Stratigraphy*). Looking north from the mouth of Kanarra Creek, to the west is a low hill with a water tower that is underlain by the Kaibab Formation and Triassic Lower Moenkopi Formation up to the Timpoweap Member (Figure 14). These strata have been thrust eastward in the hanging-wall of a splay of the Spring Creek thrust (discussed below). Just east of this hill is a resistant ridge of overturned, yellow limestone, stratigraphically overlain by yellow micritic shale, and capped by purple mudstone; the Timpoweap Member.

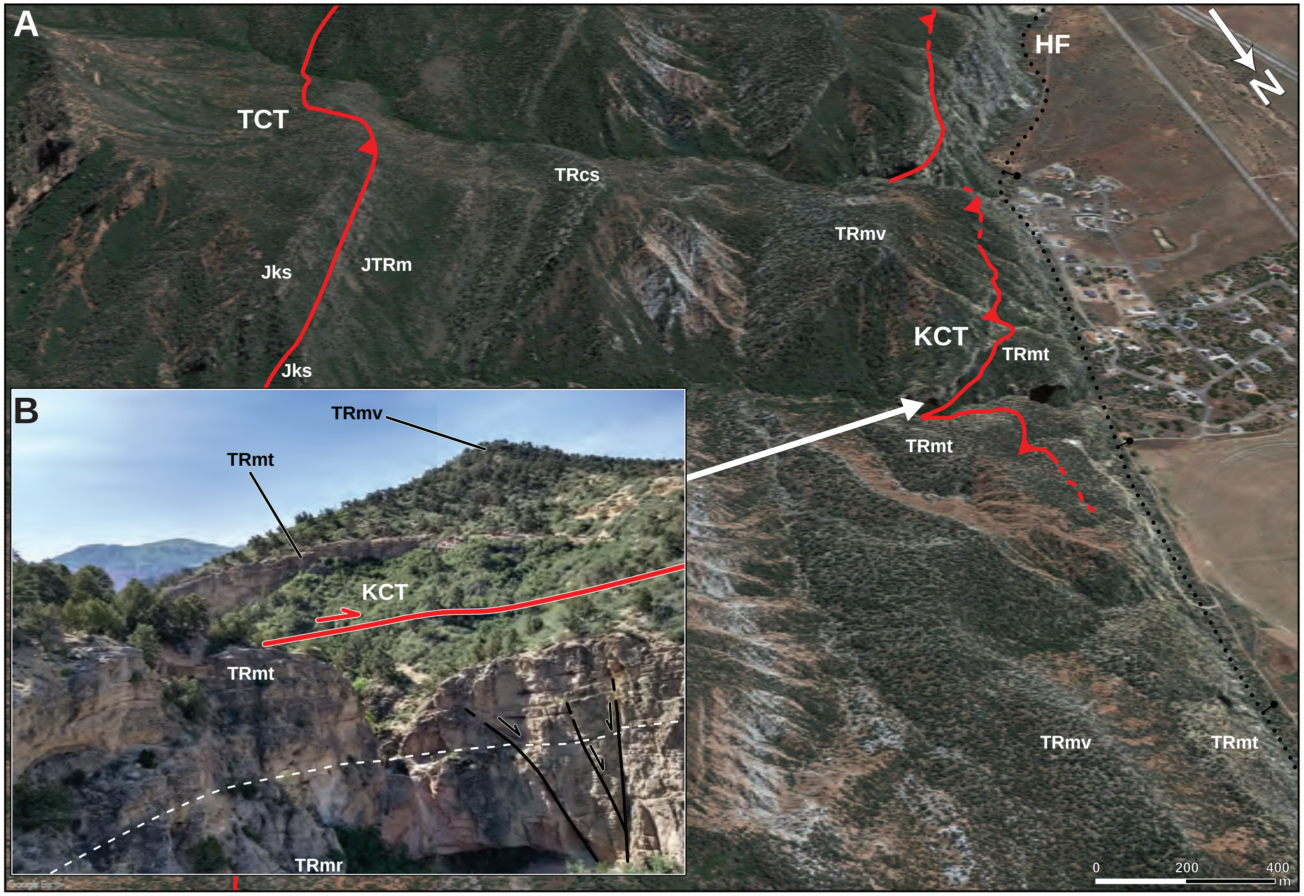

Figure 13. The Kanarra Creek thrust at Camp Creek. Google Earth 3D terrain view into Camp Creek, looking south. The Kanarra Creek thrust is seen here as an upright, west-directed thrust duplicating the Timpoweap Member. B) Kanarra Creek thrust looking southeast. Laterally variable, gradational contact (dashed white line) traced where the Rock Canyon Conglomerate weathers into hoodoos closer to the mouth of the creek (foreground).

The Timpoweap is followed eastward (up section) by the Lower Red Member and then the Virgin Limestone Member. The succession of strata, confirmed by outcrop appearance, lithology, and fossils (*c.f.* Figures 6 to 9), shows an uninterrupted, overturned, stratigraphic section up to the main trace of the Spring Creek thrust (Figure 14 inset). The Lower Red Member of the Moenkopi Formation also crops out on the western side of the ridge formed by the overturned limestone of the Timpoweap Member (Figure 3, Figure 4, and Figure 14. This repetition within the overturned stratigraphic succession marks the presence of an early thrust, the Kanarra Creek thrust, that was folded and overturned during formation of the leading anticline (Figure 3, Figure 4, and Figure 10).

The Kanarra Creek thrust can be followed further to the north as it continues along the resistant ridge defined by the limestone ledge of the Timpoweap Member. The trace of the thrust veers obliquely eastward across the ridge as it ramps up section (Figure 3 and Figure 4). Displacement along the Kanarra Creek thrust ramp is revealed on the north side of the ridge, where the Timpoweap Member is juxtaposed directly adjacent the Virgin Limestone Member (Figure 15. Further north along strike, the Kanarra Creek thrust soles into redbeds of the Moenkopi Formation, placing the Lower Red Member onto a sliver of the Middle Red Member (Figure 15A, B). A complex set of thrust splays followed by a synform in the Timpoweap Member marks the northern exposure of this part of the Kanarra Creek thrust before its main trace veers back to the west and is truncated by the Hurricane fault (Figure 3).

The northernmost appearance of the Kanarra Creek thrust in the map area is at the mouth of Short Creek (Figure 3). Here the thrust duplicates the Timpoweap Member (Figure 16. The ledge forming lower portion of the Timpoweap Member defines the hanging wall, which is thrust over the Lower Red Member, the upper yellow shales of the Timpoweap, and the lower ledge forming Timpoweap in the footwall (Figure 16A). The section here remains overturned, and the thrust is contained within these overturned

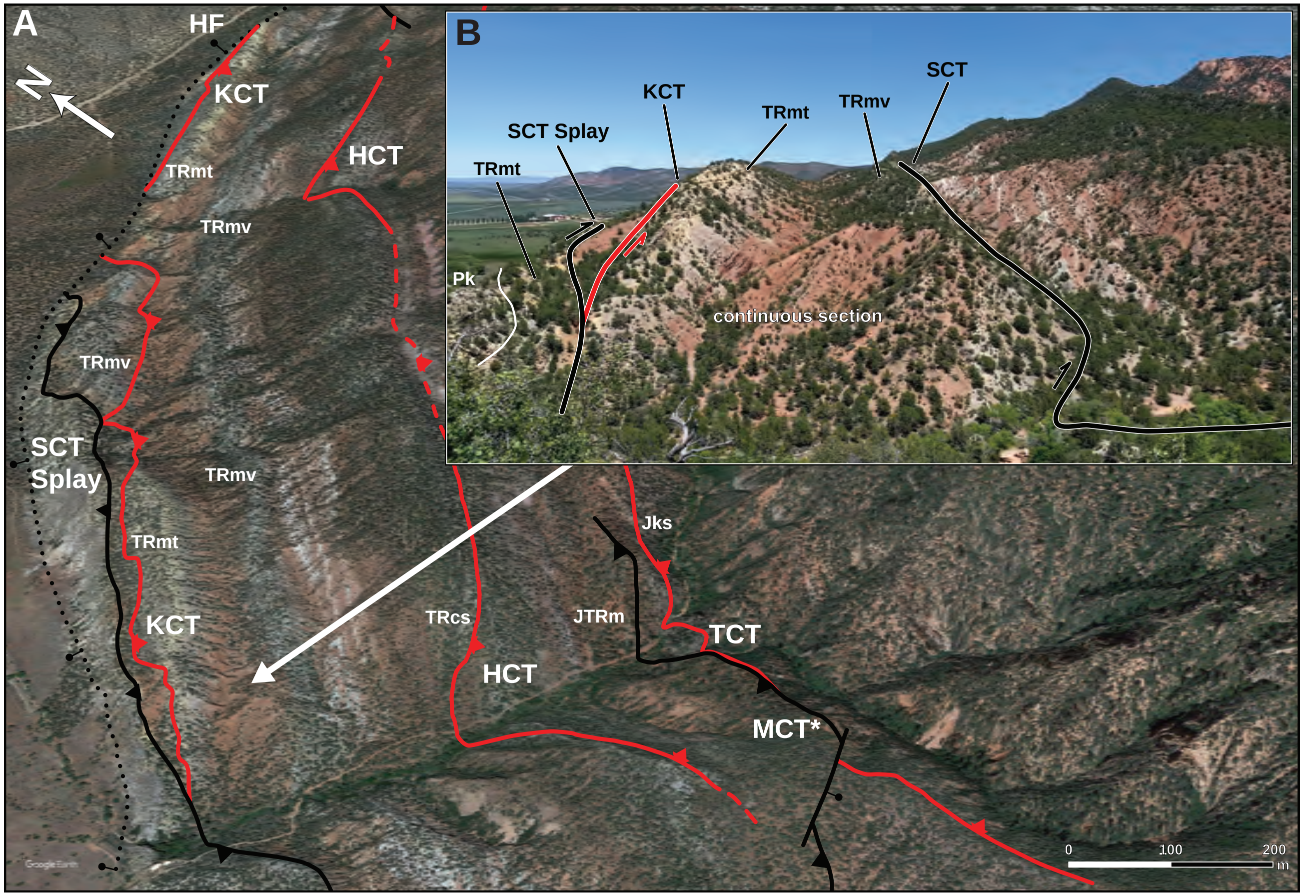

Figure 14. The Kanarra Creek thrust at Kanarra Creek. A) Google Earth 3D terrain view into Kanarra Creek looking northeast. B) Along-strike view upon ridges of the Timpoweap Member, a strike valley of Lower Red Member, the Virgin Member to the east. The Kaibab and part of the Timpoweap Member are thrust over the Kanarra Creek Thrust on the Spring Creek thrust primary splay. The Permian-Triassic unconformity (white line) is marked by Rock Canyon Conglomerate overlying the Harrisburg Member.

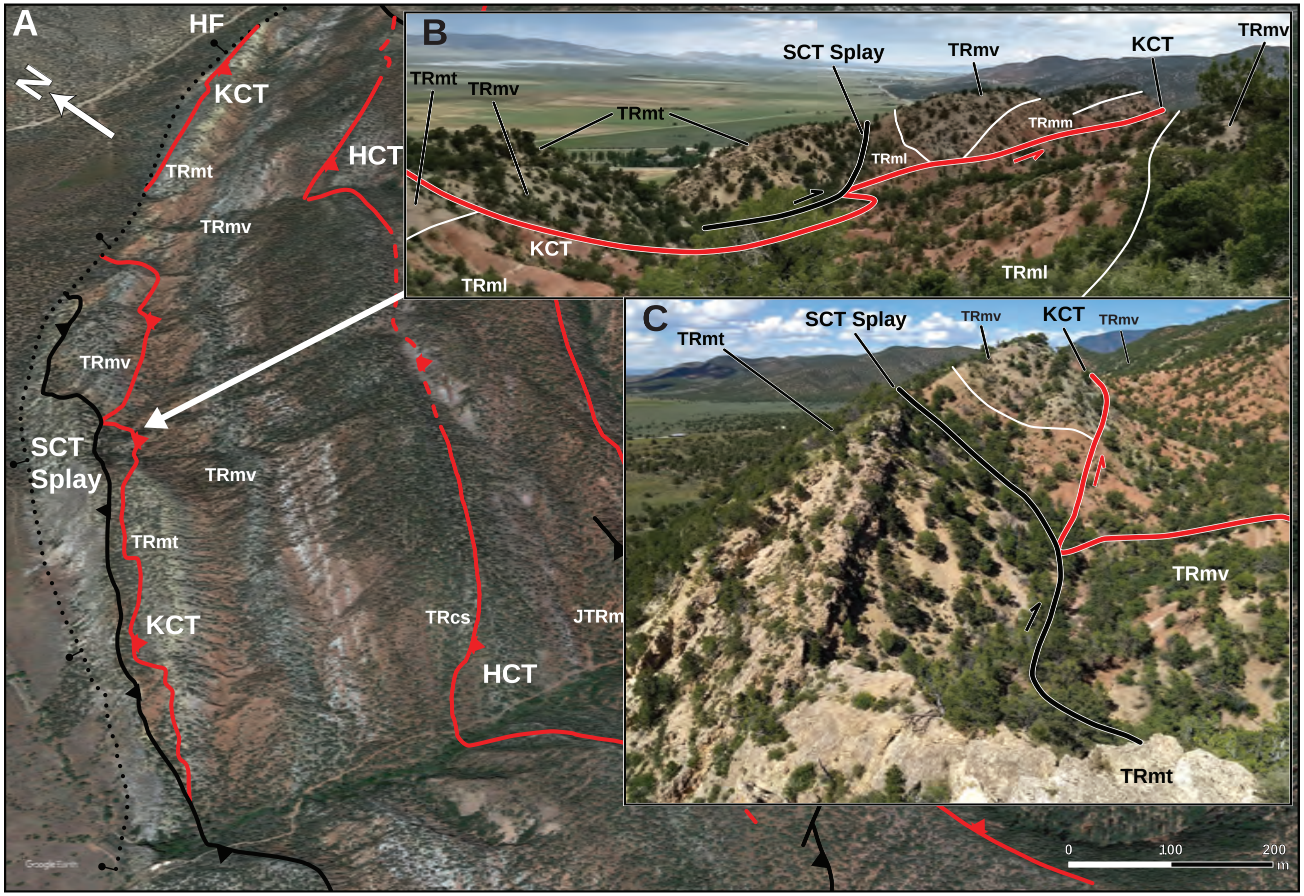

Figure 15. The Kanarra Creek thrust north of Kanarra Creek. A) Google Earth 3D terrain view looking northeast into Kanarra Creek. B) Field photo of both the Kanarra Creek thrust and the Spring Creek thrust splay, further to the north along strike. Part of the purple-gray mudstone at the top of the Timpoweap can be seen in the left midground, and the depositional contact into Lower Red is marked with a white line. C) Along-strike view of the faults in (B), taken standing on the Timpoweap looking north.

units. Along strike, to the north and to the south of Short Creek, the thrust soles into the Timpoweap member, approximately doubling its thickness, before the tips of the thrust trace are truncated by the Hurricane fault (Figure 3 and Figure 16).

5.2.2. Taylor Creek Thrust System. The Taylor Creek thrust is a significant, west-directed, flank thrust which can be traced over several kilometers along the eastern limb of the leading anticline of the Kanarra anticline (Figure 2), from its type area in Taylor Creek (Biek (2007a); Kurie (1966)) to the northernmost extent of the field area at Murie Creek (Figure 3, Figure 4). In its type area at Kolob Canyons, the thrust duplicates thin, competent ridgeformers within the Dinosaur Canyon Member and the Springdale Sandstone Member of the Jurassic Moenave Formation, and it soles into detachment layers within the Petrified Forest Member of the Chinle Formation (lower) and the Main Body of the Kayenta (upper). At Taylor Creek, several splays duplicating these units form a system of thrusts which likely share the same detachments—i.e., the Taylor Creek thrust system. Several other west-directed flank thrusts crop out along the leading anticline, (e.g., the Kanarra Creek thrust, Figure 3, Figure 4); for clarity we restrict the term "Taylor Creek thrust" to the west-directed thrusts duplicating Lower Jurassic units, primarily the Springdale Sandstone Member, as seen in the type area.

The Taylor Creek thrust is well exposed at Camp Creek (Figure 17). Here, a single splay of the thrust duplicates nearly the entire Dinosaur Canyon Member and the Springdale Sandstone Member. Erosion through the duplicated section produced a broad hill underlain by two ridge-forming ledges of the Springdale Sandstone Member. South of this ridge top, shallow, east-dipping ledges of the Springdale Sandstone define a broad, gentle fold nose in the hanging wall of the Taylor Creek thrust, indicating west-directed transport (Figure 17A). This fold in the hanging wall mimics the broad fold in the Springdale Sandstone in the hanging wall of the easternmost thrust fault of the Taylor Creek Thrust system (*c.f.* Biek (2007a), Figure 4, Plate 3).

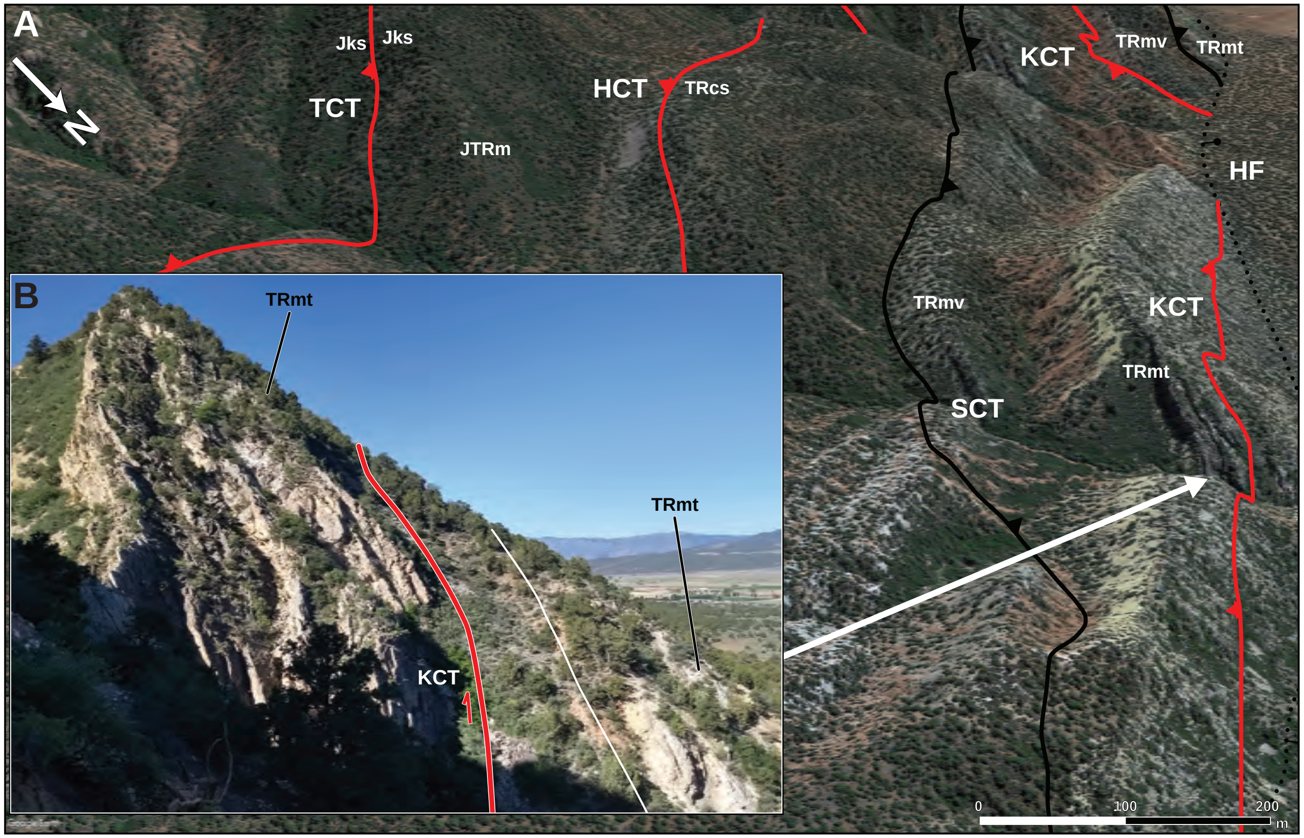

Figure 16. The Kanarra Creek thrust at Short Creek. A) Google Earth 3D terrain view southwest into Short Creek showing the overturned fold limb, overturned thrusts (Taylor Creek thrust, Hicks Creek thrust, and Kanarra Creek thrust) and the Spring Creek thrust. B) South-facing, along-strike view of duplicated Timpoweap Member along the Kanarra Creek thrust.

Figure 17. The Taylor Creek thrust at Camp Creek. A) Google Earth 3D terrain view south into Camp Creek showing the Taylor Creek thrust duplicating the Springdale Sandstone Member of the Kayenta Formation and the Dinosaur Canyon Member of the Moenave Formation. B) Edge-on field photo of the Taylor Creek thrust duplication.

Analysis of shear fracture data in the Camp Creek area yield a fault plane solution of (022, 55) with a rake of 122°, indicating a thrust fault with a minor left-lateral component of displacement. This result is consistent with the attitude of the fault, (033, 54), determined from the orientation of its map trace (Figure 3, Figure 4, and Table 3). Bedding in the footwall near the creek bed dips ~38° (Figure 3). Thus, at Camp Creek the Taylor Creek thrust is best characterized as a shallow thrust "ramp", forming an angle ~16° from bedding and thickening the Springdale Sandstone Member.

The Taylor Creek thrust system is less well-exposed in Spring Creek. Here, the steeply dipping overturned Springdale Sandstone Member is double to nearly triple its stratigraphic thickness because of multiple duplications (Figure 3). The tectonically imbricated and overthickened sandstone ledges form a prominent topographic ridge that has been eroded by the creek (Figure 18). Along the southern ridge isolated, slickensided outcrops of Springdale Sandstone on the hillside mark the presence of the thrust. A minor kink fold defined by shallow-dipping Springdale Sandstone ledges (dashed white line, Figure 18, inset) indicates the thrust splay cropping out along the ridge is a ramp which folded the overturned strata to very shallow inclinations (30-40° W). This kink fold continues up the ridge. At the top of the ridge (top right), a late-formed thrust exploited the shallow-dipping strata and displaced sandstone of the Dinosaur Canyon Member over itself to form a conspicuous truncation (Figure 3 and Figure 18). We refer to the late formed thrust that duplicates the Dinosaur Canyon Member as the Murie Creek thrust* (see "Late contraction faults"). Along the topographic ridge on the north side of Spring Creek, the primary indication of the Taylor Creek Thrust system is that the Springdale Sandstone is nearly double its normal stratigraphic thickness, suggesting at least one thrust flat is confined within the unit (Figure 3). Late thrusting of the Dinosaur Canyon Member over the Springdale Sandstone Member by the Murie Creek thrust can be traced northward just past Kanarra Creek.

Table 3. Fault plane solutions for selected thrusts in the Kanarra fold-thrust system.

Location, Fault Name	Local Bedding	Unrotated	Rotated	Fault Plane (S,D,R*)
Camp Creek, TCT	(041, 38)	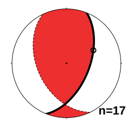	NA	(022, 25, 122)
Spring Creek, TCT	(185, 60)	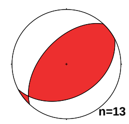	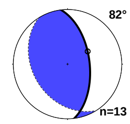	(353, 57, 105)
Kanarra Creek, TCT	(206, 42)	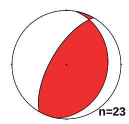	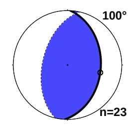	(003, 39, 82)
Kanarra Creek, MCT**	(213, 81)	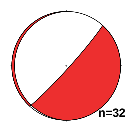	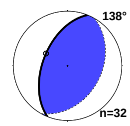	(202, 53, 85)
Kanarra Creek, SCT	(211, 57)	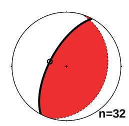	NA	(208, 64, 95)
Kanarra Creek, KCT***	(211, 57)	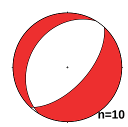	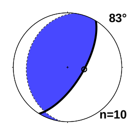	(208, 64, 95)
Short Creek, TCT	(235, 67)	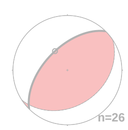	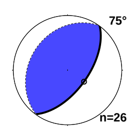	(036, 60, 91)
Short Creek, TCT****	(235, 67)	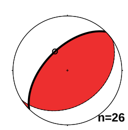	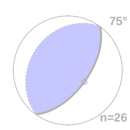	(225, 56, 83)
Murie Creek, TCT	(236, 65)	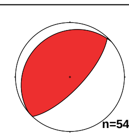	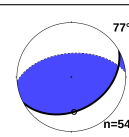	(064, 39, 71)

* Rotated to the inclination at Camp Creek (38°)

** MCT fold-thrust slickensides, see Figure 27 and accompanying text

*** May be related to movement on the folded Kanarra Creek thrust

**** Both sets are the same data, emphasis on early (top) and late (bottom) orientations.

In Spring Creek, shear fractures are best preserved on the southern ridge of Springdale Sandstone, where the thrust begins to ramp up section. The unrotated fault plane solution is presented in Figure 4. To compare to Camp Creek, the data were rotated 82°clockwise along a bearing of 185°so that the bedding inclination in the footwall (185, 60) coincides with the footwall at Camp Creek (38°). Upon this rotation, the fault plane solution (Figure 4, Table 3) yields a pre-overturning fault orientation of (353, 57)—a close match with the fault exposure in Camp Creek both in dip and angle to bedding.

At Kanarra Creek, outcrop patterns and slickensides indicate the Taylor Creek thrust continues within the Springdale Sandstone Member. Slickensided outcrops are exposed along the thrust trace. Creep of the rock may introduce more scatter in measurements along this steep ridge, but data collected along the thrust trace produce thrust-sense fault plane solutions (Figure 4, Table 3). When data are rotated so that local bedding matches the Taylor Creek thrust footwall at Camp Creek, the fault plane solution indicates a likely thrust at (003, 39)—i.e., a "flat" compared to Camp Creek (Figure 4, and Table 3). This solution also matches the present-day map pattern of an overturned thrust flat within the Springdale Sandstone Member.

North of Kanarra Creek, the outcrop pattern of the Springdale Sandstone Member changes. Discordantly dipping sets of sandstone ledges in the Springdale, near the head of the canyon north of Kanarra Creek (310036 m E; 415799 m N), indicate minimal, tops-to-the-east reactivation of the Taylor Creek thrust (Figure 4). Additional evidence for reactivation can be seen in the slickenside data collected near Short Creek (Figure 4, and Table 3). The rotated fault plane solution produces a thrust at (036, 60), and outcropping Riedel shear zones (Figure 19) show shear sense matching an overturned thrust. Yet, the fault plane solution for unrotated (present-day) data includes a potential fault which closely matches the local orientation of the thrust trace at (225, 56). Based on the outcrop pattern further south, this cannot be discounted. We show the potential for reactivation along this

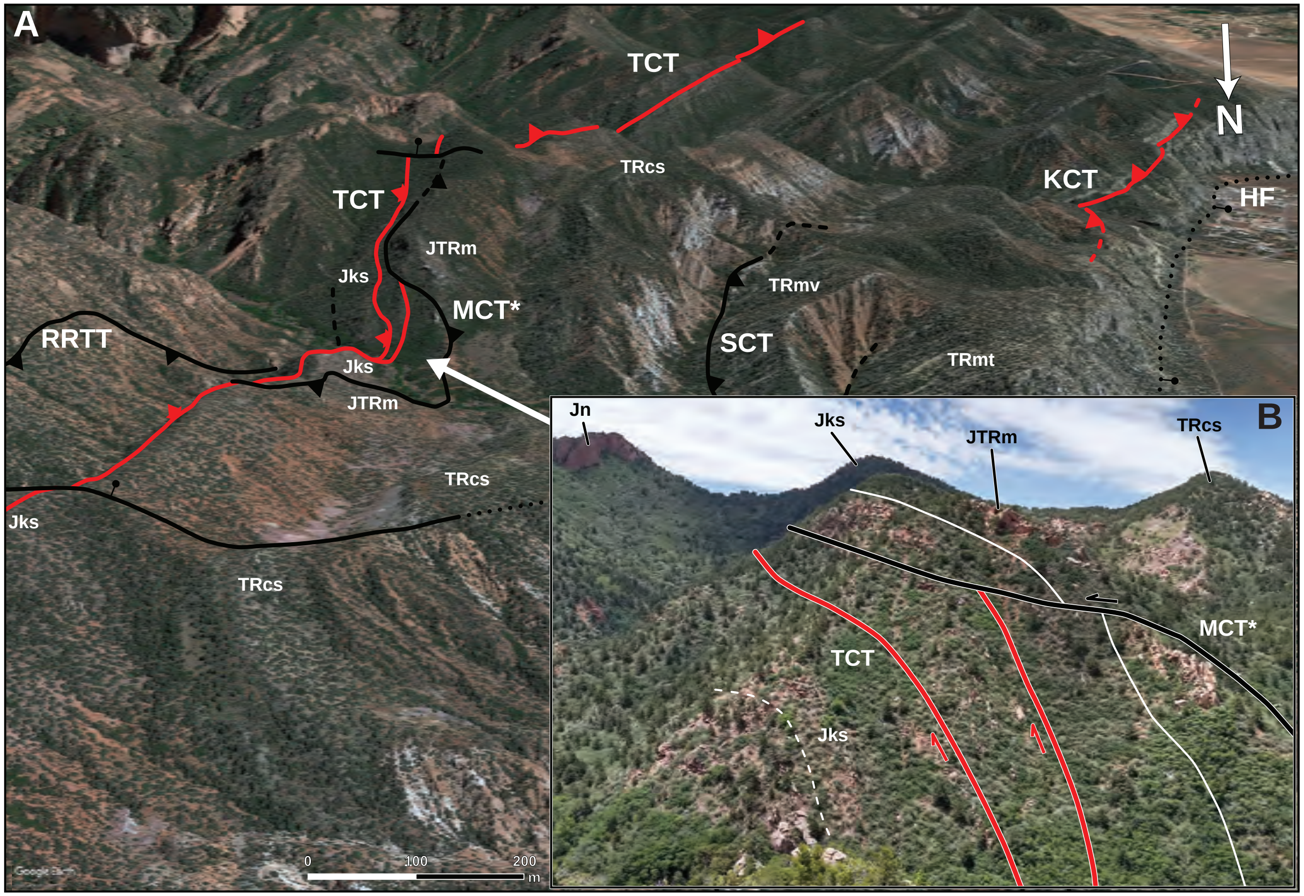

Figure 18. The Taylor Creek thrust at Spring Creek. A) Google Earth 3D terrain view south into Spring Creek. B) Closeup of the southern Springdale ridge and the Taylor Creek thrust duplications. At the bottom of the ridge, above the second duplication, strata are gently overturned, while adjacent (footwall) strata are steeply overturned, consistent with an early formed, overturned thrust ramp.

part of the thrust trace with a slightly different style of the thrust fault barbs (Figure 20. In addition, the barb style and side of the thrust are switched to indicate the location where the thrust appears to have begun limited, east-directed, movement (Figure 3, Figure 4).

At Murie Creek, isolated slickensided outcrops indicate the Taylor Creek thrust trace is exposed near the top of the southern and middle ridges of Springdale Sandstone (311667 m E, 4159286 m N; Figure 4, Table 3. Attenuation of intervening siltstones between duplicated Springdale Sandstone ledges, and a zone of well-indurated, altered siltstone between the Springdale ledges, mark the trace of the thrust (figure 20, inset). Rotation of the shear fracture data (for comparison) produces a thrust fault plane solution (062, 39), closely resembling the result at Kanarra Creek. The unrotated (present-day) data does not produce a viable thrust for either potential fault plane. This result indicates that if the Taylor Creek thrust was reactivated, only a ~1.8 km segment between Kanarra Creek and Short Creek underwent renewed, eastward movement. We trace the Taylor Creek thrust past the northern fork of Murie Creek, where it is truncated by the Murie Creek normal fault (Figure 4).

5.2.3. Hicks Creek Thrust. The thin, competent Shinarump Conglomerate Member of the Triassic Chinle Formation hosts a flank-thrust with the same style and vergence as the previous two faults, the Hicks Creek thrust (*c.f.*, Averitt (1962), the "Hicks Creek fault"). Here, the Hicks Creek thrust is less significant and its trace semi-continuous (Figure 3 and Figure 4). Averitt (1962) mapped this thrust as a normal fault at Hicks Creek in the Cedar Mountain quadrangle, but its observed style in adjacent quadrangles to the north and south (Averitt (1967); Biek (2007a); Biek and Hayden (2016); Knudsen (2014a), this paper) negates this interpretation. Similar, west-directed flank thrusts cut through the Upper Red Member and Chinle Formation at Kolob Canyons (Figure **??**).

The Hicks Creek thrust is well exposed at Kanarra Creek (Figure 21). Here, it forms a conspicuous duplication of the Shinarump Conglomerate Member. The overturned flank thrust, previously interpreted as an upright, east-directed reverse fault (**?**), hosts a ~500 meter

Figure 19. Taylor Creek thrust slickensides at Short and Murie Creek. A) Riedel shear zone defined by deformation bands in the Springdale Sandstone on the Taylor Creek thrust trace. B) Shear fracture face north of A) with R shear fracture steps that indicate the missing block moved upwards (see inset, R fracture illustration from Petit (1987); **?**. C) Dylan Webb on the outcrop measuring local bedding and shear fractures (inset). D) Example of an outcrop-scale overturned thrust with tops-to-the-east motion.

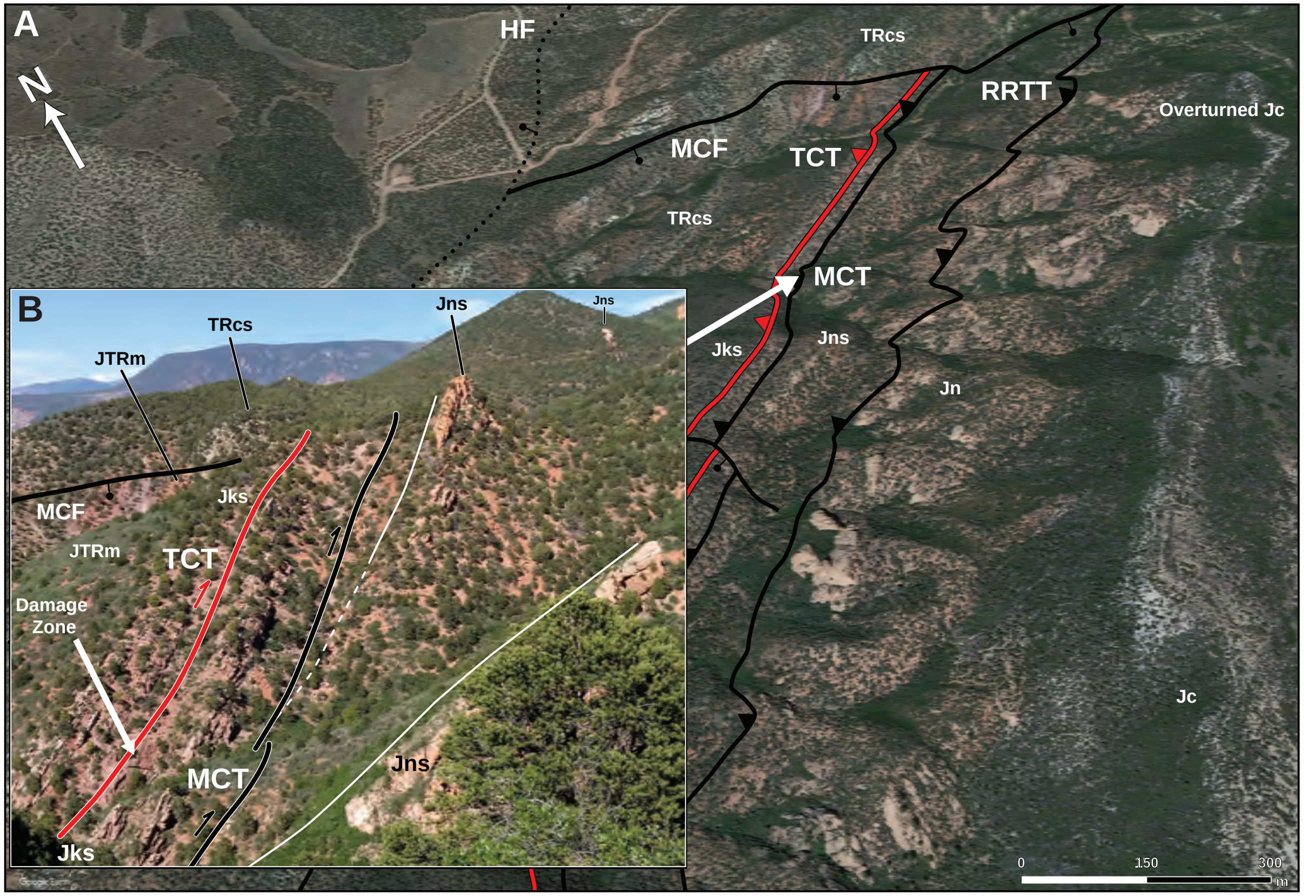

Figure 20. The Taylor Creek thrust at Short and Murie Creek. A) Google Earth 3D terrain view of the overturned Kanarra fold limb, looking northwest into Short Creek and Murie Creek. B) The Taylor Creek thrust seen looking north along strike from the Short Creek saddle into Murie Creek. A double sandstone ledge with minor siltstone interbeds marks the duplication, with a damage zone of altered rock between. Adjacent the ridge, strata are cut by the late-formed Murie Creek thrust.

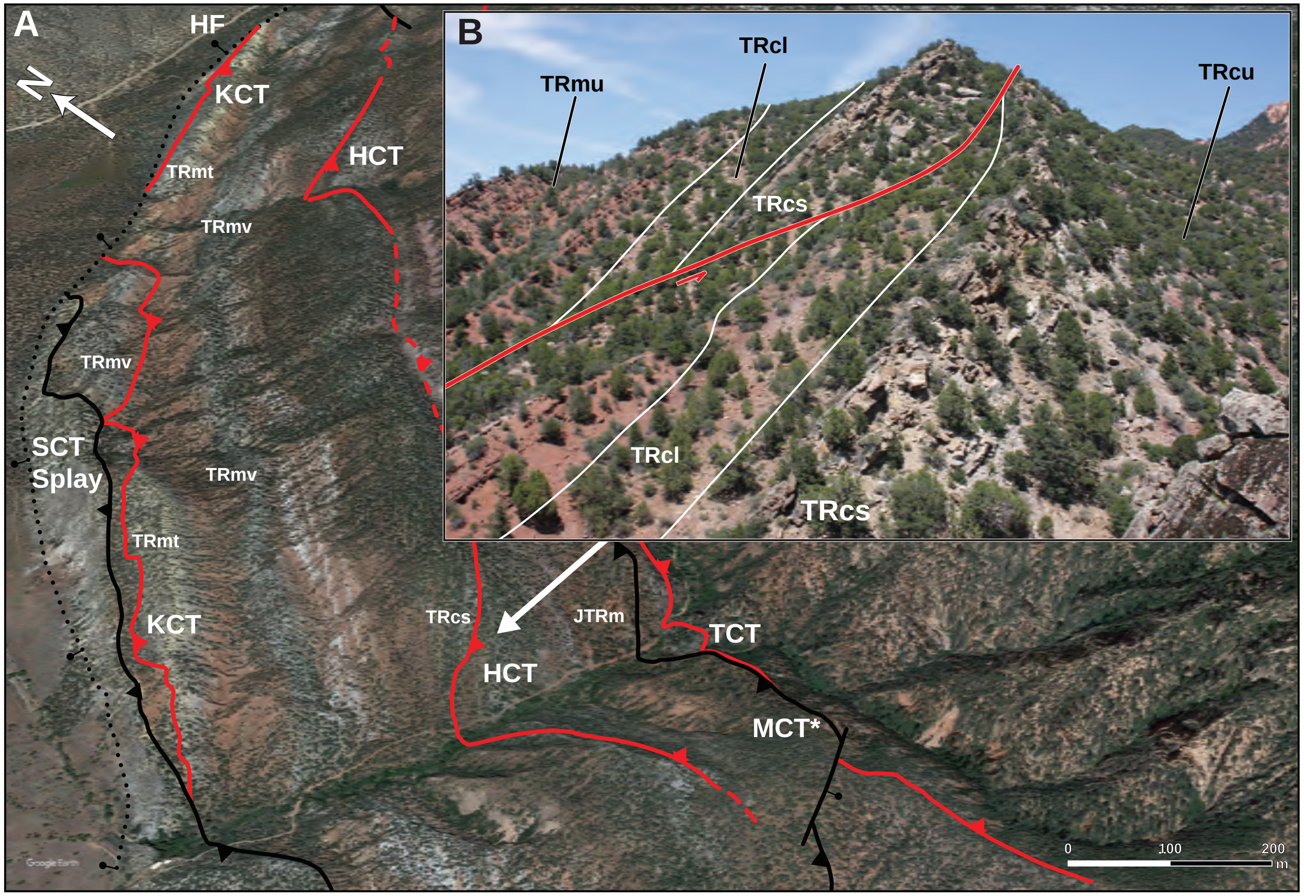

Figure 21. The Hicks Creek thrust at Kanarra Creek. A) Google Earth 3D terrain view looking northeast into Kanarra Creek. The Hicks Creek thrust Vs gently west into the creek in the foreground and displaces the Shinarump Conglomerate Member, Lower Chinle Member, and part of the Upper Red Member. B) Along-strike view of the Hicks Creek thrust duplication, from the hangingwall on the southern side of Kanarra Creek.

long duplication of the Shinarump Conglomerate and crosses the creek near (308496 m E; 4156677 m N). The lower detachment of the thrust is within the Lower Member of the Chinle Formation, and the upper detachment is in the Petrified Forest Member. The trace of the Hicks Creek thrust dies out south of Hicks Creek. A near-identical duplication is exposed in the canyon north of Kanarra Creek, and we trace the Hicks Creek thrust from here into Short Creek where it truncates against a small cross fault. It is likely the thrust soles into a higher detachment layer in the Petrified Forrest Member; this was not mappable in the field, so we query the trace of the thrust between these two Shinarump Conglomerate Member duplications. The Hicks Creek thrust becomes a major fault north of Murie Creek and at the Red Hill. Along its northern trace, the thrust cuts deeper down section, soling into a lower detachment in the Shnabkaib Member.

5.3. LATE CONTRACTION FAULTS

Late contraction thrust faults associated with formation of the Kanarra fold-thrust system are east-verging and cut across bedding. Many of these faults are kilometer-scale features (Figure 3, Figure 4). A lack of piercing points precludes determining their slip, but minimal displacement can be estimated in cross section by measuring the fault trace orientation and the magnitude of displacement consistent with the map pattern. These displacements can be tens to hundreds of meters; at Kanarra Creek, smaller thrusts displace strata up to 80 meters along their length, while larger thrusts have minimum displacements of up to 300 meters. The late thrusts commonly tectonically thin, fold, and/or truncate less competent stratigraphic units (e.g., red beds of the Moenkopi Formation). Tectonic thinning of stratigraphic layers reflects ductile flow and/or truncation along the hanging wall. The trace of late thrust faults tends to parallel the strike of bedding. Thrust fault inclinations are discordant to bedding and can achieve steep orientations, particularly when cutting through mechanically stiff layers to form "ramps" (e.g., the Navajo Sandstone). Where these faults are well-exposed and cut through competent strata, they are associated with cataclastic breccia zones several meters to tens of meters wide with varying degrees of induration. These late contraction thrusts and their connecting splays are best observed within the creek valleys that erode across the strike of the limb of the leading anticline (Figure 3, Figure 4).

5.3.1. Spring Creek Thrust System. The trace of the Spring Creek thrust is well exposed along the northern side of Spring Creek, east of the hinge zone, along the overturned limb of the leading anticline. The fault trace begins just south of Spring Creek and continues northwards for several kilometers (Figure 4, Figure 22. Its tortuous map pattern consists of several thrust *splays* which branch and curve through Moenkopi strata. Like the Taylor Creek thrust, the Spring Creek thrust is a thrust system; this thrust system adds significant structural complexity to the overturned section along the Kanarra fold (Figure 3,Figure 4, and Figure 10. We identify the "*main*" trace of the Spring Creek thrust system as the easternmost continuous thrust within the system of splays. At the surface, the main trace commonly cuts across the eastern fold limb from the Virgin Member into the Shnabkaib Member (Figure 3, Figure 12).

The *primary splay* of the Spring Creek thrust system is exposed just east of the mouth of Spring Creek, where the Timpoweap Member is thrust eastward over the Lower Red Member (Figure 3, Figure 4, and Figure 22A). The primary splay continues to the north where the Timpoweap Member is overturned, and here subsidiary splays of the Spring Creek thrust system displace the Virgin Member. These splays form a complex zone of faulting that has been dissected by the Hurricane fault, leaving discontinuous remnants of the Spring Creek thrust system along the hinge of the leading anticline of the Kanarra fold (Figure 3, Figure 4, Figure 12A,C).

The primary splay of the Spring Creek thrust system reemerges at Kanarra Creek and displaces the Fossil Mountain Member and part of the Timpoweap Member over a ridge of Lower Red and Timpoweap in the hanging wall of the Kanarra Creek thrust (Figure 14A, Figure 14B lower left). On the south side of Kanarra Creek, a connecting splay branches from the main trace of the Spring Creek thrust system (Figure 14A, lower left), accommodating displacement of the Virgin Member over the Lower Red Member that had been previously duplicated by the Kanarra Creek thrust. This connecting splay merges with the primary splay of the Spring Creek thrust on the north side of Kanarra creek (Figure 3, Figure 4). A smaller thrust splay displaces the Timpoweap Member onto the Virgin Member ridge on the south side of Kanarra Creek. Here, along the trail from the parking area (307994 m E; 4156823 m N) leading to the creek mouth, yellow limestone, shale, and tan, sand-rich limestone crops out discordantly against the Virgin Member. Yellow Timpoweap shale beds on the side of the path are contorted into meter-scale, complex folds. Steep eastward dips on the Timpoweap Member above the trail indicate folding along an east-directed thrust (Figure 3, Figure 4). Near the Timpoweap-Virgin juxtaposition, mass wasting of the Virgin Member obscures the exact location of the thrust splay and presumably the Lower Red Member along the western side of the ridge. Along this ridge, a minor normal fault associated with the Hurricane fault zone cuts obliquely across strike and truncates these Spring Creek thrust splays.

The primary splay of the Spring Creek thrust system continues northward from Kanarra Creek along the west side of the topographic ridge held up by the duplicated Timpoweap Member (Figure 3, Figure 4, Figure 15A). Near the end of the ridge, the primary splay ramps down section, exposing more of the Timpoweap Member in the hanging wall than seen at Kanarra Creek. The primary splay also truncates part of the overturned Kanarra Creek thrust and cuts out most of the Lower Red Member (Figure 3, Figure 15C). From this location, the primary splay continues along strike to the north where it is truncated by the Hurricane fault (309191 m E; 4158719 m N).

The trace of the main Spring Creek thrust first appears south of Spring Creek to the east of the primary splay (Figure 3, Figure 4, Figure 22, see also Figure 12). It cuts through the hinge zone of the leading anticline on the eastern side of a gently folded ridge of the Virgin Member, at the upright-to-overturned transition on the eastern limb of the fold (307342 m E; 4154074 m N). The thrust thins the Middle Red Member and truncates

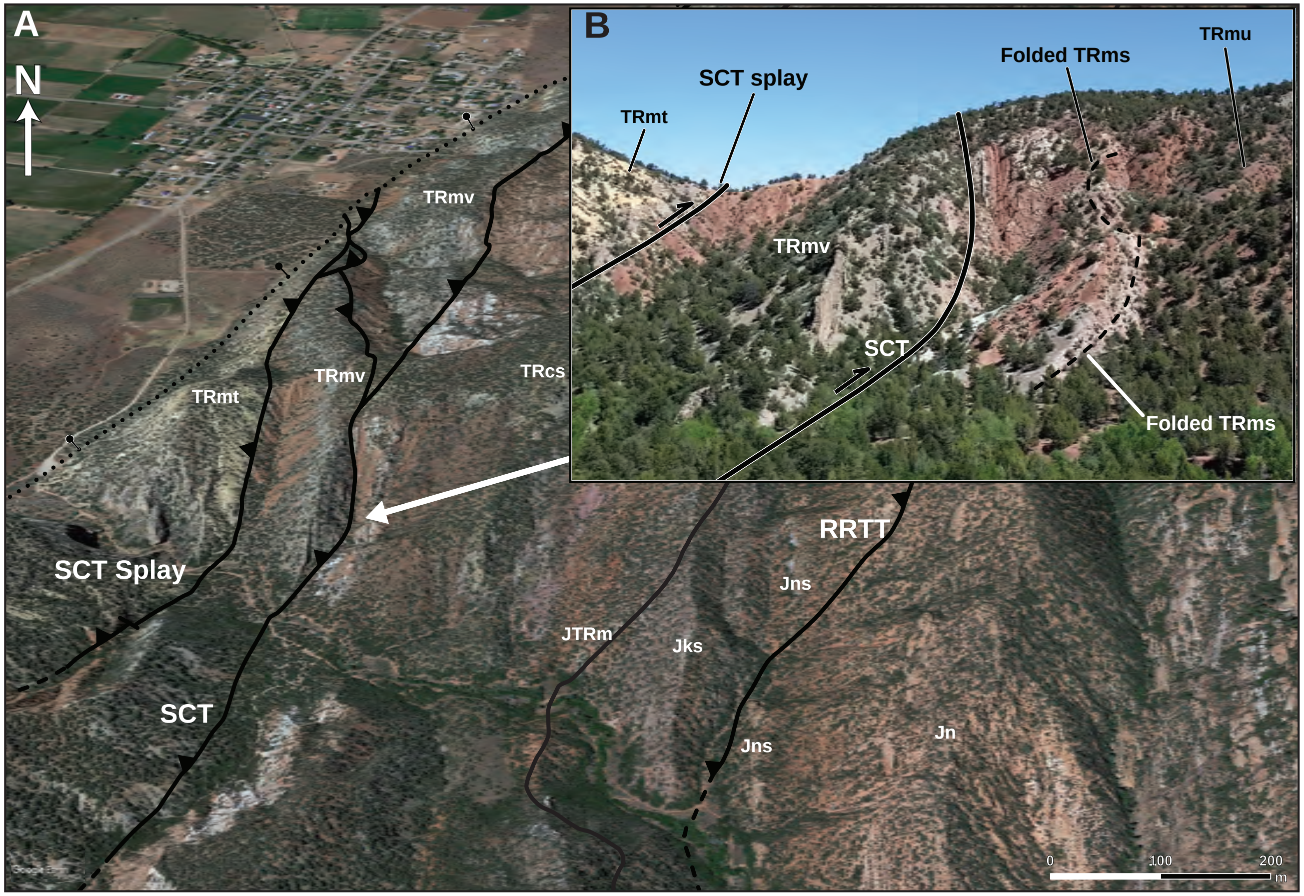

Figure 22. The Spring Creek thrust at Spring Creek. A) Google Earth 3D terrain view looking northeast into Spring Creek. To the west, the primary splay cuts the Timpoweap Member and displaces it over the Lower Red and Virgin Members. B) Closeup of the Spring Creek thrust main trace deformation zone. Displacement is accompanied by folding, as seen in the trace of a folded Shnabkaib Member gypsum layer (black dashed line).

the lower double-layer of gypsum. A few tens of meters north of the truncation, the fault is marked by a calcite-encrusted, well-indurated fault megabreccia (cataclasite), which hosts cobble- to boulder-sized clasts of slickensided and folded Virgin Member limestone (Figure 23). The trace of the main Spring Creek thrust fault can be followed along strike to the north, where west-dipping, overturned Middle Red gypsum layers crop out and the trace of the thrust is within the Middle Red Member. On the north side of Spring Creek, a prominent wall of vertical Virgin Member fins crops out in the hanging wall of this thrust—these fins were transported east and over the Middle Red Member (Figure 3, Figure 4, Figure 22).

From Spring Creek, the trace of the main Spring Creek thrust continues northward towards Kanarra Creek, juxtaposing steep overturned beds of the Virgin Member onto the Shnabkaib Member. Here, the hanging wall of the main Spring Creek thrust includes a kilometer-long, nearly-recumbent, overturned fold in the Virgin Member (Figure 12B). This fold may be part of the hinge zone of the leading anticline that was displaced east on the thrust. The folded Virgin Member forms a low ridge, with shallow west-dipping strata (~10– to 25°W) on its western side and steeper, overturned (~45– to 55°W) strata on its eastern side. On the eastern side of the ridge, the trace of the main Spring Creek thrust system displaces overturned Virgin Member beds and the Middle Red double gypsum layer over the Middle Red Member (307924 m E; 4156400 m N).

At Kanarra Creek, the main Spring Creek thrust cuts out the majority of the Middle Red Member in the same structural style seen at Spring Creek (Figure 24). Here, the thrust cuts shallow-dipping (~45– to 50°), duplicated Virgin Member in the Kanarra Creek thrust hangingwall. Near the creek bed, slickenside measurements on the Virgin Member indicate two populations of shear fractures—a set of "normal"-sense slickensides which mostly form low angles to bedding, and a set of thrust-sense slickensides, also at low angles to bedding (Figure 4, Table **??**{{tab3, Figure 25B,D). Both populations include strike-slip shear fractures with minor normal-sense and thrust-sense displacement, indicated by their

Figure 23. Spring Creek thrust megabreccia at Spring Creek. A) Kink fold on outcrop of brecciated limestone in the Virgin Member along the Spring Creek thrust. Hammer beneath Dylan Webb is placed parallel to the fold axis. B) Flaggy breccia clasts (examples outlined in white), variably slickensided and oriented. C) Cobble-sized, slickensided clasts (white arrow) within a recrystallized calcite matrix. D) Botyroidal calcite-encrusted outcrop containing several boulder-sized, angular clasts, some slickensided (arrows).

slickenline rakes (Figure 25B inset, Figure 25C). Rotation of the normal sense shear fracture data to where bedding dips 38°E (analogous to an “earlier” stage of folding at Camp Creek) yields a fault plane solution with a west-directed thrust at 27°to bedding Figure 4, Table 3. Once restored, the “normal-sense” shear fractures are consistent with movement along the early Kanarra Creek thrust which was later folded and overprinted. Fault plane solutions from the thrust-sense shear fracture population indicate a steep, east-directed thrust which matches the local orientation of the main trace of the Spring Creek thrust (208, 64—see Figure 4, Table 3). The Spring Creek thrust shallows to the north to (209, 45), where it exploits the shallow bedding on the duplicated Virgin Member.

North of Kanarra Creek, the main Spring Creek thrust ramps up section and places the Virgin Member over the Shnabkaib Member (Figure 26). This juxtaposition of the Virgin Member against the Shnabkaib Member continues another 3.5 km from Kanarra Creek into Short Creek. Only the main thrust trace is present within Short creek, again placing the Virgin Member against the Shnabkaib Member (Figure 3, Figure 4, Figure 6). The thrust trace veers westwards as it ramps down section from the Shnabkaib Member to the Lower Red Member. As the thrust truncates the Virgin Member, it veers northward into sub-parallelism with the strike of bedding (310690 m E, 4159590 m N). Within Murie Creek, displacement along the main Spring Creek thrust completely cuts out the Lower Red Member, placing the Timpoweap Member against the Virgin Member. Just to the north of the creek mouth, the thrust is truncated by the Hurricane fault (311370 m E, 4159990 m N).

5.3.2. Murie Creek Thrust System. East of Spring Creek, several late, east-directed thrusts are exposed in the Jurassic section near the syncline axis of the Kanarra fold-thrust system. We group the first two of these thrusts together as the Murie Creek thrust system. The main Murie Creek thrust is a longer, continuous thrust that crops out near Kanarra Creek (308910 m E; 4156517 m N) within the Kayenta Formation and can be traced for five kilometers to the north. Displacement along this thrust is revealed by folding and truncation of Kayenta strata at the upper contact of the Springdale Sandstone Member

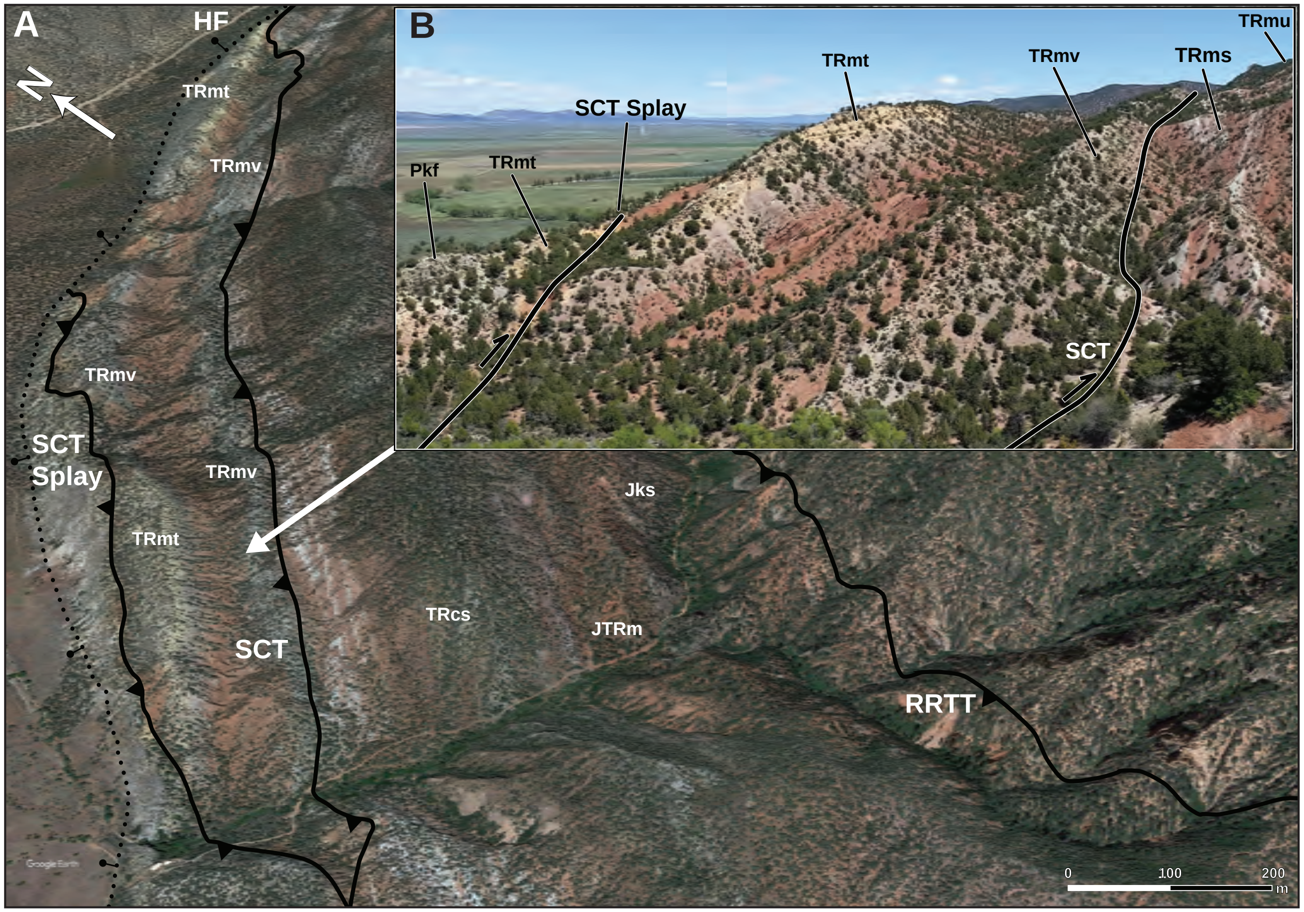

Figure 24. The Spring Creek thrust at Kanarra Creek. A) Google Earth 3D terrain view looking northeast into Kanarra Creek. To the west, the Spring Creek thrust primary splay displaces Permian-Triassic strata over the Lower Red Member. B) Along-strike view to the north of the Spring Creek thrust main trace and Spring Creek thrust primary splay. The Timpoweap and Virgin Members are displaced over younger Moenkopi strata. To the west, Lower Red Member adjacent the Timpoweap indicates the Kanarra Creek thrust trace.

Figure 25. Spring Creek thrust slickensides at Kanarra Creek. A) Slickensided outcrop of the Virgin Member. Examples marked by white arrows, slip direction by black arrows. Inset from Allmendinger et al. (1989), modified from Petit (1987). View northeast, Daniel Quick for scale. B) Thrust-sense shear fracture. White arrow points to inset, with tops-to-the-east motion. C) Slickensided outcrop near the fault, north of Kanarra Creek. D) View west onto slickenside northeast of (A); stereonet: bedding black, shear fracture red.

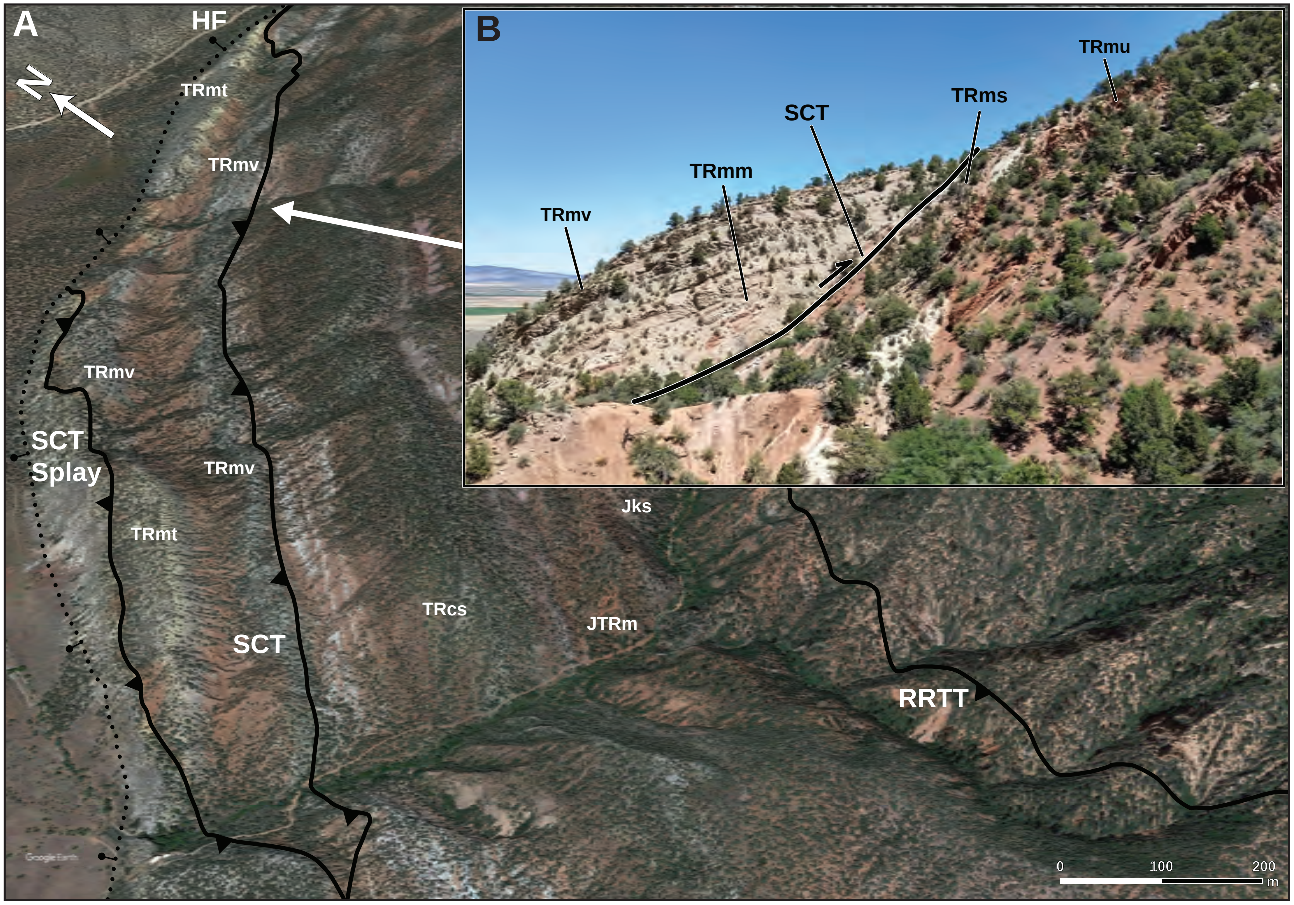

Figure 26. Spring Creek thrust north of Kanarra Creek. A) Google Earth 3D terrain view looking northeast into Kanarra Creek. B) The Spring Creek thrust main trace seen looking north within an unnamed stream cut just north of Kanarra Creek. Te structural pattern of the Virgin Member being displaced over and truncating the Shnabkaib Member is continued here. A sliver of the Middle Red Member containing a thick, double layer of gypsum persists all along the Spring Creek thrust hangingwall.

in Kanarra Creek. The shorter, discontinuous thrust is in the Dinosaur Canyon Member of the Moenave Formation. We show it as an independent thrust rather than a splay of the main Murie Creek thrust (Figure 4; see also Figure 18 and Figure 22). For clarity, we refer to this discontinuous thrust as the Murie Creek thrust*.

The Murie Creek thrust* crops out south of Spring Creek where it displaces the Dinosaur Canyon Member over the Springdale Sandstone (307900 m E, 4154070 m N). The thrust is well exposed where Spring Creek erodes through the topographic ridge underlain by sandstones of the Springdale Sandstone Member. Looking south along this ridge, a thick, persistent sandstone ledge in the Dinosaur Canyon Member forms a prominent "T" discordance where it is folded and displaced over itself along the thrust plane (Figure 3, Figure 4, Figure 18. Bedding above the thrust is overturned and shallow-dipping (~30°), whereas bedding beneath the thrust is steeply overturned (~65– to 70°). Looking north of Spring Creek along the continuation of this topographic ridge, the structural pattern is repeated but partially obscured by mass wasting and vegetation (see Figure 28B later in this section). High on the topographic ridge, the thrust visibly displaces the lower Springdale Sandstone Member contact before petering out. Further north towards Kanarra Creek, the Murie Creek thrust* recurs for a short distance where it again thrusts the Dinosaur Canyon Member over the Springdale Sandstone Member (Figure 4, Figure 21A, lower right). Truncation of the Petrified Forest Member of the Chinle Formation indicates the thrust may initiate further down section, but the contact is complicated by mass wasting and by a late cross fault (308220 m E; 4155780 m N). North of Kanarra Creek, fractured Dinosaur Canyon Member and discordance with Springdale Sandstone bedding at the contact indicate the presence of the Murie Creek thrust*, but displacement is visibly diminished and the thrust peters out (308940 m E, 4156670 m N).

The trace of the main Murie Creek thrust initiates just south of Kanarra Creek where the the main body of the Kayenta Formation is dramatically thinned by the fault (Figure 3, Figure 4; 308730 m E, 4156050 m N). The main thrust crops out along the

Kanarra Creek Falls trail, where the creek has eroded through the topographic ridge formed by the Dinosaur Canyon and Spring Creek Sandstone Members. The thrust is marked where overturned sandstones of the Springdale Sandstone Member define an east-verging fold in the hanging wall of the thrust (Figure 27. The fold is a composite fold-thrust structure. We interpret faults in the nose and on the front limb of this fold as small, older, east-directed thrusts which were subsequently folded. These faults are well exposed along the trail on the north side of the creek where slickensides show normal separation, but rotation of the steep west-dipping (~81°W) bedding back to the local average orientation along the ridge (~45°W) shows a pre-folding thrust sense of motion with an average dip ~10°greater than bedding (Figure 4, Table 3). To the north, the Kayenta Formation thins dramatically as the main Murie Creek thrust fault continues along the Springdale Sandstone Member-Kayenta Formation contact north towards Short Creek (Figure 3, Figure 4,see also Figure 31 later in this section). Estimates of thinning of this unit, based on published thicknesses for the area (e.g., Biek and Hayden, 2016) as well as our thickness measurements, indicate a 63% reduction from a 120 meters to 46 meters along the main body of the Kayenta Formation. We interpret the reduced thickness is a result of movement along the Murie Creek thrust, and east-directed thrusting of the Springdale Sandstone Member over the Kayenta Formation. The main trace of the Murie Creek thrust can be followed north to Murie Creek where the thrust is truncated by the Murie Creek normal fault, along with the rest of the fold limb (Figure 3, Figure 4, Figure 32 later in this section).

5.3.3. Red Rock Trail Thrust. The Red Rock Trail thrust is the easternmost thrust along the Kanarra fold-thrust system. It can be mapped from Spring Creek to the Red Hill in Cedar City (Figure 2) and crops out in Parowan Gap as well (see discussion below). It begins within the Kayenta Formation near the Springdale Sandstone Member–Kayenta Formation contact in Spring Creek and cuts up section through the Navajo Sandstone, forming a persistent, poorly consolidated cataclasite zone at the Kayenta–Navajo contact (Figure 3, Figure 4, Figure 28). Here, a resistant lens of the Shurtz Tongue of the Navajo

Figure 27. Murie Creek thrust fold-thrust at Kanarra Creek. A) Fold-thrust structure in the Springdale Sandstone on the Murie Creek thrust hangingwall, tops-to-the-east motion. Folded thrusts with tops-to-the-east motion in solid red. B) Outcrop of the fold limb where it is exposed on the trail at the north side of Kanarra Creek. C) P fractures along the fold limb outcrop in (B). D) Slickensided shear fracture surface with well-developed, lunate R fractures (see illustration Allmendinger et al. (1989), modified from Petit (1987).

crops out from the creek bed, striking obliquely to adjacent strata. This lens is truncated and offset 150 meters to the north along the southernmost expression of the Red Rock Trail thrust as it ramps up section. The cliffs near the contact are mantled with talus of pervasively slickensided clasts derived from the fault damage zone. The cataclasite zone is well exposed and readily accessible on the Red Rock Trail (308700 m E; 4155320 m N). The fault damage zone associated with the Red Rock Trail thrust is mapped as a cataclasite (i.e., Jnc) derived from the Navajo Sandstone (Figure 3, Figure 4). As with other thrusts along the Kanarra fold, the Red Rock Trail thrust is more likely a thrust fault system, but individual thrusts within the cataclasite are difficult to trace. Within the central section of the Kanarra fold-thrust system, the Red Rock Trail thrust forms the contact between the Kayenta Formation and the cataclasite developed in the Navajo Sandstone.

North of Spring Creek, talus aprons of cataclasite appear on the Kayenta-Navajo cliff face, indicating the presence of the Red Rock Trail thrust damage zone. Direct accessibility is poor due to the steepness of the cliff. The Red Rock Trail thrust crops out along the Red Rock Trail, and it is here that a damage zone consisting of a semi-coherent megabreccia—outcrop-sized clasts of faulted Navajo surrounded by a matrix of smaller clasts—is well exposed (Figure 29). At the fault contact with the Kayenta, planar-bedded, steeply overturned sandstone of the Navajo Formation are pervasively slickensided and host sets of deformation bands. Further east into the damage zone, remnant steep, upright bedding indicates fault-related discordance with overturned Navajo Formation in the hanging wall of the thrust. Approximately 100 meters east along the Red Rock trail and further into the Navajo, the megabreccia gives way to intact rock.

At Kanarra Creek, near the entrance to the Kanarra Falls slot canyon, the trace of the Red Rock Trail thrust is marked by strong discordance in bedding dips between channel sands in the Kayenta Formation and planar sandstone beds of the Navajo Sandstone. This discordance reflects folding of the Kayenta Formation along the thrust (Figure 30). In the foreground of Figure 30, beds of Navajo Sandstone have been rotated to vertical and in

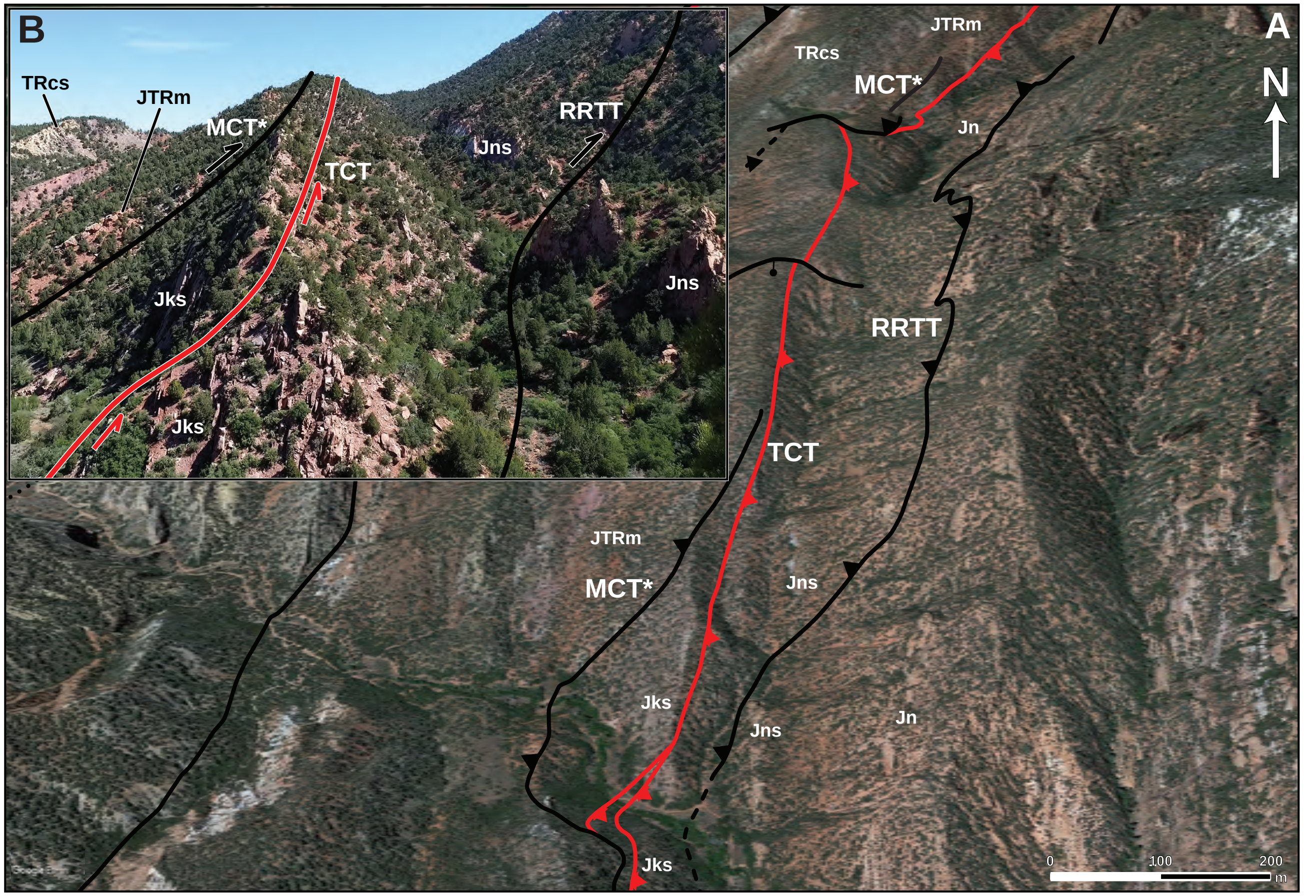

Figure 28. Red Rock Trail thrust at Spring Creek. A) Google Earth 3D terrain view looking north into Spring Creek. The Red Rock trail thrust cuts the Shurtz Tongue of the Navajo as it makes its way up section. B) Field photo of Shurtz Tongue lens displaced by the thrust looking north past Spring Creek along the strike of the Springdale ridge. Also shown is the Murie Creek thrust* (left midground).

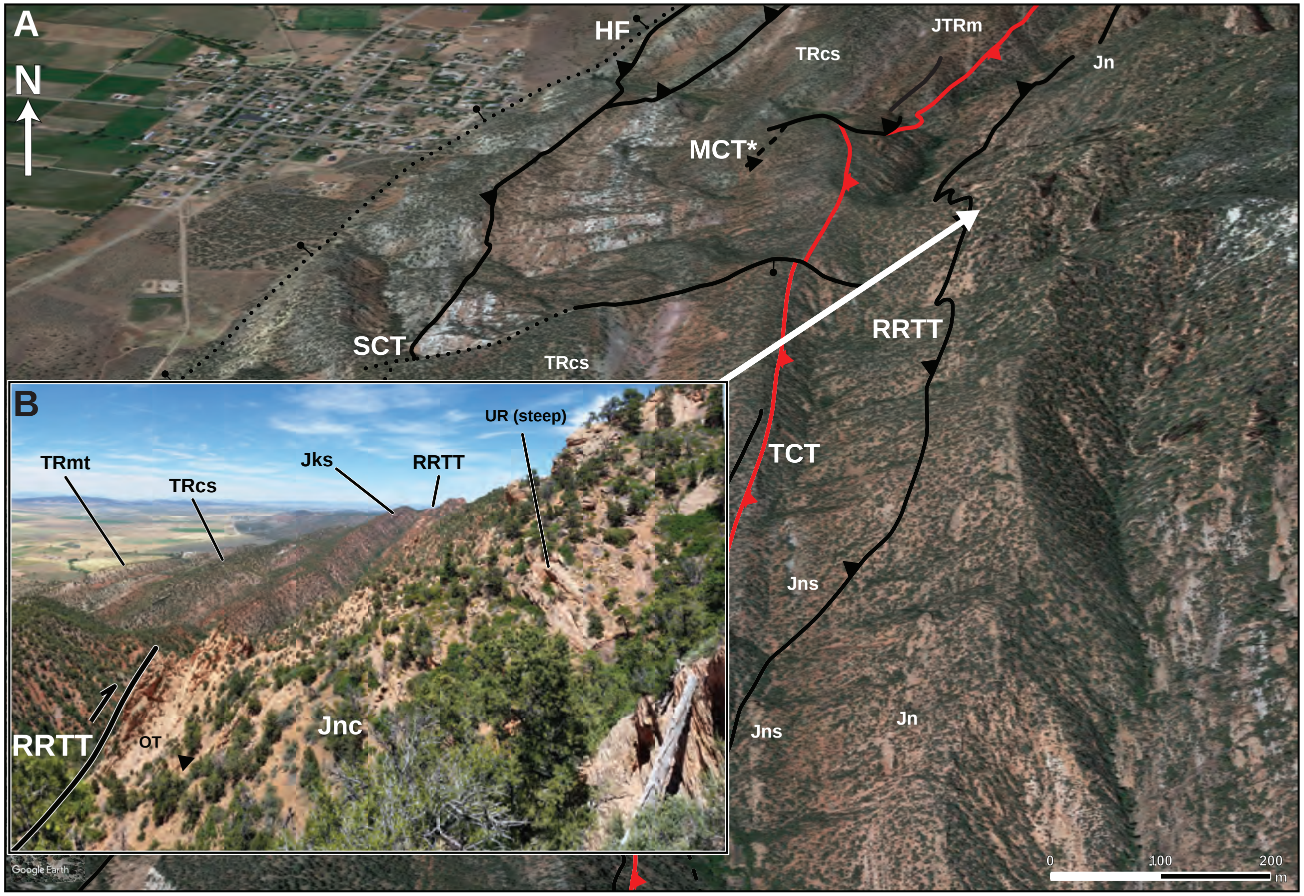

Figure 29. Red Rock Trail thrust at the Red Rock Trail. A) Google Earth 3D terrain view looking north into Spring Creek. B) View of the Red Rock trail thrust, looking northeast while standing on the Red Rock Trail after crossing the thrust contact. Foreground: overturned, west-dipping Navajo sandstone beds are thrust over steep, upright, east-dipping beds. Background: distant saddle labelled "RRTT" is formed by shallow, overturned Shurtz Tongue (see Figure 31).Photo by John P. Hogan.

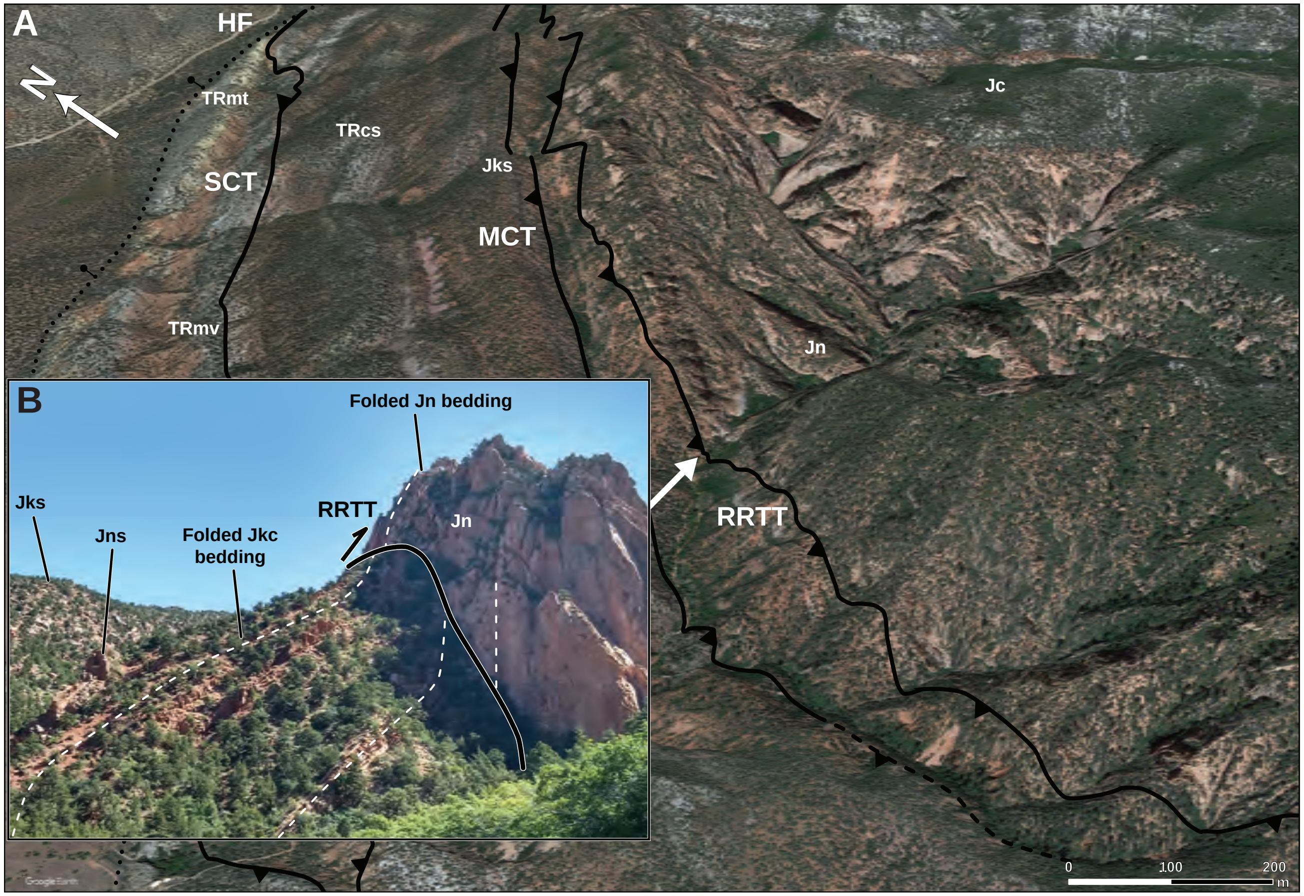

Figure 30. Red Rock Trail thrust at Kanarra Creek. A) Google Earth 3D Terrain view of the Red Rock Trail thrust, looking northeast into Kanarra Creek. Late-formed thrusts (Spring Creek thrust, Murie Creek thrust) shown for reference to the map. B) View looking northeast onto Jurassic units exposed near Kanarra Creek. Folded Kayenta abuts steep, overturned Navajo Sandstone along the Red Rock Trail thrust. Part of this contact may be complicated by the presence of an older, east-dipping thrust (e.g., Averitt (1967).

the canyon to the east they return to upright, gentle eastward dips. To the north of the slot canyon, steeply overturned, folded planar beds of the Navajo Sandstone, seen in the background of figure 31, are in fault contact with significantly thinned, shallow-dipping, overturned strata of the Kayenta Formation. Though the Red Rock Trail thrust appears to dip steeply to the east (i.e., verge west) at Kanarra Creek, the dominant vergence along the thrust is to the east. Here the thrust contact may be complicated by the presence of an older, east-dipping thrust (see Averitt (1967)). However, we associate this earlier interpretation with sinistral, out-of-the-syncline flexural slip and disharmonic folding of thin Kayenta sandstone lenses adjacent to a thick, competent control unit, the Navajo Sandstone—see discussion for further details.

At the saddle by the next canyon to the north (Figure 3, Figure 4; 310000 m E, 4157700 m N) the Cedar City Tongue of the Kayenta is attenuated with a minimum 62% reduction in thickness along the Red Rock Trail thrust (Figure 31B). The thrust contact dips moderately westward (~50°), and overturned beds of the Kayenta Formation are displaced over steeply dipping, overturned Navajo Sandstone. East of the fault contact, the damage zone persists for 200-300 meters into the Navajo Sandstone. Talus of slickensided cataclasite mantle the tops of the cliff (Figure 31B). In this view, the damage zone can be traced from the foreground, through the vegetation, into the background to include steeply dipping, isolated outcrops of Navajo Sandstone. The Red Rock Trail thrust and damage zone continue northward along the cliffs in the Navajo Sandstone. At the flatiron near the head of Murie Creek (311970 m E; 4159330 m N), both the Kayenta Formation and the Navajo Sandstone are overturned and dipping ~45– to 55°to the west along the east verging thrust (Figure 32). Sharp deflection of Carmel strata into steep, overturned orientations (Figure 32A, right, dashed white line in the Carmel) suggests the thrust cuts up section. The high-strain zone is characterized by a great density of fractures, imparting a “shattered” appearance to the

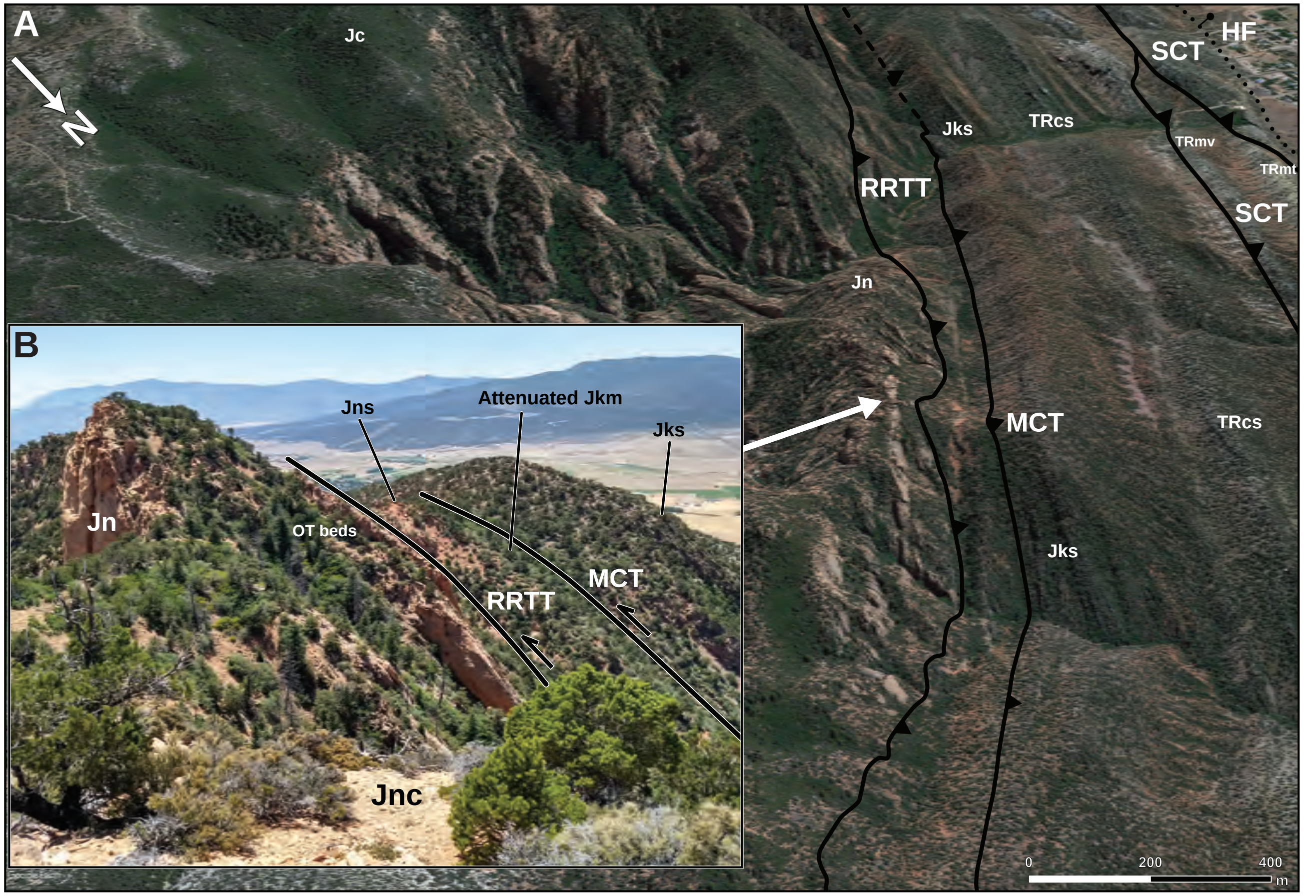

Figure 31. Red Rock Trail thrust at the Kanarra Creek saddle. A) Google Earth 3D terrain view looking southwest into a stream cut north of Kanarra Creek. Here, the Red Rock trail thrust is marked by a wide fault megabreccia zone (Jnc) at the Navajo contact and attenuated Kayenta strata. Likewise, thinned Main Body Kayenta between the Springdale Sandtone and Shurtz Tongue marks the Murie Creek thrust contact in the background. Slickensided talus clasts mantle pervasively fractured but cohesive outcrop in the foreground.

Navajo Sandstone within the cataclasite zone (Figure 32 B). Movement within the cataclasite zone appears to have rotated isolated outcrops of "relict bedding clasts" of Navajo Sandstone to shallow, westward dips (Figure 32B, right midground).

The Red Rock Trail thrust and damage zone continue northwards and abut against the Murie Creek fault (Figure 3, Figure 4, Figure 32; (313000 m E; 4159750 m N). Though Averitt (1962) does not appear to have found the trace of the Red Rock Trail thrust in the Cedar Mountain Quadrangle, we infer its location here through the Navajo Sandstone and link it with the thrust at the Red Hill (Figure 2).

5.4. EXTENSION FAULTS

The Kanarra fold-thrust system is cross-cut by later extension faults. These notably include the Hurricane fault, as well as smaller faults associated with the Basin and Range transition zone (Figure 1 and Figure 2). These smaller faults are largely restricted to the High Plateaus immediately adjacent the Kanarra fold-thrust system. Prominent examples of transition zone faults are the Cougar Mountain, Bear Trap Canyon, and "Lone Tree Mountain" faults ((Averitt, 1962; Biek and Hayden, 2016; Biek et al., 2010; Gregory and Williams, 1947; Knudsen, 2014a). Displacement along the transition zone faults rotates the "regional" dip adjacent the Kanarra fold-thrust system syncline axis, which approaches 6°east in the field area and 3– to 5°west near Cedar City. Other extension faults with ambiguous temporal relationships between Sevier folding and Basin and Range tectonism are "cross faults". Cross faults along the Kanarra fold vary in size from tens of meters to kilometers in length (e.g., the Murie Creek fault). These cross faults, particularly the larger structures, may reflect reactivation of Proterozoic transfer zone faults (i.e., present-day basement lineaments) along the Cordilleran hinge line in Sevier time ((Paulsen and Marshak, 1999; Picha and Gibson, 1985; Quick et al., 2020; Thomas, 2006).

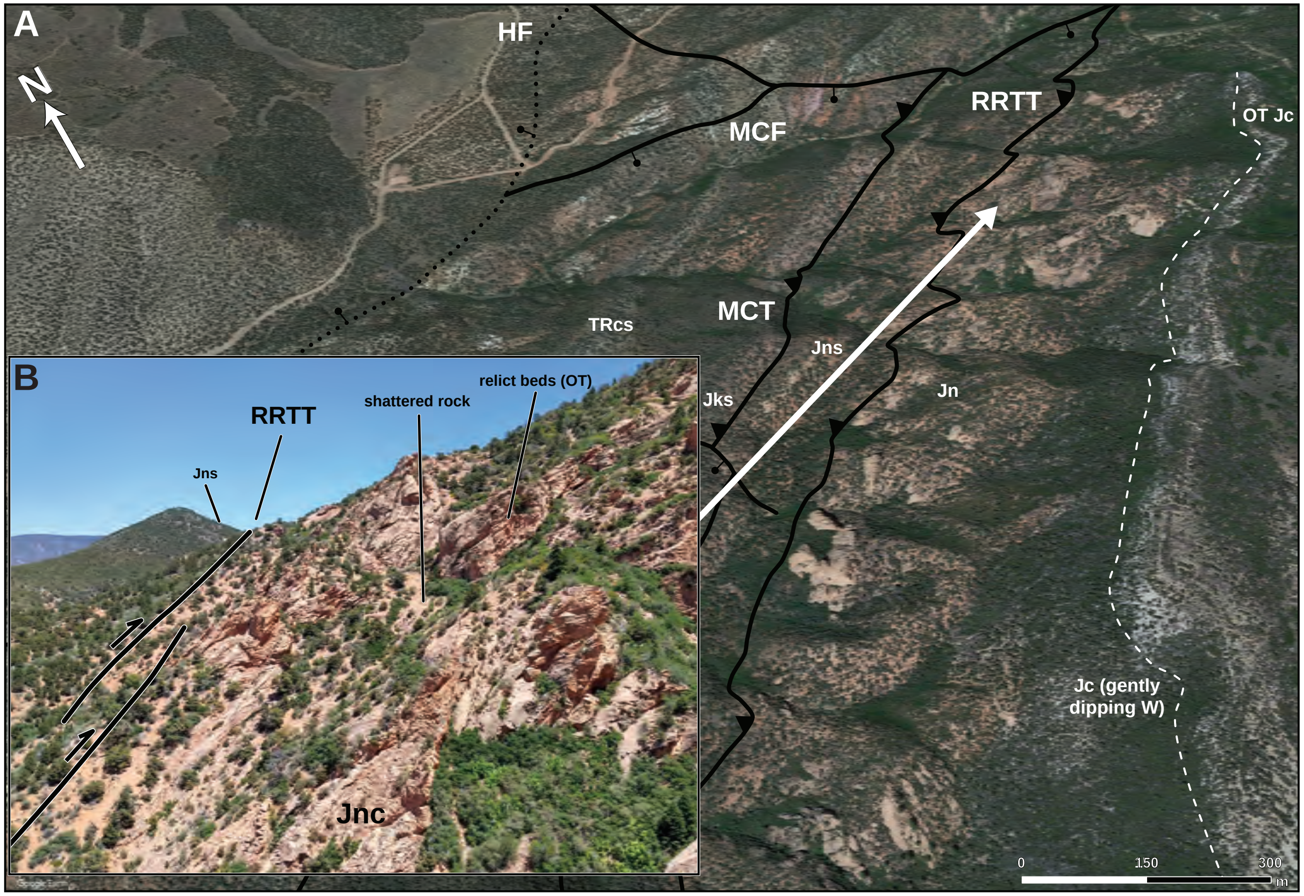

Figure 32. Red Rock Trail thrust at Short and Murie Creek. A) Google Earth 3D terrain view looking north into Short Creek and Murie Creek. Gently east-dipping Carmel steepens and overturns near the fault zone (white dashed line). B) View of the Red Rock Trail thrust contact on the southern fork of Murie Creek. The contact is partially occluded where it Vs westward, down the hillside. Isolated outcrops of pervasively fractured Navajo Sandstone mantled by slickensided talus define a megabreccia shear zone tens of meters wide.

5.4.1. Cross Faults. Where exposed along the Kanarra fold-thrust system, cross faults tend to cut across bedding nearly orthogonal to strike. They appear to be exclusive to the overturned limb of the leading anticline (Figure 3, Figure 4). Estimates of displacement along many of these faults indicate a greater horizontal (i.e., strike-slip) component than vertical (i.e., dip-slip) component (e.g., the Murie Creek fault in Averitt (1962); the Thunderbird Gardens Trail fault mapped by Knudsen (2014a) (see *Discussion*, Figure 35 and Figure 36) and thus, many of them are likely to represent "tear faults" or lateral ramps that developed during folding. An example is the approximately 800-meter-long cross fault along the Spring Creek saddle (see Figure 18 and Figure 29), with right-lateral separation and limited down-to-the-south vertical displacement, that offsets the Shnabkaib Member to the Springdale Sandstone (Figure 3 and Figure 4, notable cutoffs at the Shinarump outcrop north of the saddle (308150 m E; 4155290 m N) and along the Springdale Sandstone Member (308390 m E; 4155290 m N); see also Biek and Hayden (2016)). The extent of this fault is unclear, as its western trace is concealed beneath a landslide deposit along part of the Red Rock Trail. Spatial relationships between the Shnabkaib Member north and south of the Spring Creek saddle (Figure 3 and Figure 4) indicate it may either disturb or truncate against the Spring Creek thrust trace. Another, smaller cross fault antithetic to the Spring Creek saddle cross fault is revealed by offset across the Shnabkaib Member further to the north (Figure 3, Figure 4, (308150 m E; 4155654 m N)). Along the rest of the fold limb other, smaller cross faults are endemic to competent units in the Jurassic section, and particularly affect the Dinosaur Canyon Member, Springdale, and Shurtz Tongue of the Navajo. Two examples of large cross faults of the Kanarra fold-thrust system are the Murie Creek fault—the largest, and the northern boundary of the field area—and a similar, unnamed fault of opposite polarity at the Red Hill (the Thunderbird Gardens Trail fault of this study). These two faults displace much of the "salient" northern section of the Kanarra fold-thrust system upward and to the east (Figure 2).

5.4.2. Hurricane Fault Splays. The Hurricane fault crosscuts the Kanarra fold-thrust system displacing the trailing western limb of the anticline in the hanging wall down to the west (Figure 3 and Figure 4). The main trace of the Hurricane fault is largely concealed beneath colluvium and alluvial fan deposits from the Hurricane cliffs. However, subsidiary normal faults associated with Basin and Range extension can produce complex horse configurations ((Biek, 2003b, 2007a; Biek et al., 2010; Hurlow and Biek, 2003). Several large splays of the Hurricane fault, south of the study area, displace Moenkopi strata down onto Permian units or completely cut out the Paleozoic section (Figure 2; Biek (2007a); Biek et al. (2010). Within the central portion of the Kanarra fold-thrust system, far fewer splays of the Hurricane fault are present and crop out near (less than 150 meters) the main trace of the Hurricane fault. We recognize one notable splay just south of Kanarra Creek along the Kanarra Creek trail (previously discussed); the other splays are largely restricted to Camp Creek.

The best exposed Hurricane fault splays in the central area of the fold crop out en-echelon at the mouth of Camp Creek, where they complicate the leading anticline hinge zone (Figure 3, Figure 4; (305800 m E; 4153000 m N)). Here short (less than 250 meter-long), low displacement normal faults form gently curved fault traces sub-parallel to the local strike of bedding. In Figure 11, two of the three mappable splays can be seen; the largest (westernmost) is a synthetic fault splay, and the eastern, middle splay is antithetic to the Hurricane fault. Slickenside measurements and map patterns indicate down-to-the-west movement on the western and eastern splays, with little lateral motion (most slickenline rakes are between 87-93°). The middle, antithetic splay forms a miniature horst of Rock Canyon Conglomerate (Figure 11C). The largest and westernmost splay at Camp Creek forms a prominent, steeply west-dipping (65– to 70°) fault scarp along the Rock Canyon Conglomerate Member. A trail leading into Camp Creek directly follows the scarp strike for ~50 meters as it climbs in elevation, allowing good access to slickensides. Near the start of the trail, black banded, chert-rich Fossil Mountain Member is exposed in the footwall of the splay, with Rock Canyon Conglomerate unconformably mantling it (Figure 11C, inset). The splay displaces an outcrop of ledge-forming lower Timpoweap Member down to the west, where it rests beside the upper contact of the Fossil Mountain Member. Thus, based on the observed dip slip movement, minimal stratigraphic separation along this splay (i.e., throw) is in the tens of meters. Further east into Camp Creek, steep, west-dipping fractures with minimal detectable displacement outcrop on the canyon walls (Figure 11B). These observations indicate more deformation and may represent a damage zone associated with the fault. This suggests a short zone (10s of meters) of decreasing displacement east from the main Hurricane fault zone.

6. DISCUSSION

In southwestern Utah, deformation associated with the leading edge of the Sevier fold-thrust belt resulted in formation of multiple thrusts (e.g., the Square Top Mountain thrust, Iron Springs Gap Thrust, and Red Rock Trail thrust) and prominent folds (e.g., Virgin Dome, Pintura Anticline, and the Kanarra Anticline, see Figure 1 and Figure 2). These contractional structures are the result of regional layer-parallel compression associated with plate convergence along the Cordilleran orogen. The hanging wall cover rocks were translated along a detachment several hundred meters above the crystalline basement within the Cambrian Bright Angel Shale and, potentially, the lower incompetent layers of the Bonanza King Formation (Biek et al. (2010); Hintze (2005), see cross sections A-A' and B-B'). Folding and thrusting are closely associated, and these fold-thrust structures (e.g., Butler et al. (2020)) are thought to have localized blind thrust ramps during folding (Biek, 2003a,b).

The initial stages of folding likely involved multilayer buckling ("break-thrust" folds of Currie et al. (1962); Fischer et al. (1992); Willis (1893), followed by thrusting (Eisenstadt and De Paor (1987); "fault propagation folding" of Williams and Chapman (1983); Cawood and Bond (2020), Figure 15, p. 18). During buckling, many of these folds developed fold accommodation faults, or flank thrusts (e.g., Cloos (1961, 1964); Eisenstadt and De Paor (1987); Faill and Wells (1974); Mitra (2002a). These flank thrusts likely formed due to significant differences in thickness and competence between the currently exposed, relatively thin Paleozoic-Mesozoic ridge formers—namely the Timpoweap, Shinarump Conglomerate, and Springdale Sandstone Members—and much thicker, incompetent units—the Triassic redbeds, Petrified Forest Member, and Kayenta Formation. Long-wavelength buckling of thick, competent "control" units—the Bonzanza King–Nopah Dolomite, Mississippian Redwall Limestone, Permian Queantoweap Sandstone, and Jurassic Navajo Sandstone—may have determined the development of flank thrusts by inducing more intense buckling of thinner adjacent competent layers (e.g., Davis et al. (2011); Fischer et al. (1992); **?**, p. 384-390). Initial buckling within thin, competent layers transitions to accommodation of folding via thrusting once the layer can no longer fold (e.g., (Biek (2003a), A-A' and B-B'; Biek (2003b)), D-D', the west-directed, Hicks Creek thrust equivalent at Silver Reef).

The Virgin Dome, Pintura anticline, and Kanarra fold all exhibit similar structural styles, as they share a stratigraphy with similar mechanical strength properties. Early development of flank thrusts within competent units on the limbs of gentle to open folds is an intrinsic characteristic of many folds of southwestern Utah (e.g., the Silver Reef thrusts on the Virgin Dome; see Biek (2003a,b)). The presence of flank-thrusts in the nascent stages of folding greatly affects the structural evolution of the fold as the amount of shortening increases; for example, along the strike of the axis of the leading anticline of the Kanarra fold-thrust system. At Camp Creek, early formed flank thrusts (e.g., Kanarra Creek thrusts, Taylor Creek thrusts) along the east-dipping, upright limb of the open leading anticline are upright west-verging thrusts (Figure 3, Figure 4). Along strike to the north, the amount of shortening increases and leads to development of a fold style with many attributes of a fault propagation fold, including a gently dipping trailing fold limb and a steeply dipping, overturned leading fold limb (Figure 10; *c.f.* Davis et al. (2011), p. 414–428). Early formed flank thrusts along the eastern limb (e.g., Taylor Creek thrusts, Figure 10 and Figure 17) were rotated, along with the stratigraphy, into steeply dipping to overturned orientations as the fold tightened. The resulting geometry of stratigraphic units juxtaposed along overturned early formed flank thrusts (e.g., Hicks Creek thrust, see Figure 21) previously led to separation-based interpretations of these faults as normal faults, which is a misrepresentation of these folded thrusts and obscures their true structural significance. Slip will cease along an early formed flank thrust if the fault plane is rotated into an unfavorable orientation for failure with respect to the regional stress field (e.g., Kanarra Creek thrust, Figure 14). In contrast, early formed flanks thrusts on the trailing limb of the fold, such as the Spring Creek thrusts, remain in favorable orientations for continued slip along the fault plane and continued to do so as the fold continued to tighten with increased shortening. This is demonstrated by displacement of the folded Kanarra Creek thrust by the Spring Creek thrust (Figure 10, Figure 14, Figure 15). Earlier movement along the Spring Creek thrusts at depth resulted in the development of a fault-bend fold in the trailing limb of the anticline, imparting a broad crest profile similar to a box fold for the Kanarra anticline (Figure 10, Figure 33).

Higher degrees of shortening in the central section of the Kanarra fold-thrust system resulted in lockup of the leading anticline, syncline, and early formed flank thrusts on the leading overturned limb. In addition to continued slip on faults in a favorable orientation for failure, new, late fold accommodation thrust faults (e.g., Murie Creek thrusts, Red Rock Trail thrusts) formed in response to fold lockup within a continued layer-parallel compressive stress field (e.g., Jadamec and Wallace (2014), Figure 12, p. 122; Mitra (2002a), Figure 15 p. 686; Mitra (2002b), Figure 4, p. 1679). These late fold accommodation thrust faults are spatially associated with the hinge zones of the leading anticline and syncline, and thus are examples of "forelimb shear thrusts" (see Mitra (2002a)). While the Murie Creek thrusts are relatively short and of low displacement, the Red Rock Trail thrust is in a favorable location and orientation to eventually link with the blind thrust deeper in the core of this fold-thrust structure (Figure 10. It is our contention that these faults become hard-linked in

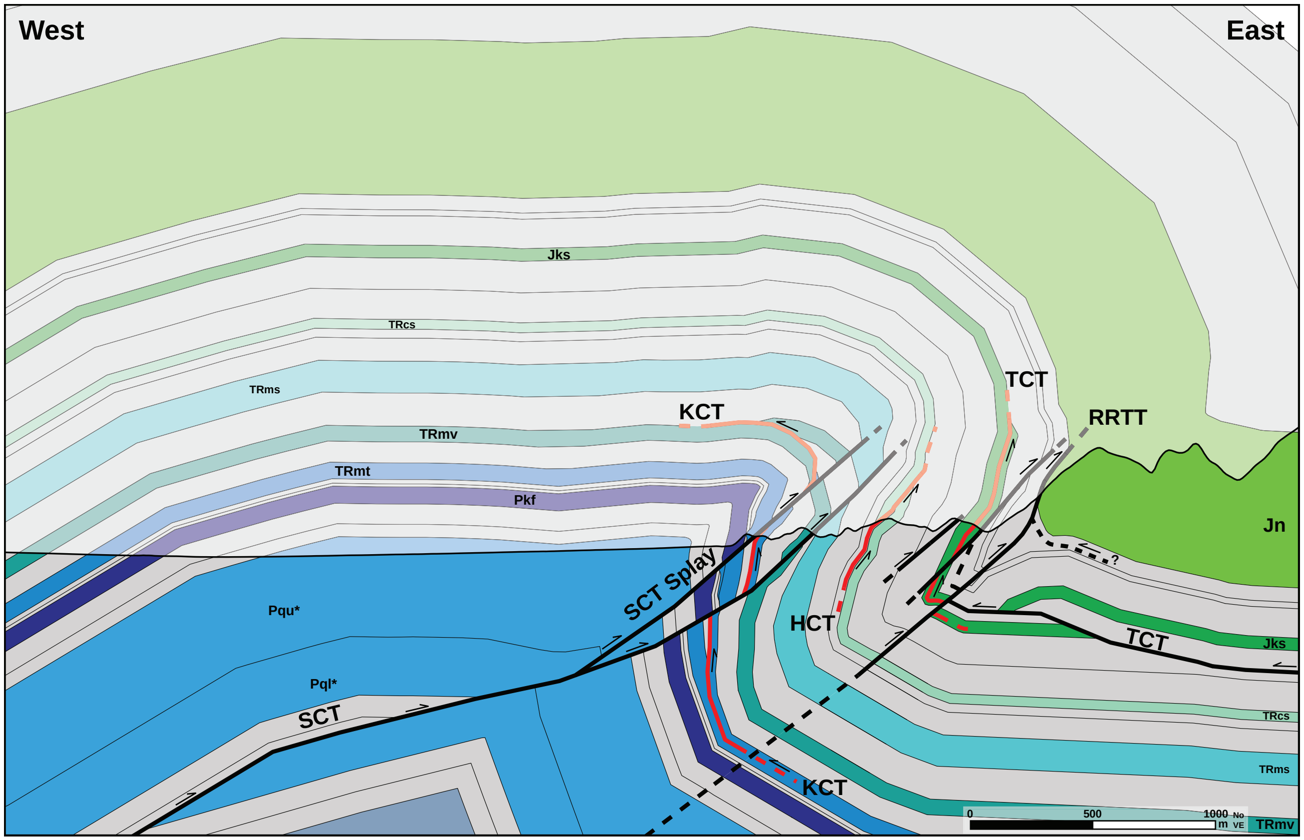

Figure 33. Blowup of the cross section of the Kanarra fold-thrust system at Kanarra Creek. Early formed thrusts (fold accommodation faults) which were overturned at later stages of Kanarra fold development are colored in red. Late-forming thrusts comprise a dextral shear zone across the fold limb, dissecting earlier flank thrusts. Displacement along the Red Rock Trail thrust is estimated here to be approximately 250 meters. Sinistral flexural slip within the syncline core which may be responsible for the structural relationships at Kanarra Creek (Figure 30B) is represented by the dashed, queried detachment beneath the Navajo. All abbreviations on Figure 10.

the subsurface in the vicinity of Short Creek to form a "break thrust" (see Eisenstadt and De Paor (1987); Fischer et al. (1992). Thus, the Red Rock Trail thrust is a throughgoing thrust fault that defines the leading edge of the Sevier fold-thrust belt in southwestern Utah.

6.1. THE KANARRA FOLD-THRUST SYSTEM AND THE PINTURA ANTICLINE

Dissection of the Kanarra fold-thrust system by the Hurricane fault yielded spectacular exposures of the leading anticline-syncline pair and associated thrust faults of the Kanarra fold-thrust system in its footwall block, the Hurricane Cliffs. The burial of the hanging wall block of the Hurricane fault, and with it the trailing limb of the Kanarra anticline, beneath late Tertiary to Quaternary sediments and volcanics of Cedar Valley obfuscates the full tectonic significance of the Kanarra fold-thrust system to the Sevier fold-thrust-belt. This is borne out in a long-lived debate regarding the relationship between the Virgin anticline, Pintura anticline, and the Kanarra anticline (see Hurlow and Biek 2003 for a complete summary) and the timing of Sevier deformation in southwestern Utah ((Biek et al., 2010)).

The Pintura anticline, from early on, has been depicted as a broad gentle anticline separated from the smaller, tighter Kanarra anticline by an intervening syncline (e.g., (Gardner, 1941), Figure 2A p. 249). The folds were beveled by erosion and the angular unconformity capped by Tertiary clastics. The younger Hurricane fault is pictured cutting the western limb of the Kanarra anticline near the axis of the intervening syncline, isolating the partially eroded Pintura anticline within the rotated hanging wall of the Hurricane fault (e.g., (Gardner, 1941), Figure 2F p. 249). Gardner (1941) notes "down-turning" of the hanging wall strata as the contact with the Hurricane fault is approached enhances the intervening syncline, a process he attributes to gravitational "sag". More recent mapping of the Pintura 7.5 minute quadrangle by Hurlow and Biek (2003) substantiate these findings and their cross-section shows a similar broad Pintura anticline, a faulted intervening syncline, and a tighter faulted Kanarra anticline.

Cook (1957) called into the question the existence of the Pintura anticline. Cook noted that when bedding in the Carmel Formation is rotated to horizontal, the contact between the underlying Navajo Sandstone and Carmel Formation everywhere dips more steeply to the northwest; the east dipping limb of the Pintura anticline is missing or poorly exposed. Hurlow and Biek (2003) confirmed Cook's result and described two plausible interpretations of the data: 1) the Pintura anticline is a west dipping homocline (i.e., Cook's model), 2) the Pintura anticline is a broad anticline that shares an east dipping limb with the intervening syncline that was modified by reverse drag along the Hurricane fault (i.e., Hurlow and Biek's (2003) preferred model).

The results of our work have bearing on resolving the relationship of the Pintura anticline to the Kanarra anticline. The geologic cross-section (Figure 10) depicts a complete profile through the Kanarra fold-thrust system "restored" to the Cretaceous (i.e., prior to dissection by the Hurricane fault). In our structural interpretation, the Kanarra anticline is a compound fold, with a broad, sub horizontal hinge zone flanked by a leading anticline on the east and by a trailing anticline to the west. The trace of the Hurricane fault closely parallels the trace of the hinge zone of the *leading anticline* in the composite Kanarra anticline (Figure 3). As previously suggested, during Basin and Range extension, the Hurricane fault exploits the hinge-zone of the leading anticline and likely the underlying thrust as well (Biek et al., 2010; Grant et al., 1994; Threet, 1963b). Downward displacement of the trailing limb of the composite Kanarra fold (Figure 10) in the hanging wall of the Hurricane fault would result in a west-dipping homocline. The presence of the intervening syncline can be attributed to the development of a "roll-over anticline" and antithetic normal faults as the contact with the Hurricane fault is approached (see (Davis et al., 2011), Figure 8.3.1, p. 433). However, downward displacement and clockwise rotation of the hanging wall along a listric normal Hurricane fault could create the appearance that the western trailing anticline is a separate "Pintura" anticline. Clockwise rotation of the broad sub horizontal hinge zone would appear to be the shared east-dipping limb of the intervening syncline, with the dismembered leading anticline isolated and representing the traditional Kanarra anticline. Hanging wall strata adjacent to the Hurricane fault would still be subjected to modification by development of a rollover anticline and antithetic faults. In either scenario, the “Pintura anticline” was cleaved from the compound Kanarra anticline that formed as part of the Kanarra fold-thrust system. The relative stratigraphic ages used previously to constrain the timing of the formation of the “Pintura anticline” to be between early and late Campanian time (~84 to 72 Ma; see (Biek et al., 2010)) constrain the formation of the Kanarra fold-thrust system.

6.2. THE KANARRA FOLD-THRUST SYSTEM AT RED HILL

The northern terminus of the Kanarra fold-thrust system is well exposed at the Red Hill near Cedar City; one of Utah’s iconic geologic exposures ((Hintze, 2005)). Again, the fold has been dissected by the Hurricane fault along the axial trace of the leading anticline (Figure 2). The western trailing limb of the anticline has been displaced along with the hanging wall beneath the sediment fill in Cedar Valley with the eastern limb of the anticline and leading syncline well exposed in the footwall. Partial closure of the northerly plunging nose of the fold is preserved. The amount of shortening at Red Hill is greater than along Camp Creek but less than along Kanarra Creek. The lower degree of shortening is reflected in the upright, gentle to steeply dipping stratigraphic section along leading eastern limb of the anticline with moderate, additional structural complexity from faulting along the limb. Nevertheless, some of these faults (e.g., the Hicks Creek thrust) were previously classified based upon observed separation as normal faults (e.g., Averitt (1962); Hintze (2005)), obscuring the true relationship of these faults to folding and to the Sevier fold-thrust belt. Based upon our unpublished mapping and with consideration for the characteristic structural style of the Kanarra fold-thrust system (Figure 10) we present a geologic cross-section for the Red Hill at Cretaceous time (Figures 34, 35, and 36).

The profile through the Kanarra fold-thrust system at the Red Hill shares several features with the central portion of the system at Kanarraville (Figure 10). The anticline at Red Hill is an asymmetric, composite fold-thrust structure modified by late thrust fault propagation. It developed above the basal detachment in the Cambrian Bright Angel Shale above the basement-cover contact and a blind break-thrust ramp (Figure 34). Slip along the early formed Spring Creek flank-thrust forms a fault-bend fold within the trailing limb of the fold to produce a compound fold profile. The influence of the kink-axes on the fold profile gradually diminishes upwards such that the fold has a rounded profile more typical of buckle folds. The early formed Hicks Creek flank thrust on the eastern limb has been steepened by rotation of the limb during folding but remains upright. Duplication of the stratigraphic section along this west-verging flank thrust thickens the east-dipping limb and broadens out the hinge-zone of the leading anticline of the fold (Figures 34, 35, and 36) Another, smaller early formed flank thrust west of the Hicks Creek thrust duplicates the Shnabkaib Member by folding and displacement. We interpret several faults as later-forming fold accommodation faults which truncate the earlier Hicks Creek thrust. These include previously mapped normal faults, which we interpret as the Coal Creek thrust system. The Coal Creek thrusts (Figure 35 and Figure 36) are late, west-verging "hinge wedge thrusts" (e.g., Cloos (1961), Figures 12–14, p. 113–115; Mitra (2002a), Figure 8, p. 680) and likely formed in response to hinge zone tightening and displacement along the Red Rock Trail thrust. They duplicate Upper Moenkopi and Chinle units in the footwall of the Hicks Creek thrust and displace the Hicks Creek thrust several tens of meters west within the subsurface along the fold limb, though aggregate slip on each splay is higher (100s of meters).

The Red Rock Trail thrust is also present at the Red Hill. Here it has ramped higher up section compared to Kanarra Creek and displaces the Navajo Sandstone over the Carmel Formation (Figure 35). Like the cross-section through the fold-thrust system at Kanarraville, the Red Rock Trail thrust is a late forming forelimb shear thrust in a favorable location and orientation to merge with the blind thrust ramp deeper within the fold. Construction of the

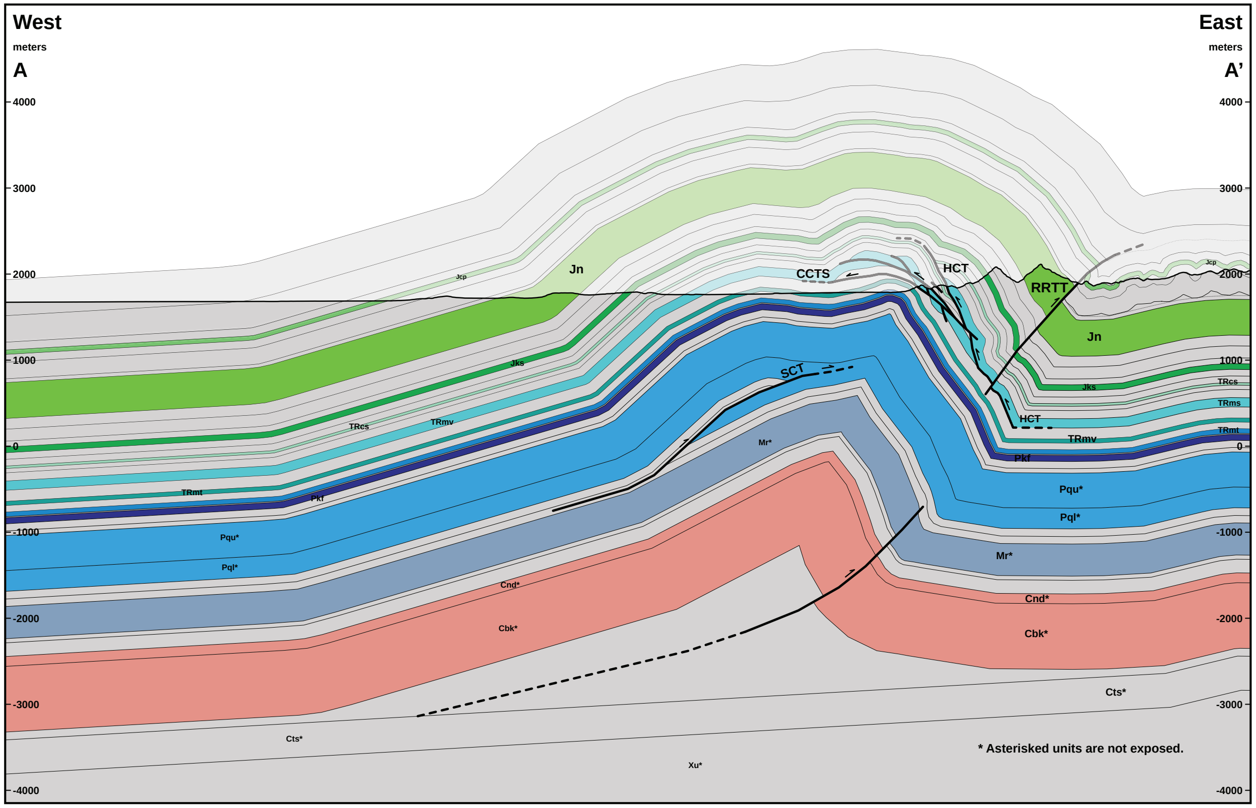

Figure 34. Cross section of the Kanarra fold at the Red Hill. Restored Sevier structure circa 80 Ma, based on unpublished mapping along Coal Creek and mapping by Knudsen (2014a). Eroded geology is faded out. Unexposed, thick, competent layers (Cbk-Cnd, Mr, Pq) are colored according to age; exposed ridge-former colors correspond to the maps in the study area (Figure 3, Figure 4). Present-day topography is included to emphasize the ridge-formers. Structure west of the Hurricane Cliffs, within the present-day Cedar Valley graben, does not represent present-day bedrock geology. Unexposed structure constrained by surface control, fold style, and assumption of buckle folding before break-thrust faulting. CTTS—Coal Creek thrust system.

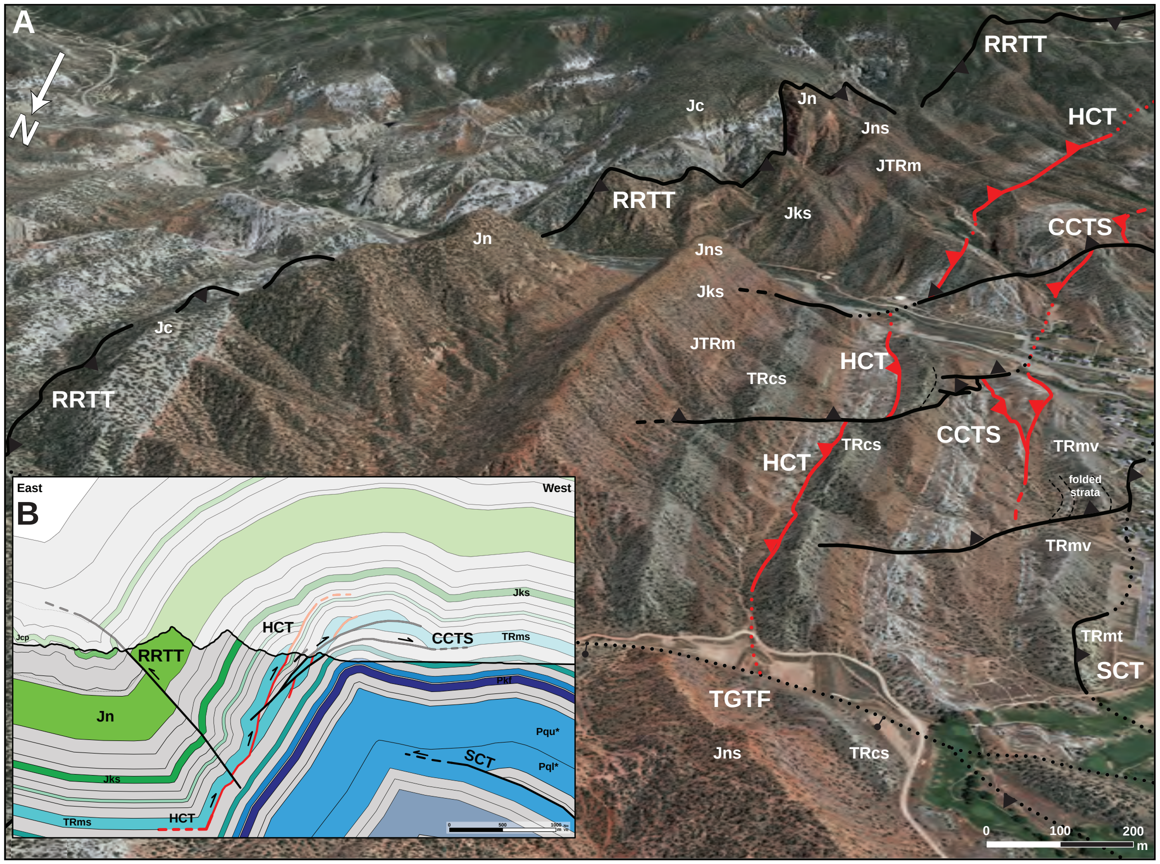

Figure 35. Kanarra fold-thrust system at the Red Hill, looking southeast. A) Google Earth 3D terrain view southeast onto the east limb of the Kanarra fold-thrust system at the Red Hill adjacent Cedar City. Coal Creek thrust system cuts obliquely across the earlier set Nearby, the Spring Creek thrust breaches the surface, bringing up Timpoweap strata. B) Partial large-scale blowup of the cross section drawn in Move™of the Kanarra fold-thrust system at the Red Hill, reflected to match the southeast view of (A).

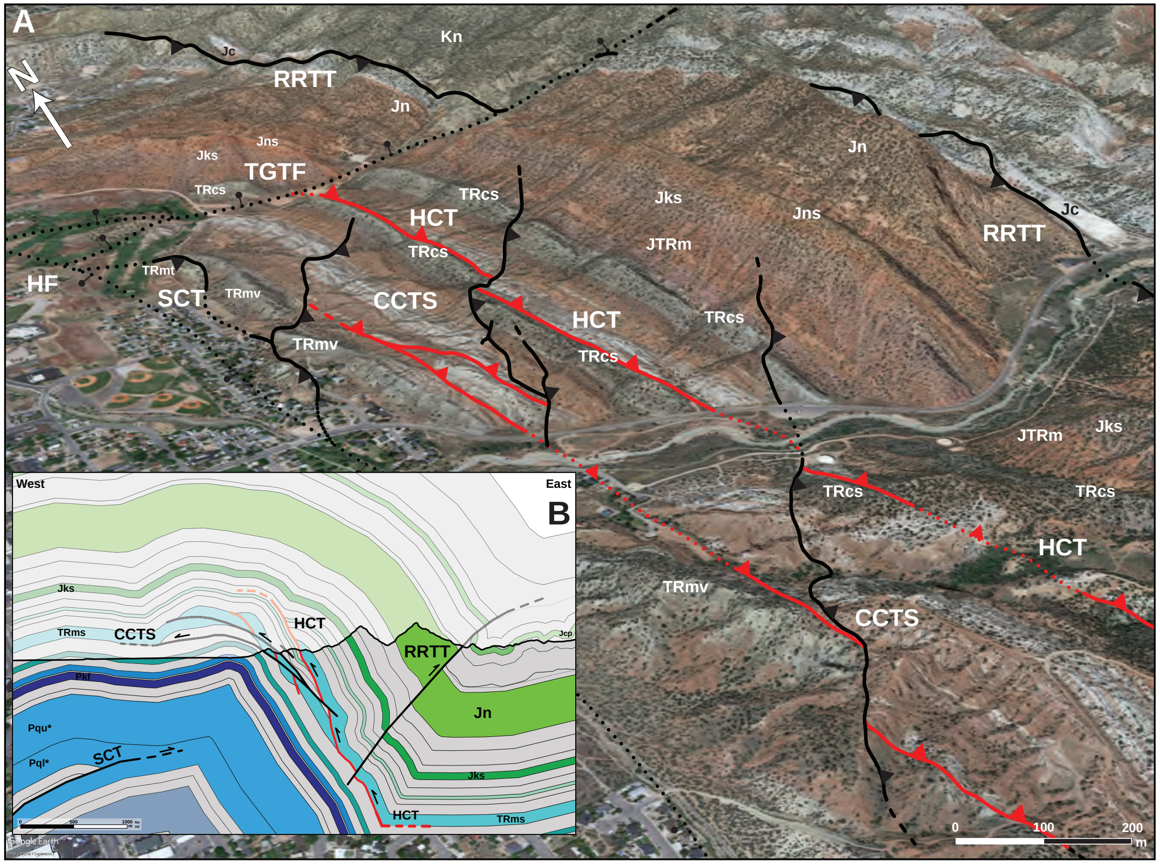

Figure 36. Kanarra fold-thrust system at the Red Hill, looking northeast. A) Google Earth 3D terrain view with Landsat/Copernicus imagery looking northeast onto the east limb of the Kanarra fold-thrust system at the Red Hill adjacent Cedar City. This approximately along-strike view shows their gentle-moderate dips (e.g., right midground). B) Partial large-scale blowup of the cross section drawn in Move™ of the Kanarra fold-thrust system at the Red Hill.

cross-section for the amount of shortening required at the Red Hill indicates these two faults are not hard-linked (Figure 34). Nonetheless, the position of the Red Rock Trail thrust here confirms that the Kanarra fold-thrust system defines the leading edge of the Sevier Orogeny in southwest Utah.

6.2.1. Salient and Recess Development Along the Kanarra Fold-Thrust System. The Kanarra fold-thrust system is defined by broad open curves along its strike (Figure 2). Near Cedar City the curve is concave towards the hinterland and forms a salient. Just south of Kanarraville, the system curves to be concave towards the foreland and forms a recess. The presence of salients and recesses are a common feature of many orogens, including the Sevier fold-thrust belt (Quick et al., 2020). The presence of salients and recesses may reflect variation in stratigraphy (e.g., Chapman and DeCelles (2015)), sediment thickness (Paulsen and Marshak (1999)), and variation in the shape of the rifted-continental margin, that are the embayments and promontories that define the hingeline (Thomas (2006)). The presence of strike-slip transform faults, separating different rift-basins in the Precambrian basement contributes to development of an irregular hingeline to the extended continental crust. Along strike variation in the temporal and spatial advancement of the leading edge of the Sevier fold-and-thrust belt front was largely inherited from the structure of the rifted Precambrian crystalline basement of western North America (Picha (1986); Picha and Gibson (1985); Quick et al. (2020)). We suggest that the close spatial association of the Kanarra fold-thrust system with the Cordilleran hingeline (Figure 1) indicates that structural inheritance is a contributing factor to the formation of salients and recesses that characterize this structural system (Figure 2). In addition, we suspect localization of the Murie Creek normal fault just north of Kanarraville and the “Thunderbird Gardens Trail” normal fault just north of Cedar City, sub-parallel to the Paragonah Lineament (see Figure 1) along reactivated transform faults in the basement led to the along strike displacement of this fold-thrust system (Figure 2).

6.2.2. The Kanarra Fold-Thrust System and Advancement of the Sevier Deformation Front. The Kanarra fold-thrust system represents the leading edge of the Sevier deformation front in southwest Utah. In the central portion of the Kanarra fold-thrust system, The Red Rock Trail thrust hard-links down section with the basal-decollement in the Cambrian Bright Angel Shale, forming a break thrust (Figure 10 and Figure 34. The thrust displaces Navajo Sandstone, and the distinctive cataclastic Navajo Sandstone over the Carmel Formation. This distinctive spatial relationship of fault related units is well exposed along the prominent topographic ridge of Navajo Sandstone at the entrance to Parowan Gap in the Red Hills (Anderson and Dinter, 2010; Biek et al., 2015; Maldonaldo and Williams, 1993a; Threet, 1963a). Cropping out in the low hills on the eastern side of the ridge, is an east verging thrust that places the distinctive cataclasite Navajo Sandstone over tightly folded and fractured, laminated micritic limestone of the Carmel Formation—we recognize this as the Red Rock Trail thrust. The thrust is in fault contact with the Navajo Sandstone ridge along a down to the east steep, normal fault.

To the east of the Red Rock Trail thrust, two other east-verging thrusts are well exposed in Parowan Gap (see Anderson and Dinter (2010); Biek et al. (2015)). The eastern most thrust fault has been traditionally recognized as the main trace of the Iron Springs thrust (see Anderson and Dinter (2010); Biek et al. (2015); Maldonaldo and Williams (1993a); Threet (1963a)). These thrusts are of lower displacement, placing Carmel Formation over the lower Iron Springs Formation and lower Iron Springs Formation over upper Iron Springs Formation suggesting low displacement. Uncertainty and disagreement in the identification of the Cretaceous units in Parowan Gap, particularly the presence or absence of the Straight Cliffs and Naturita Formations, will affect the interpretation of the displacement on these thrusts (Anderson and Dinter, 2010; Biek et al., 2015; Enriquez St. Pierre and Johnson, 2021; Maldonaldo and Williams, 1993a; Threet, 1963a). These thrusts are beveled off along an angular unconformity that is capped by the late Cretaceous to early Eocene Grand Castle

Formation. Slight displacement of the unconformable contact by the thrust constrains the waning stages of movement on these thrusts to the early Eocene (Anderson and Dinter, 2010; Biek et al., 2015).

Correlation of the Iron Springs Gap thrust where it crops out in its type locality in the Three Peaks area with the eastern thrusts exposed in Parowan Gap is questionable due to disparity in the spatial relationship with the Red Rock Trail thrust. The Iron Springs Gap thrust of the Three Peaks crops out to the west of the Kanara fold-thrust system and the Red Rock Trail thrust (Figure 1). In Parowan Gap, the thrusts east of the Red Rock Trail thrust would reverse this spatial relationship if they are correlated with the Iron Springs Gap thrust. However, considering the structural style of the Kanarra fold-thrust system, the thrusts east of the Red Rock Trail thrust at Parowan Gap more likely formed as out of the syncline thrusts. These late fold accommodation faults of lower displacement potentially sole into the Temple Cap Formation detachment underlying the buckle fold train at the Red Hill (e.g., Averitt and Threet (1973); Knudsen (2014a)) rather than into the regional basal decollement in southwest Utah (e.g., Biek et al. (2010); Van Kooten (1988)). In addition, restoration of the Red Hills horst to its location pre- Basin and Range extension would place it closer to the Markagunt Plateau further supporting the correlation of Sevier structures in Parowan Gap as part of the Kanarra fold-thrust system as previously suggested by Threet (1963b) and Biek et al. (2015).

Correlation of the Iron Springs Gap thrust with the thrusts exposed in Parowan Gap is also unlikely due to disparity in the temporal relationships of these thrusts. Quick et al. (2020) constrained emergence of the Iron Springs Gap thrust in the type location of the Three Peaks to 100 Ma. The timing of movement on the Iron Springs Gap thrust is tens of millions of years earlier than motion on the thrusts in Parowan Gap which is constrained to be late Cretaceous to early Eocene. However, timing constraints on the movement of the Kanarra fold-thrust system in the south (i.e., the former Pintura anticline) of ~84 to 72 Ma (Hurlow and Biek (2003)) are in closer agreement with the stratigraphic constraints in

Parowan Gap. Recognition of the Red Rock Trail thrust in Parowan gap, and the associated late fold accommodation faults, alleviates the apparent discrepancy in the timing of thrusting in southwest Utah.

Advancement of the Sevier deformation front in southwestern Utah is episodic. Quick et al. (2020) connected movement along the Irons Springs Gap thrust at 100 Ma with the late Albian early Cenomanian magmatic flare-up in the Cordilleran arc. They suggested that accelerated subduction, associated with a period of global plate reorganization, contributed to a magmatic flare-up in the Cordilleran arc. This event, along with steepening of the orogenic wedge, triggered widespread thrusting across the retroarc Sevier deformation belts. The timing of deformation of the Kanarra fold-thrust system in southwest Utah (~84-72 Ma) also corresponds with a period of widespread thrusting in central Utah (e.g., Paxton thrust, Gunnison thrust, Charleston-Nebo thrust) and in northern Utah and southwest Wyoming (e.g., Crawford thrust, Absaroka thrust) as well as overlapping with major magmatic flare-ups in the Cordilleran arc (see Quick et al. (2020), Figure 9 p. 85). This close temporal relationship between magmatic activity in the arc and widespread deformation in the Sevier fold-thrust belt requires further investigation.

6.2.3. The Kanarra Fold-Thrust System and Sediment Dispersal in the Sevier Foreland. The temporal and spatial advancement of topographic highs and lows associated with the progression of the Sevier deformation front across southwest Utah significantly influences the redistribution of sediment in the Sevier foreland basin. The emergence of the Irons Springs thrust in the late Albanian to earliest Cenomanian correlates with movement on the Keystone-Muddy Mountain thrust, the Pavant thrust, the Charleston Nebo thrust, and the Willard thrust system (see Quick et al. (2020), Figure 9, p. 85). The deformation front advances eastward in southwest Utah with the development of the Kanarra fold-thrust system in the Campanian to early Eocene. During this time, the Kanarra fold-thrust system likely formed a substantial, linear, topographic high with associated strike valleys that extended over a hundred kilometers, from Tocqueville to north of Parowan Gap along the edge of the Markagunt Plateau (Figure 1).

Investigation of Cretaceous stratigraphy in southwest Utah documented the foredeep of the Sevier orogeny was broken up into several discrete sub-basins presumably due to reactivation of northeast-trending structures in the basement as normal faults (see Figure 10 of Enriquez St. Pierre and Johnson (2021)). Creation of northeast trending topographic highs and lows associated with horsts and grabens is suggested to have controlled the fluvial drainage patterns of the main axial river systems in what is now the plateau province. The Sevier fold-thrust belt and wedge top being well west of the edge of the Markagunt Plateau. This interpretation may have merit for the eastern plateaus adjacent to the Western Interior Cretaceous Seaway, however, it mischaracterized the Kanarra fold-thrust system as a Laramide age monocline rather than the leading edge of the Sevier fold-thrust belt during the late Cretaceous to early Eocene (see Figures 1 and 2 of Enriquez St. Pierre and Johnson (2021)). We suggest the distribution of Cretaceous depocenters and fluvial drainage patterns sub-parallel to the Sevier deformation on the Markagunt Plateau and to the immediate west more likely reflect the development of significant topographic features in response to the episodic advancement of the leading edge of the Sevier fold-thrust belt in southwest Utah.

7. CONCLUSIONS

Detailed geologic mapping and structural analysis of the central portion of the traditional "Kanarra anticline", near Kanarraville, Utah brings additional clarity to the regional tectonic significance of this structure to the geology of southwest Utah. Folding and thrusting are inextricably linked in all stages of deformation associated with contractional shortening during the Sevier orogeny such that we identify this structure as the *Kanarra fold-thrust system*. The traditional "Kanarra anticline" of the literature represents only the leading, tight, upright to overturned anticline of a broad composite fold-thrust structure (i.e., the *Kanarra anticline*). The *Kanarra anticline* of the Kanarra fold-thrust system has an overall form of a "box fold" in that its crest includes an open, upright, trailing anticline as well as the leading anticline now exposed as the surface (see Figure 10). Secondary structures associated with contractional deformation within the hinge of the leading anticline, as well as a blind thrust beneath the leading anticline, were in a favorable orientation to be reactivated during younger Basin and Range extension resulting in strain localization and formation of the Hurricane fault. The trace of the Hurricane fault variably dissected the hinge zone of the leading anticline such that scattered remnants of the hinge zone crop out discontinuously along the strike of the entire structure. The true crest of the composite fold, as well as the trailing anticline, were down dropped in the hanging wall of the Hurricane fault and are obscured by younger Tertiary and Quaternary clastics and volcanics in the half-grabens created along the strike of the fault. The consequences of Basin and Range deformation resulted in recognition of an apparent anticline, the Pintura anticline, and an intervening syncline, separate from the traditional Kanarra anticline. We demonstrate the Pintura anticline is part of the trailing anticline on the broad crest of the composite *Kanarra anticline* that is part of the Kanarra fold-thrust system. Stratigraphic relationships associated with the "Pintura anticline" apply to the Kanarra fold-thrust system and constrain the timing of deformation to be late Cenomanian to early Eocene (Hurlow and Biek, 2003).

Mapped thrust faults associated with the Kanarra fold-thrust system can be divided into early (e.g., flank thrusts) and late (forelimb shear and out of the syncline) fold accommodation thrust faults. Early formed flank thrusts are common to many folds in this area (e.g., the Virgin anticline). The Taylor Creek thrust system on the eastern limb of the leading anticline of the Kanarra anticline is the best-known example of one of these faults (see (Biek, 2007a)). Early formed flank thrusts on this eastern limb (e.g., Taylor Creek thrusts) were folded and overturned along with the stratigraphic section in the central portion of the Kanarra fold-thrust system. This additional structural complexity resulted in several faults previously being misidentified as normal faults rather than as folded thrusts. Rotation of these thrust into an unfavorable orientation for continued slip resulted in fault lock up. However, early formed flank thrusts on the trailing western limb remain in a favorable orientation for slip and affected both the early development of the Kanarra anticline, as well cross-cutting and displacing folded thrusts on the overturned eastern limb (e.g., the Spring Creek thrusts). Upon hinge lockup, late forming forelimb shear and out of the syncline thrusts within the overturned eastern limb developed a kilometer-scale dextral shear zone (e.g., Jadamec and Wallace (2014); Mitra (2002a)) shared by the leading anticline and syncline (see Figure 10). Of these faults, the Red Rock Trail thrust was in a favorable position and orientation to grow and eventually merge with the blind thrust beneath the Kanarra anticline to form a "break-thrust" (Eisenstadt and De Paor, 1987; Fischer et al., 1992). The Red Rock Trail thrust transports the stratigraphic section in the Kanarra anticline to the east and on top of the Jurrassic to late Cretaceous strata of the Markagunt Plateau.

The Red Rock Trail thrust and its distinctive Navajo Sandstone cataclasite can be traced from its inception north of Spring Creek along the contact between the Kayenta Formation and Navajo Sandstone well to the north. At the Red Hill, Cedar City, the Red Rock Trail thrust has climbed section and places Navajo Sandstone over folded Jurassic Carmel Formation. In Parowan Gap, the distinctive pairing of the Navajo Sandstone cataclasite on top of tightly folded and overturned Carmel Formation preserves a remnant of the Red Rock Trail thrust at the western end of the gap. The overturned Carmel and Iron Springs Formation in the gap represent the eastern limb of the leading anticline of the Kanarra fold-thrust system—a system which can be traced for a minimum distance of ~90 km from the southern terminus near Toquerville to north of Parowan Gap. We associate the thrusts east of the Red Rock Trail thrust in Parowan Gap as late fold accommodation faults (i.e., out of the syncline thrusts) with the Kanarra fold-thrust system. This reconciles the apparent conflict in the timing of emergence of the Iron Springs Gap thrust at Three Peaks at ~100 Ma (Quick et al. (2020)) with the movement on the Kanarra fold-thrust system constrained to being between Campanian to early Eocene (~84 to 56 Ma).

The Kanarra fold-thrust system represents the leading edge of the Sevier fold-thrust belt in southwest Utah during the late Cretaceous. The Sevier fold-thrust deformation front appears to have advanced episodically from the Iron Springs Gap thrust at 100 Ma (Quick et al. (2020)) to the Red Rock Trail thrust in the late Campanian. This is suggestive that movement on Sevier thrusts may be temporally tied to episodes of magmatic flare-ups in the Cordilleran arc (DeCelles and Graham, 2015; DeCelles et al., 2009; Lageson et al., 2001; Quick et al., 2020; Yonkee et al., 2019). During the early to late Cretaceous, and potentially persisting into the Eocene, the Keystone-Muddy Mountain-Tule Spring-Square Top Mountain- Blue Mountain-Iron Springs Gap-Canyon Range thrust system in the Cenomanian and the Kanarra fold-thrust system in the Campanian would present substantial north-south, linear topographic highs flanked by linear valleys that stretched over 100 km in southwestern Utah. These imposing topographic features would have severe consequences for sediment provenance and dispersal in the associated Cordilleran foreland basin.

ACKNOWLEDGEMENTS

John P. Hogan extends his thanks to Robert “Bob” Laudon for welcoming him to be a part of the field camp many years ago and sharing his thoughts, as well as his recollections of past conversations with Sheldon “Kerry” Grant, on the geology of the area. Additional hearty thanks goes to Michael Wizevich, Jonathan Obrist-Farner, and Jason Kaiser, for their insights and discussions regarding the geologic significance of many field exposures to the geology of southwest Utah as well as their friendship and comradery while teaching the Missouri S&T field camp.

William Chandonia would also like to thank Jason Kaiser for his help with logistics in Utah and sharing methods for measuring shear fractures. Tyler R. Knudsen gave his time to meet in the field and shared his knowledge of the stratigraphy, which assisted with interpretations in the Chinle Formation. William also acknowledges Brennan Brunsvick, Trey Anglim, Dylan Webb, and Daniel Quick for their valuable assistance helping him in the field. Petroleum Experts' Move™software was invaluable to the study workflow and creating cross sections. This work was also enhanced by Richard Allmendinger's programs GMDE, FaultKin, and Stereonet. Paul Inkenbrandt's CSL code facilitated the compiling and styling of our references. The study was funded by two grants from the American Association of Petroleum Geologists Foundation Grants-in-Aid program, one grant from the Geological Society of America Graduate Student Research Grant program, and the Chancellor's Fellowship and Radcliffe Scholarship from Missouri University of Science and Technology.

REFERENCES

R. W. Allmendinger. GMDE–Extracting quantitative information from geologic maps. *Geosphere*, 16(6):1495–1507, 2020. doi: https://doi.org/10.1130/GES02253.1.

R. W. Allmendinger, J. W. Gephart, and R. A. Marrett. Notes on fault slip analysis. In Allmendinger, R.W., Aydin, A., Engelder, T., and Pollard, D. D., editors, *Quantitative Interpretation of Joints and Faults*, Annual Meeting 1989, page 59. Geologial Society of America, 1989.

R. W. Allmendinger, N. Cardozo, and D. M. Fisher. *Structural Geology Algorithms: Vectors and Tensors*. Cambridge University Press, 2012. doi: https://doi.org/10.1017/CBO9780511920202.

L. P. Anderson and D. A. Dinter. Deformation and sedimentation in the southern Sevier foreland, Red Hills, southwestern Utah. In Carney S. M., Tabet, D. E., and Johnson, C. L., editors, *Geology of South-Central Utah*, Publication 39, pages 338–366. Utah Geological Association, 2010.

R. L. Armstrong. Sevier orogenic belt in Nevada and Utah. *Geological Society of America Bulletin*, 79(4):429–458, 1968. doi: https://doi.org/10.1130/0016-7606(1968)79[429:SOBINA]2.0.CO;2.

P. Averitt. Geology and coal resources of the Cedar Mountain quadrangle, Iron County, Utah, 1962.

P. Averitt. Geologic map of the Kanarraville quadrangle, Iron County, Utah, 1967.

P. Averitt and R. L. Threet. Geologic map of the Cedar City quadrangle, Iron County, Utah, 1973.

R.F. Biek. Geologic map of the Harrisburg Junction quadrangle, Washington County, Utah, 2003a.

R.F. Biek. Geologic map of the Hurricane 7.5' quadrangle, Washington County, Utah, 2003b.

R.F. Biek. Geologic map of the Kolob Arch quadrangle and part of the Kanarraville quadrangle, Washington and Iron Counties, Utah, 2007a.

R.F. Biek. Geologic map of the Kolob Reservoir quadrangle, Washington and Iron Counties, Utah, 2007b.

R.F. Biek and J. M. Hayden. Geologic map of the Kanarraville quadrangle, Iron County, Utah, 2016.

R.F. Biek, P.D. Rowley, J.M. Hayden, D.B Hacker, G.C Willis, L.F. Hintze, R.E. Anderson, and K.D. Brown. Geologic map of the St.. George and east part of the Clover Mountains 30' x 60' Quadrangles, Washington and Iron Counties, Utah, 2010.

R.F. Biek, P.D. Rowley, J.J. Anderson, F. Maldonaldo, D.B. Hacker, J.G Eaton, R. Hereford, E.D. Sable, H.F. Filkorn, and B. Matyjasik. Geologic map of the Panguitch 30' x 60' Quadrangle, Garfield, Iron, and Kane Counties, Utah, 2015.

B. C. Burchfiel and Gregory A. Davis. Structural framework and evolution of the southern part of the Cordilleran orogen, western United States. *American Journal of Science*, 272(2):97–118, 1972. doi: https://doi.org/10.2475/ajs.272.2.97.

R.W.H. Butler, C.E. Bond, M.A. Cooper, and H. Watkins. Fold–thrust structures—where have all the buckles gone? In Bond, C.E. and Lebit, H. D., editors, *Folding and Fracturing of Rocks—50 Years of Research since the Seminal Text Book of J. G. Ramsay*, Special Publication 487, pages 21–44. Geological Society of London, 2020. doi: https://doi.org/10.1144/SP487.7.

K. Carpenter. Where the sea meets the land—the unresolved Dakota problem in Utah. In MacLean, J. S., Biek, R. F., and Huntoon, J. E., editors, *Geology of Utah's Far South*, Publication 43, pages 357–372. Utah Geological Association, 2014.

A. J. Cawood and C. E. Bond. Broadhaven revisited: A new look at models of fault–fold interaction. In Bond, C.E. and Lebit, H. D., editors, *Folding and Fracturing of Rocks—50 Years of Research since the Seminal Text Book of J. G. Ramsay*, Special Publication 487, pages 105–126. Geological Society of London, 2020. doi: https://doi.org/10.1144/SP487.11.

J. B. Chapman and P. G. DeCelles. Foreland basin stratigraphic control on thrust belt evolution. *Geology*, 43(7):579–582, 2015. doi: 10.1130/G36597.1.

T.C. Chidsey, J.S. DeHamer, E.E. Hartwick, Keith Johnson, D.D. Schelling, Douglas Sprinkel, D.K. Strickland, John Vrona, and David Wavrek. Petroleum geology of Covenant oil field, central Utah thrust belt. In Willis, G.C., Hylland, M.D., Clark, D.L., and Chidsey, T.C., Jr., editors, *Central Utah — Diverse Geology of a Dynamic Landscape*, Publication 36, pages 273–296. Utah Geological Association, 2007.

E. Cloos. Bedding slips, wedges, and folding in layered sequences. *Extrait de Comptes Rendus de la Société Géologique de Finlande*, 33, 1961.

E. Cloos. Wedging, bedding plane slips, and gravity tectonics in the Appalachians. In *Tectonics of the Southern Appalachians*, number 1 in Memoir, pages 63–70. Virginia Polytechnic Institute Geological Sciences, 1964.

K. N. Constenius. Late Paleogene Extensional collapse of the Cordilleran foreland fold and thrust belt. *GSA Bulletin*, 108(1):20–39, 1996. doi: https://doi.org/10.1130/0016-7606(1996)108<0020:LPECOT>2.3.CO;2.

K.N. Constenius, R.P. Esser, and P. W. Layer. Extensional collapse of the Charleston-Nebo Salient and its relationship to space-time variations in Cordilleran orogenic belt tectonism and continental stratigraphy. In Reynolds, R.G. and Flores, R.M., editors, *Cenozoic Systems of the Rocky Mountain Region*, pages 303–353. Rocky Mountain Section SEPM (Society for Sedimentary Geology), 2003.

E. F. Cook. Geology of the Pine Valley Mountains, Utah. Technical report, Utah Geological and Mineralogical Survey, 1957.

J. B Currie, H. W Patnode, and R. P. Trump. Development of folds in sedimentary strata. *GSA Bulletin*, 73(6):655–673, 1962. doi: https://doi.org/10.1130/0016-7606(1962)73[655:DOFISS]2.0.CO;2.

C. D. A. Dahlstrom. Balanced cross sections. *Canadian Journal of Earth Sciences*, 6(4): 743–757, 1969a. doi: https://doi.org/10.1139/e69-069.

G. H. Davis, S .J. Reynolds, and C. F. Kluth. *Structural Geology of Rocks and Regions (Third Ed.)*. John Wiley & Sons, 2011.

P. G. DeCelles. Late Jurassic to Eocene evolution of the Cordilleran thrust belt and foreland basin system, western U.S.A. *American Journal of Science*, 304(2):105–168, 2004. doi: https://doi.org/10.2475/ajs.304.2.105.

P. G. DeCelles and J. C. Coogan. Regional structure and kinematic history of the Sevier fold-and-thrust belt, central Utah. *GSA Bulletin*, 118(7-8):841–864, 2006. doi: https://doi.org/https:/doi.org/10.1130/B25759.1.

P. G. DeCelles and S.A. Graham. Cyclical processes in the North American Cordilleran orogenic system. *Geology*, 43(6):499–502, 2015. doi: https://doi.org/10.1130/G36482.1.

Peter G. DeCelles, Mihai N. Ducea, Paul Kapp, and George Zandt. Cyclicity in Cordilleran orogenic systems. *Nature Geoscience*, 2(4):251–257, 2009. doi: https://doi.org/10.1038/ngeo469.

R. V. Di Fiori, S. P. Long, A. C. Fetrow, K. E. Snell, J. W. Bonde, and J. D. Vervoort. The role of shortening in the Sevier Hinterland within the U.S. Cordilleran retroarc thrust system—insights from the Cretaceous Newark Canyon Formation in Central Nevada. *Tectonics*, 40(5):31, 2021. doi: https://doi.org/10.1029/2020TC006331.

M. N. Ducea, S. R. Paterson, and P. G. DeCelles. High-volume magmatic events in subduction systems. *Elements*, 11(2):99–104, 2015. doi: https://doi.org/10.2113/gselements.11.2.99.

C. E. Dutton. Report on the geology of the high plateaus of Utah, U.S. Geographical and Geological Survey of the Rocky Mountain Region. Technical Report unserialized monograph, U.S. Government Printing Office, 1880.

G. Eisenstadt and D. G. De Paor. Alternative model of thrust-fault propagation. *Geology*, 15(7):630–633, 1987. doi: https://doi.org/10.1130/0091-7613(1987)15<630:AMOTP>2.0.CO;2.

G. A. Enriquez St. Pierre and C. L. Johnson. Faulty foundations—Early breakup of the southern Utah Cordilleran foreland basin. *GSA Bulletin*, 2021. doi: https://doi.org/10.1130/B35872.1.

R. T. Faill. Kink-Band Folding, Valley and Ridge Province, Pennsylvania. *GSA Bulletin*, 84(4):1289–1314, 1973. doi: https://doi.org//10.1130/0016-7606(1973)84<1289:KFVARP>2.0.CO;2.

R. T. Faill and R. B. Wells. Geology and mineral resources of the Millerstown quadrangle, Perry, Juniata, and Snyder counties, Atlas 136. Technical report, Commonwealth of Pennsylvania Department of Environmental Resources, 1974.

M. P. Fischer, N. B. Woodward, and M. M. Mitchell. The kinematics of break-thrust folds. *Journal of Structural Geology*, 14(4):451–460, 1992. doi: https://doi.org/10.1016/0191-8141(92)90105-6.

R. J. Fleck and M. D. Carr. The age of the Keystone thrust—laser-fusion 40Ar/39Ar dating of foreland basin deposits, southern Spring Mountains, Nevada. *Tectonics*, 9(3): 467–476, 1990. doi: https://doi.org/10.1029/TC009i003p00467.

L.S. Gardner. The Hurricane fault in southwestern Utah and northwestern Arizona. *American Journal of Science*, 239(4):241–260, 1941. doi: https://doi.org/10.2475/ajs.239.4.241.

M.A. Giallorenzo, M.L. Wells, W.A. Yonkee, D.F. Stockli, and B.P. Wernicke. Timing of exhumation, Wheeler Pass thrust sheet, southern Nevada and California—Late Jurassic to middle Cretaceous evolution of the southern Sevier fold-and-thrust belt. *GSA Bulletin*, 130(3-4):558–579, 2018. doi: https://doi.org/10.1130/B31777.1.

S.K Grant, L. W. Fielding, and M. A Noweir. Cenozoic fault patterns in southwestern Utah and their relationships to structures of the Sevier orogeny. In R.E Blackett and Moore J. N, editors, *Cenozoic Geology and Geothermal Systems of Southwestern Utah*, Publication 23, pages 139–153. Utah Geological Association, Utah Geological Association, 1994.

H.E. Gregory and N.C. Williams. Zion National Monument, Utah. *GSA Bulletin*, 58(3):211–244, 1947. doi: https://doi.org/10.1130/0016-7606(1947)58[211:ZNMU]2.0.CO;2.

Michael Hautmann, Andrew B. Smith, Alistair J. McGowan, and Hugo Bucher. Bivalves from the Olenekian (Early Triassic) of south-western Utah: Systematics and evolutionary significance. *Journal of Systematic Palaeontology*, 11(3):263–293, 2013. doi: https://doi.org//10.1080/14772019.2011.637516.

D. M. Herring and D. C. Greene. The western Utah thrust belt in the larger context of the Sevier orogeny. In J.B. Comer, P.C. Inkenbrandt, K.A. Krahulec, and M.L. Pinnell, editors, *Resources and Geology of Utah's West Desert*, Publication 45, pages 131–146. Utah Geological Association, Utah Geological Association, 2016.

L. F. Hintze. Stratigraphy and structure of the Beaver Dam Mountains, southwestern Utah. In Griffin, D.T. and Phillips, W.R., editors, *Thrusting and Extensional Structures and Mineralization in the Beaver Dam Mountains, Southwestern Utah*, Publication 15, pages 1–36. Utah Geological Association, 1986.

L. F. Hintze. *Utah's Spectacular Geology—How It Came to Be*. Brigham Young University Department of Geology, 2005.

R. Hofmann, M. Hautmann, M. Wasmer, and H. Bucher. Palaeoecology of the Spathian Virgin Formation (Utah, USA) and its implications for the Early Triassic recovery. *Acta Palaeontologica Polonica*, 58(1):149–173, 2013. doi: https://doi.org/10.4202/app.2011.0060.

Richard Hofmann, Michael Hautmann, Arnaud Brayard, Alexander Nützel, Kevin G. Bylund, James F. Jenks, Emmanuelle Vennin, Nicolas Olivier, and Hugo Bucher. Recovery of benthic marine communities from the end-Permian mass extinction at the low latitudes of eastern Panthalassa. *Palaeontology*, 57(3):547–589, 2014. doi: https://doi.org//10.1111/pala.12076.

H.A. Hurlow and R.F. Biek. Geologic map of the Pintura quadrangle, Washington County, Utah, 2003.

M. A. Jadamec and W. K. Wallace. Thrust-breakthrough of asymmetric anticlines–observational constraints from surveys in the Brooks Range, Alaska. *Journal of Structural Geology*, 62:109–124, 2014. doi: https://doi.org/10.1016/j.jsg.2014.01.012.

T. R. Knudsen. Interim geologic map of the Cedar City 7.5-minute quadrangle, Iron County, Utah, 2014a.

A. E. Kurie. Recurrent structural disturbance of Colorado Plateau margin near Zion National Park, Utah. *GSA Bulletin*, 77(8):867–872, 1966. doi: https://doi.org/10.1130/0016-7606(1966)77[867:RSDOCP]2.0.CO;2.

D. R. Lageson, J. G. Schmitt, B. K. Horton, T. J. Kalakay, and B. R. Burton. Influence of Late Cretaceous magmatism on the Sevier orogenic wedge, western Montana. *Geology*, 29(8):723–726, 2001. doi: https://doi.org/10.1130/0091-7613(2001)029<0723:IOLCMO>2.0.CO;2.

S. P. Long. Magnitudes and spatial patterns of erosional exhumation in the Sevier hinterland, eastern Nevada and western Utah, USA–insights from a Paleogene paleogeologic map. *Geosphere*, 8(4):881–901, 2012. doi: https://doi.org/10.1130/GES00783.1.

S. P. Long. An upper-crustal fold province in the hinterland of the Sevier orogenic belt, eastern Nevada, U.S.A.—a Cordilleran Valley and Ridge in the Basin and Range. *Geosphere*, 11(2):404–424, 2015. doi: https://doi.org/10.1130/GES01102.1.

Earl M. P. Lovejoy. Age of structural differentiation between the Colorado Plateaus and Basin and Range provinces in southwestern Utah—comment and reply—COMMENT. *Geology*, 6(9):572–572, 1978. doi: https://doi.org/10.1130/0091-7613(1978)6<572a:AOSDBT>2.0.CO;2.

S. G. Lucas and L. H. Tanner. The Springdale Member of the Kayenta Formation, Lower Jurassic of Utah-Arizona. In Harris, J.D., Lucas, S. G., Spielmann, J. A., Lockley, M.G., Milner, R. C., and Kirkland, J. I., editors, *The Triassic-Jurassic Terrestrial Transition*, Bulletin 37, pages 71–76. New Mexico Museum of Natural History and Science, 2006.

S. G. Lucas, K. Krainer, and A.R.C. Milner. The type section and age of the Timpoweap Member and stratigraphic nomenclature of the Triassic Moenkopi Group in southwestern Utah. In Lucas, S.G. and Spielmann, J.A., editors, *Triassic of the American West*, Bulletin 40, pages 109–117. New Mexico Museum of Natural History and Science, 2007.

F. Maldonaldo and V.S. Williams. Geologic map of the Parowan Gap quadrangle, Iron County, Utah, 1993a.

R. Marrett and R.W. Allmendinger. Kinematic analysis of fault-slip data. *Journal of Structural Geology*, 12(8):973–986, 1990. doi: https://doi.org/10.1016/0191-8141(90)90093-E.

S. Mitra. Fold-accommodation faults. *AAPG Bulletin*, 86(4):671–693, 2002a. doi: https://doi.org/10.1306/61EEDB7A-173E-11D7-8645000102C1865D.

S. Mitra. Structural Models of Faulted Detachment Folds. *American Association of Petroleum Geologists Bulletin*, 86(9):1673–1694, 2002b. ISSN 0149-1423. doi: 10.1306/61EEDD3C-173E-11D7-8645000102C1865D.

R.J. Muir. Digital field mapping—making the change from paper to touchscreen technology. *Geology Today*, 31(6):232–236, 2015. doi: https://doi.org//10.1111/gto.12120.

A. M. Nowir and S.K Grant. Balanced cross-section across the southern Utah overthrust belt (Otb). *Qatar University Science Journal*, 15(1):195–204, 1995.

W.R. Page, S.C. Lundstron, V.V Langenheim, J.B Workman, S. Mahan, J.B. Paces, G.L. Dixon, P.D. Rowley, B.C. Burchfiel, J.W. Bell, and E.I. Smith. Geologic and geophysical maps of the Las Vegas 30' x 60' Quadrangle, Clark and Nye counties, Nevada, and Inyo County, California, 2005.

T. Paulsen and S. Marshak. Origin of the Uinta recess, Sevier fold–thrust belt, Utah—influence of basin architecture on fold–thrust belt geometry. *Tectonophysics*, 312 (2):203–216, 1999. doi: https://doi.org/10.1016/S0040-1951(99)00182-1.

D. G. Perry and B. D. E. Chatterton. Late Early Triassic brachiopod and conodont fauna, Thaynes Formation, southeastern Idaho. *Journal of Paleontology*, 53(2):307–319, 1979.

J.P. Petit. Criteria for the sense of movement on fault surfaces in brittle rocks. *Journal of Structural Geology*, 9(5):597–608, 1987. doi: https://doi.org/10.1016/0191-8141(87)90145-3.

F. Picha. The influence of preexisting tectonic trends on geometries of the Sevier orogenic belt and its foreland in Utah. In Peterson, J.A., editor, *Paleotectonics and Sedimentation in the Rocky Mountain Region, United States*, Memoir 41, pages 309–320. American Association of Petroleum Geologists, 1986. doi: https://doi.org/10.1306/M41456C14.

F. Picha and R. I. Gibson. Cordilleran hingeline—late Precambrian rifted margin of the North American craton and its impact on the depositional and structural history, Utah and Nevada. *Geology*, 13(7):465–468, 1985. doi: https://doi.org/10.1130/0091-7613(1985)13<465:CHLPRM>2.0.CO;2.

G. N. Pipiringos and R. B. O'Sullivan. Principal unconformities in Triassic and Jurassic rocks, western interior United States—a preliminary survey. Technical report, U.S. Geological Survey, 1978.

E. J. Pujols, D. F. Stockli, K. N. Constenius, and B. K. Horton. Thermochronological and geochronological constraints on Late Cretaceous unroofing and proximal sedimentation in the Sevier orogenic belt, Utah. *Tectonics*, 39(7):32, 2020. doi: https://doi.org/10.1029/2019TC005794.

J. D. Quick, J. P. Hogan, M. Wizevich, J. Obrist-Farner, and J. L. Crowley. Timing of deformation along the Iron Springs thrust, southern Sevier fold-and-thrust belt, Utah—evidence for an extensive thrusting event in the mid-Cretaceous. *Rocky Mountain Geology*, 55(2):75–89, 2020. doi: https://doi.org/10.24872/rmgjournal.55.2.75.

P.D. Rowley, V.S. Williams, D.J. Maxwell, D.B. Hacker, L.W. Snee, and J.H. Mackin. Interim geologic map of the Cedar City 30' x 60' Quadrangle, Iron and Washington Counties, Utah, 2006.

D. A. Sprinkel, H. H. Doelling, B. J. Kowallis, G. Waanders, and P. A. Kuehne. Early results of a study of the Middle Jurassic strata in the Sevier fold and thrust belt, Utah. In Sprinkel, D. A., Yonkee, W. A., and Chidsey, T. C., Jr., editors, *Sevier Thrust Belt–Northern and Central Utah and Adjacent Areas*, number Publication 40, pages 151–172. Utah Geological Association, 2011.

D. A. Steed. Geology of the Virgin River Gorge, northwest Arizona. Technical report, Brigham Young University, 1980. 3 plates.

M. E. Stewart and W. J. Taylor. Structural analysis and fault segment boundary identification along the Hurricane fault in southwestern Utah. *Journal of Structural Geology*, 18 (8):1017–1029, 1996. doi: https://doi.org/10.1016/0191-8141(96)00036-3.

W. L. Stokes. What is the Wasatch line? In Hill, J., editor, *Symposium on Geology of the Cordilleran Hingeline*, pages 11–25. Rocky Mountain Association of Geologists, 1976.

W.L. Stokes, L.F. Hintze, and Jr. Madsen, J.H. Geologic map of Utah, 1963.

William Thomas. Tectonic inheritance at a continental margin. *GSA today : a publication of the Geological Society of America*, 16(2):4–11, 2006. doi: https://doi.org/10.1130/1052-5173(2006)016[4:TIAACM]2.0.CO;2.

R.L. Threet. Geology of the Parowan Gap area, Iron County, Utah. In E.B. Heylmun, editor, *Guidebook to the Geology of Southwestern Utah–Transition between the Basin-Range and Colorado Plateau Provinces*, Twelfth Annual Field Conference, pages 136–145. Intermountain Association of Petroleum Geologists, Intermountain Association of Petroleum Geologists, 1963a.

R.L. Threet. Structure of the Colorado Plateau margin near Cedar City, Utah. In E.B. Heylmun, editor, *Guidebook to the Geology of Southwestern Utah–Transition between the Basin-Range and Colorado Plateau Provinces*, Twelfth Annual Field Conference, pages 104–117. Intermountain Association of Petroleum Geologists, Intermountain Association of Petroleum Geologists, 1963b.

G.K. Van Kooten. Structure and hydrocarbon potential beneath the Iron Springs laccolith, southwestern Utah. *Geological Society of America Bulletin*, 100(10):1533–1540, 1988. doi: https://doi.org/10.1130/0016-7606(1988)100<1533:SAHPBT>2.3.CO;2.

J. D. Walker, B. Tikoff, J. Newman, R. Clark, J. Ash, J. Good, E. G. Bunse, A. Möller, M. Kahn, R. T. Williams, Z. Michels, J. E. Andrew, and C. Rufledt. StraboSpot data system for structural geology. *Geosphere*, 15(2):533–547, 2019. doi: https://doi.org/10.1130/GES02039.1.

F. Wang, J. Chen, X. Dai, and H. Song. A new Dienerian (Early Triassic) brachiopod fauna from South China and implications for biotic recovery after the Permian–Triassic extinction. *Papers in Palaeontology*, 3(3):425–439, 2017. doi: https://doi.org/10.1002/spp2.1083.

B. Wernicke, G.J. Axen, and J. K. Snow. Basin and Range extensional tectonics at the latitude of Las Vegas, Nevada. *Geological Society of America Bulletin*, 100(11):1738–1757, 1988. doi: https://doi.org/10.1130/0016-7606(1988)100<1738:BARETA>2.3.CO;2.

G. Williams and T. Chapman. Strains developed in the hangingwalls of thrusts due to their slip/propagation rate—a dislocation model. *Journal of Structural Geology*, 5(6): 563–571, 1983. doi: https://doi.org/10.1016/0191-8141(83)90068-8.

B. Willis. The Mechanics of Appalachian Structure. In Powell, J. W., editor, *Thirteenth Annual Report of the United States Geological Survey to the Secretary of the Interior, 1891-1892—Part 2*, pages 217–281. U.S. Government Printing Office, 1893. doi: https://doi.org/10.3133/70039920.

G. C. Willis. The Utah thrust system—an overview. In Spangler, L.W. and Allen, C.J., editors, *Geology of Northern Utah and Vicinity*, Publication 27, pages 1–9. Utah Geological Association, 1999.

S. J. Wyld, J. W. Rogers, and P. Copeland. Metamorphic evolution of the Luning-Fencemaker fold-thrust belt, Nevada—illite crystallinity, metamorphic petrology, and 40Ar/39Ar geochronology. *Geology*, 111(1):17–38, 2003. doi: https://doi.org/10.1086/344663.

W. A. Yonkee and A. B. Weil. Tectonic evolution of the Sevier and Laramide belts within the North American Cordillera orogenic system. *Earth-Science Reviews*, 150:531–593, 2015. doi: https://doi.org/10.1016/j.earscirev.2015.08.001.

W. A. Yonkee, B. Eleogram, M. L. Wells, D. F. Stockli, S. Kelley, and D. E. Barber. Fault slip and exhumation history of the Willard Thrust Sheet, Sevier fold-thrust belt, Utah—relations to wedge propagation, hinterland uplift, and foreland basin sedimentation. *Tectonics*, 38(8):2850–2893, 2019. doi: https://doi.org/10.1029/2018TC005444.

.

SECTION

2. SUMMARY AND CONCLUSIONS

Detailed geologic mapping, cross sections, and fault slip analyses along the central and northern portion of the Kanarra fold-thrust system clarify its tectonic significance in southwest Utah. This work answers three major scientific questions involving the development of the Sevier fold-thrust belt in southwest Utah, and the significance of the Kanarra fold and its place in the Sevier fold-thrust belt, including 1) how fold and thrust belts advance at the leading edge; 2) what the role of folding and faulting is in defining the structural architecture of the leading edge; and 3) where the leading edge of the Sevier fold-thrust belt is located in southwest Utah.

The presence and nature of fold accommodation faults (*c.f.* at all scales, which have formed several fold-thrust systems along the exposed fold limb, indicate that the Kanarra fold thrust system developed initially as a leading edge asymmetric buckle fold, within which folding and thrusting occurred simultaneously in a distributed fashion according to the mechanical response of its constituent stratigraphic layers. The traditional *Kanarra anticline* only represents a portion of the hinge zone of this fold-thrust structure, with the "Pintura anticline" forming its broad hinge zone and trailing limb. This work is the first to employ such a mechanism of development regarding the Kanarra fold and the Sevier leading edge in southwest Utah. Regarding the first question, this mechanism is transferrable to other fold-thrust belts (e.g., and better reflects the real-world processes involved in layer-parallel contraction at the leading edge than purely kinematic models.

Thrust faults mapped in the field along the Kanarra fold-thrust system can be categorized as early (i.e., flank thrusts) and late (forelimb shear and out of the syncline) fold accommodation faults. Earlier thrusts were west-directed and formed due to the mechanical response of relatively thin, competent layers to regional layer parallel shortening. Later thrusts displace strata eastward and formed as a consequence of lockup of the fold prior to movement along the Red Rock Trail thrust. The Red Rock Trail thrust is a major, regional scale feature which developed as a break thrust in an ideal position and orientation to merge with the regional detachment beneath the growing Kanarra fold-thrust system. Thus the Red Rock Trail thrust forms the leading edge of the Sevier fold-thrust belt in southwest Utah. Displacement along the thrust and its damage zone are traceable from Kanarraville to Parowan Gap.

Regarding the second question, early-formed thrusts on the front limb of the fold continued to displace strata until they rotated into a position which prevented continued movement and locked up. Those on the back limb of the fold, i.e. the Spring Creek thrust, were not rotated and continued to move, modifying the shape of the fold crest and eventually cutting across the front limb of the fold. Late-formed, east-directed thrusts formed a foreland-directed shear zone as forelimb shear thrusts once the leading syncline hinge locked and could not accommodate more folding. This process culimnated in the development of the Red Rock trail thrust, which has been preserved at the moment of fold break-through. This is a unique and important discovery, as most leading edge thrusts are observed in much later stages of development.

Regarding the third question, the Red Rock trail thrust is a previously unrecognized, regional-scale thrust at the leading edge in southwest Utah. Its presence challenges the traditional paradigm in this research space, under which most authors place the Sevier leading edge further to the west. The Red Rock trail thrust marks the leading edge, and thus our structural framework for this area of Utah must change to reflect this reality.

Finally, this work touches on the broader significance of the Kanarra fold in relation to large-scale magmatic and sedimentation processes during Sevier deformation. The Kanarra fold-thrust system comprised the Sevier fold-thrust deformation front during the Late Cretaceous in southwestern Utah. It formed due to episodic, layer-parallel contractional deformation along a regional detachment in the Cambrian Bright Angel Shale, advancing ahead of the Iron Springs thrust several million years after Iron Springs thrusting. This suggests periodic deformation associated with magmatic flareups in the Cordilleran arc far to the west of the fold-thrust front. The scale of the fold—including Parowan Gap, likely ~100 km in length—and formation of the Kanarra fold-thrust system with other regional folds in southwest Utah (i.e., the Virgin anticline) would have produced topographic highs which controlled the distribution and provenance of sedimentation in the region and its adjacent foreland basin.

REFERENCES

R. W. Allmendinger. GMDE–Extracting quantitative information from geologic maps. *Geosphere*, 16(6):1495–1507, 2020. doi: https://doi.org/10.1130/GES02253.1.

R. W. Allmendinger, J. W. Gephart, and R. A. Marrett. Notes on fault slip analysis. In Allmendinger, R.W., Aydin, A., Engelder, T., and Pollard, D. D., editors, *Quantitative Interpretation of Joints and Faults*, Annual Meeting 1989, page 59. Geologial Society of America, 1989.

R. W. Allmendinger, N. Cardozo, and D. M. Fisher. *Structural Geology Algorithms: Vectors and Tensors*. Cambridge University Press, 2012. doi: https://doi.org/10.1017/CBO9780511920202.

L. P. Anderson and D. A. Dinter. Deformation and sedimentation in the southern Sevier foreland, Red Hills, southwestern Utah. In Carney S. M., Tabet, D. E., and Johnson, C. L., editors, *Geology of South-Central Utah*, Publication 39, pages 338–366. Utah Geological Association, 2010.

R. L. Armstrong. Sevier orogenic belt in Nevada and Utah. *Geological Society of America Bulletin*, 79(4):429–458, 1968. doi: https://doi.org/10.1130/0016-7606(1968)79[429:SOBINA]2.0.CO;2.

P. Averitt. Geology and coal resources of the Cedar Mountain quadrangle, Iron County, Utah, 1962.

P. Averitt. Geologic map of the Kanarraville quadrangle, Iron County, Utah, 1967.

P. Averitt and R. L. Threet. Geologic map of the Cedar City quadrangle, Iron County, Utah, 1973.

R.F. Biek. Geologic map of the Harrisburg Junction quadrangle, Washington County, Utah, 2003a.

R.F. Biek. Geologic map of the Hurricane 7.5' quadrangle, Washington County, Utah, 2003b.

R.F. Biek. Geologic map of the Kolob Arch quadrangle and part of the Kanarraville quadrangle, Washington and Iron Counties, Utah, 2007a.

R.F. Biek. Geologic map of the Kolob Reservoir quadrangle, Washington and Iron Counties, Utah, 2007b.

R.F. Biek and J. M. Hayden. Geologic map of the Kanarraville quadrangle, Iron County, Utah, 2016.

R.F. Biek, P.D. Rowley, J.M. Hayden, D.B Hacker, G.C Willis, L.F. Hintze, R.E. Anderson, and K.D. Brown. Geologic map of the St.. George and east part of the Clover Mountains 30' x 60' Quadrangles, Washington and Iron Counties, Utah, 2010.

R.F. Biek, P.D. Rowley, J.J. Anderson, F. Maldonaldo, D.B. Hacker, J.G Eaton, R. Hereford, E.D. Sable, H.F. Filkorn, and B. Matyjasik. Geologic map of the Panguitch 30' x 60' Quadrangle, Garfield, Iron, and Kane Counties, Utah, 2015.

B. C. Burchfiel and Gregory A. Davis. Structural framework and evolution of the southern part of the Cordilleran orogen, western United States. *American Journal of Science*, 272(2):97–118, 1972. doi: https://doi.org/10.2475/ajs.272.2.97.

R.W.H. Butler, C.E. Bond, M.A. Cooper, and H. Watkins. Fold–thrust structures—where have all the buckles gone? In Bond, C.E. and Lebit, H. D., editors, *Folding and Fracturing of Rocks—50 Years of Research since the Seminal Text Book of J. G. Ramsay*, Special Publication 487, pages 21–44. Geological Society of London, 2020. doi: https://doi.org/10.1144/SP487.7.

K. Carpenter. Where the sea meets the land—the unresolved Dakota problem in Utah. In MacLean, J. S., Biek, R. F., and Huntoon, J. E., editors, *Geology of Utah's Far South*, Publication 43, pages 357–372. Utah Geological Association, 2014.

A. J. Cawood and C. E. Bond. Broadhaven revisited: A new look at models of fault–fold interaction. In Bond, C.E. and Lebit, H. D., editors, *Folding and Fracturing of Rocks—50 Years of Research since the Seminal Text Book of J. G. Ramsay*, Special Publication 487, pages 105–126. Geological Society of London, 2020. doi: https://doi.org/10.1144/SP487.11.

J. B. Chapman and P. G. DeCelles. Foreland basin stratigraphic control on thrust belt evolution. *Geology*, 43(7):579–582, 2015. doi: 10.1130/G36597.1.

T.C. Chidsey, J.S. DeHamer, E.E. Hartwick, Keith Johnson, D.D. Schelling, Douglas Sprinkel, D.K. Strickland, John Vrona, and David Wavrek. Petroleum geology of Covenant oil field, central Utah thrust belt. In Willis, G.C., Hylland, M.D., Clark, D.L., and Chidsey, T.C., Jr., editors, *Central Utah — Diverse Geology of a Dynamic Landscape*, Publication 36, pages 273–296. Utah Geological Association, 2007.

E. Cloos. Bedding slips, wedges, and folding in layered sequences. *Extrait de Comptes Rendus de la Société Géologique de Finlande*, 33, 1961.

E. Cloos. Wedging, bedding plane slips, and gravity tectonics in the Appalachians. In *Tectonics of the Southern Appalachians*, number 1 in Memoir, pages 63–70. Virginia Polytechnic Institute Geological Sciences, 1964.

K. N. Constenius. Late Paleogene Extensional collapse of the Cordilleran foreland fold and thrust belt. *GSA Bulletin*, 108(1):20–39, 1996. doi: https://doi.org/10.1130/0016-7606(1996)108<0020:LPECOT>2.3.CO;2.

K.N. Constenius, R.P. Esser, and P. W. Layer. Extensional collapse of the Charleston-Nebo Salient and its relationship to space-time variations in Cordilleran orogenic belt tectonism and continental stratigraphy. In Reynolds, R.G. and Flores, R.M., editors, *Cenozoic Systems of the Rocky Mountain Region*, pages 303–353. Rocky Mountain Section SEPM (Society for Sedimentary Geology), 2003.

E. F. Cook. Geology of the Pine Valley Mountains, Utah. Technical report, Utah Geological and Mineralogical Survey, 1957.

J. B Currie, H. W Patnode, and R. P. Trump. Development of folds in sedimentary strata. *GSA Bulletin*, 73(6):655–673, 1962. doi: https://doi.org/10.1130/0016-7606(1962)73[655:DOFISS]2.0.CO;2.

C. D. A. Dahlstrom. Balanced cross sections. *Canadian Journal of Earth Sciences*, 6(4): 743–757, 1969a. doi: https://doi.org/10.1139/e69-069.

G. H. Davis, S .J. Reynolds, and C. F. Kluth. *Structural Geology of Rocks and Regions (Third Ed.)*. John Wiley & Sons, 2011.

P. G. DeCelles. Late Jurassic to Eocene evolution of the Cordilleran thrust belt and foreland basin system, western U.S.A. *American Journal of Science*, 304(2):105–168, 2004. doi: https://doi.org/10.2475/ajs.304.2.105.

P. G. DeCelles and J. C. Coogan. Regional structure and kinematic history of the Sevier fold-and-thrust belt, central Utah. *GSA Bulletin*, 118(7-8):841–864, 2006. doi: https://doi.org/https:/doi.org/10.1130/B25759.1.

P. G. DeCelles and S.A. Graham. Cyclical processes in the North American Cordilleran orogenic system. *Geology*, 43(6):499–502, 2015. doi: https://doi.org/10.1130/G36482.1.

Peter G. DeCelles, Mihai N. Ducea, Paul Kapp, and George Zandt. Cyclicity in Cordilleran orogenic systems. *Nature Geoscience*, 2(4):251–257, 2009. doi: https://doi.org/10.1038/ngeo469.

R. V. Di Fiori, S. P. Long, A. C. Fetrow, K. E. Snell, J. W. Bonde, and J. D. Vervoort. The role of shortening in the Sevier Hinterland within the U.S. Cordilleran retroarc thrust system—insights from the Cretaceous Newark Canyon Formation in Central Nevada. *Tectonics*, 40(5):31, 2021. doi: https://doi.org/10.1029/2020TC006331.

M. N. Ducea, S. R. Paterson, and P. G. DeCelles. High-volume magmatic events in subduction systems. *Elements*, 11(2):99–104, 2015. doi: https://doi.org/10.2113/gselements.11.2.99.

C. E. Dutton. Report on the geology of the high plateaus of Utah, U.S. Geographical and Geological Survey of the Rocky Mountain Region. Technical Report unserialized monograph, U.S. Government Printing Office, 1880.

G. Eisenstadt and D. G. De Paor. Alternative model of thrust-fault propagation. *Geology*, 15(7):630–633, 1987. doi: https://doi.org/10.1130/0091-7613(1987)15<630:AMOTP>2.0.CO;2.

G. A. Enriquez St. Pierre and C. L. Johnson. Faulty foundations—Early breakup of the southern Utah Cordilleran foreland basin. *GSA Bulletin*, 2021. doi: https://doi.org/10.1130/B35872.1.

R. T. Faill. Kink-Band Folding, Valley and Ridge Province, Pennsylvania. *GSA Bulletin*, 84(4):1289–1314, 1973. doi: https://doi.org//10.1130/0016-7606(1973)84<1289:KFVARP>2.0.CO;2.

R. T. Faill and R. B. Wells. Geology and mineral resources of the Millerstown quadrangle, Perry, Juniata, and Snyder counties, Atlas 136. Technical report, Commonwealth of Pennsylvania Department of Environmental Resources, 1974.

M. P. Fischer, N. B. Woodward, and M. M. Mitchell. The kinematics of break-thrust folds. *Journal of Structural Geology*, 14(4):451–460, 1992. doi: https://doi.org/10.1016/0191-8141(92)90105-6.

R. J. Fleck and M. D. Carr. The age of the Keystone thrust—laser-fusion 40Ar/39Ar dating of foreland basin deposits, southern Spring Mountains, Nevada. *Tectonics*, 9(3): 467–476, 1990. doi: https://doi.org/10.1029/TC009i003p00467.

L.S. Gardner. The Hurricane fault in southwestern Utah and northwestern Arizona. *American Journal of Science*, 239(4):241–260, 1941. doi: https://doi.org/10.2475/ajs.239.4.241.

M.A. Giallorenzo, M.L. Wells, W.A. Yonkee, D.F. Stockli, and B.P. Wernicke. Timing of exhumation, Wheeler Pass thrust sheet, southern Nevada and California—Late Jurassic to middle Cretaceous evolution of the southern Sevier fold-and-thrust belt. *GSA Bulletin*, 130(3-4):558–579, 2018. doi: https://doi.org/10.1130/B31777.1.

S.K Grant, L. W. Fielding, and M. A Noweir. Cenozoic fault patterns in southwestern Utah and their relationships to structures of the Sevier orogeny. In R.E Blackett and Moore J. N, editors, *Cenozoic Geology and Geothermal Systems of Southwestern Utah*, Publication 23, pages 139–153. Utah Geological Association, Utah Geological Association, 1994.

H.E. Gregory and N.C. Williams. Zion National Monument, Utah. *GSA Bulletin*, 58(3):211–244, 1947. doi: https://doi.org/10.1130/0016-7606(1947)58[211:ZNMU]2.0.CO;2.

Michael Hautmann, Andrew B. Smith, Alistair J. McGowan, and Hugo Bucher. Bivalves from the Olenekian (Early Triassic) of south-western Utah: Systematics and evolutionary significance. *Journal of Systematic Palaeontology*, 11(3):263–293, 2013. doi: https://doi.org//10.1080/14772019.2011.637516.

D. M. Herring and D. C. Greene. The western Utah thrust belt in the larger context of the Sevier orogeny. In J.B. Comer, P.C. Inkenbrandt, K.A. Krahulec, and M.L. Pinnell, editors, *Resources and Geology of Utah's West Desert*, Publication 45, pages 131–146. Utah Geological Association, Utah Geological Association, 2016.

L. F. Hintze. Stratigraphy and structure of the Beaver Dam Mountains, southwestern Utah. In Griffin, D.T. and Phillips, W.R., editors, *Thrusting and Extensional Structures and Mineralization in the Beaver Dam Mountains, Southwestern Utah*, Publication 15, pages 1–36. Utah Geological Association, 1986.

L. F. Hintze. *Utah's Spectacular Geology—How It Came to Be*. Brigham Young University Department of Geology, 2005.

R. Hofmann, M. Hautmann, M. Wasmer, and H. Bucher. Palaeoecology of the Spathian Virgin Formation (Utah, USA) and its implications for the Early Triassic recovery. *Acta Palaeontologica Polonica*, 58(1):149–173, 2013. doi: https://doi.org/10.4202/app.2011.0060.

Richard Hofmann, Michael Hautmann, Arnaud Brayard, Alexander Nützel, Kevin G. Bylund, James F. Jenks, Emmanuelle Vennin, Nicolas Olivier, and Hugo Bucher. Recovery of benthic marine communities from the end-Permian mass extinction at the low latitudes of eastern Panthalassa. *Palaeontology*, 57(3):547–589, 2014. doi: https://doi.org//10.1111/pala.12076.

H.A. Hurlow and R.F. Biek. Geologic map of the Pintura quadrangle, Washington County, Utah, 2003.

M. A. Jadamec and W. K. Wallace. Thrust-breakthrough of asymmetric anticlines–observational constraints from surveys in the Brooks Range, Alaska. *Journal of Structural Geology*, 62:109–124, 2014. doi: https://doi.org/10.1016/j.jsg.2014.01.012.

T. R. Knudsen. Interim geologic map of the Cedar City 7.5-minute quadrangle, Iron County, Utah, 2014a.

A. E. Kurie. Recurrent structural disturbance of Colorado Plateau margin near Zion National Park, Utah. *GSA Bulletin*, 77(8):867–872, 1966. doi: https://doi.org/10.1130/0016-7606(1966)77[867:RSDOCP]2.0.CO;2.

D. R. Lageson, J. G. Schmitt, B. K. Horton, T. J. Kalakay, and B. R. Burton. Influence of Late Cretaceous magmatism on the Sevier orogenic wedge, western Montana. *Geology*, 29(8):723–726, 2001. doi: https://doi.org/10.1130/0091-7613(2001)029<0723:IOLCMO>2.0.CO;2.

S. P. Long. Magnitudes and spatial patterns of erosional exhumation in the Sevier hinterland, eastern Nevada and western Utah, USA–insights from a Paleogene paleogeologic map. *Geosphere*, 8(4):881–901, 2012. doi: https://doi.org/10.1130/GES00783.1.

S. P. Long. An upper-crustal fold province in the hinterland of the Sevier orogenic belt, eastern Nevada, U.S.A.—a Cordilleran Valley and Ridge in the Basin and Range. *Geosphere*, 11(2):404–424, 2015. doi: https://doi.org/10.1130/GES01102.1.

Earl M. P. Lovejoy. Age of structural differentiation between the Colorado Plateaus and Basin and Range provinces in southwestern Utah—comment and reply—COMMENT. *Geology*, 6(9):572–572, 1978. doi: https://doi.org/10.1130/0091-7613(1978)6<572a:AOSDBT>2.0.CO;2.

S. G. Lucas and L. H. Tanner. The Springdale Member of the Kayenta Formation, Lower Jurassic of Utah-Arizona. In Harris, J.D., Lucas, S. G., Spielmann, J. A., Lockley, M.G., Milner, R. C., and Kirkland, J. I., editors, *The Triassic-Jurassic Terrestrial Transition*, Bulletin 37, pages 71–76. New Mexico Museum of Natural History and Science, 2006.

S. G. Lucas, K. Krainer, and A.R.C. Milner. The type section and age of the Timpoweap Member and stratigraphic nomenclature of the Triassic Moenkopi Group in southwestern Utah. In Lucas, S.G. and Spielmann, J.A., editors, *Triassic of the American West*, Bulletin 40, pages 109–117. New Mexico Museum of Natural History and Science, 2007.

F. Maldonaldo and V.S. Williams. Geologic map of the Parowan Gap quadrangle, Iron County, Utah, 1993a.

R. Marrett and R.W. Allmendinger. Kinematic analysis of fault-slip data. *Journal of Structural Geology*, 12(8):973–986, 1990. doi: https://doi.org/10.1016/0191-8141(90)90093-E.

S. Mitra. Fold-accommodation faults. *AAPG Bulletin*, 86(4):671–693, 2002a. doi: https://doi.org/10.1306/61EEDB7A-173E-11D7-8645000102C1865D.

S. Mitra. Structural Models of Faulted Detachment Folds. *American Association of Petroleum Geologists Bulletin*, 86(9):1673–1694, 2002b. ISSN 0149-1423. doi: 10.1306/61EEDD3C-173E-11D7-8645000102C1865D.

R.J. Muir. Digital field mapping—making the change from paper to touchscreen technology. *Geology Today*, 31(6):232–236, 2015. doi: https://doi.org//10.1111/gto.12120.

A. M. Nowir and S.K Grant. Balanced cross-section across the southern Utah overthrust belt (Otb). *Qatar University Science Journal*, 15(1):195–204, 1995.

W.R. Page, S.C. Lundstron, V.V Langenheim, J.B Workman, S. Mahan, J.B. Paces, G.L. Dixon, P.D. Rowley, B.C. Burchfiel, J.W. Bell, and E.I. Smith. Geologic and geophysical maps of the Las Vegas 30' x 60' Quadrangle, Clark and Nye counties, Nevada, and Inyo County, California, 2005.

T. Paulsen and S. Marshak. Origin of the Uinta recess, Sevier fold–thrust belt, Utah—influence of basin architecture on fold–thrust belt geometry. *Tectonophysics*, 312 (2):203–216, 1999. doi: https://doi.org/10.1016/S0040-1951(99)00182-1.

D. G. Perry and B. D. E. Chatterton. Late Early Triassic brachiopod and conodont fauna, Thaynes Formation, southeastern Idaho. *Journal of Paleontology*, 53(2):307–319, 1979.

J.P. Petit. Criteria for the sense of movement on fault surfaces in brittle rocks. *Journal of Structural Geology*, 9(5):597–608, 1987. doi: https://doi.org/10.1016/0191-8141(87)90145-3.

F. Picha. The influence of preexisting tectonic trends on geometries of the Sevier orogenic belt and its foreland in Utah. In Peterson, J.A., editor, *Paleotectonics and Sedimentation in the Rocky Mountain Region, United States*, Memoir 41, pages 309–320. American Association of Petroleum Geologists, 1986. doi: https://doi.org/10.1306/M41456C14.

F. Picha and R. I. Gibson. Cordilleran hingeline—late Precambrian rifted margin of the North American craton and its impact on the depositional and structural history, Utah and Nevada. *Geology*, 13(7):465–468, 1985. doi: https://doi.org/10.1130/0091-7613(1985)13<465:CHLPRM>2.0.CO;2.

G. N. Pipiringos and R. B. O'Sullivan. Principal unconformities in Triassic and Jurassic rocks, western interior United States—a preliminary survey. Technical report, U.S. Geological Survey, 1978.

E. J. Pujols, D. F. Stockli, K. N. Constenius, and B. K. Horton. Thermochronological and geochronological constraints on Late Cretaceous unroofing and proximal sedimentation in the Sevier orogenic belt, Utah. *Tectonics*, 39(7):32, 2020. doi: https://doi.org/10.1029/2019TC005794.

J. D. Quick, J. P. Hogan, M. Wizevich, J. Obrist-Farner, and J. L. Crowley. Timing of deformation along the Iron Springs thrust, southern Sevier fold-and-thrust belt, Utah—evidence for an extensive thrusting event in the mid-Cretaceous. *Rocky Mountain Geology*, 55(2):75–89, 2020. doi: https://doi.org/10.24872/rmgjournal.55.2.75.

P.D. Rowley, V.S. Williams, D.J. Maxwell, D.B. Hacker, L.W. Snee, and J.H. Mackin. Interim geologic map of the Cedar City 30' x 60' Quadrangle, Iron and Washington Counties, Utah, 2006.

D. A. Sprinkel, H. H. Doelling, B. J. Kowallis, G. Waanders, and P. A. Kuehne. Early results of a study of the Middle Jurassic strata in the Sevier fold and thrust belt, Utah. In Sprinkel, D. A., Yonkee, W. A., and Chidsey, T. C., Jr., editors, *Sevier Thrust Belt–Northern and Central Utah and Adjacent Areas*, number Publication 40, pages 151–172. Utah Geological Association, 2011.

D. A. Steed. Geology of the Virgin River Gorge, northwest Arizona. Technical report, Brigham Young University, 1980. 3 plates.

M. E. Stewart and W. J. Taylor. Structural analysis and fault segment boundary identification along the Hurricane fault in southwestern Utah. *Journal of Structural Geology*, 18 (8):1017–1029, 1996. doi: https://doi.org/10.1016/0191-8141(96)00036-3.

W. L. Stokes. What is the Wasatch line? In Hill, J., editor, *Symposium on Geology of the Cordilleran Hingeline*, pages 11–25. Rocky Mountain Association of Geologists, 1976.

W.L. Stokes, L.F. Hintze, and Jr. Madsen, J.H. Geologic map of Utah, 1963.

William Thomas. Tectonic inheritance at a continental margin. *GSA today : a publication of the Geological Society of America*, 16(2):4–11, 2006. doi: https://doi.org/10.1130/1052-5173(2006)016[4:TIAACM]2.0.CO;2.

R.L. Threet. Geology of the Parowan Gap area, Iron County, Utah. In E.B. Heylmun, editor, *Guidebook to the Geology of Southwestern Utah–Transition between the Basin-Range and Colorado Plateau Provinces*, Twelfth Annual Field Conference, pages 136–145. Intermountain Association of Petroleum Geologists, Intermountain Association of Petroleum Geologists, 1963a.

R.L. Threet. Structure of the Colorado Plateau margin near Cedar City, Utah. In E.B. Heylmun, editor, *Guidebook to the Geology of Southwestern Utah–Transition between the Basin-Range and Colorado Plateau Provinces*, Twelfth Annual Field Conference, pages 104–117. Intermountain Association of Petroleum Geologists, Intermountain Association of Petroleum Geologists, 1963b.

G.K. Van Kooten. Structure and hydrocarbon potential beneath the Iron Springs laccolith, southwestern Utah. *Geological Society of America Bulletin*, 100(10):1533–1540, 1988. doi: https://doi.org/10.1130/0016-7606(1988)100<1533:SAHPBT>2.3.CO;2.

J. D. Walker, B. Tikoff, J. Newman, R. Clark, J. Ash, J. Good, E. G. Bunse, A. Möller, M. Kahn, R. T. Williams, Z. Michels, J. E. Andrew, and C. Rufledt. StraboSpot data system for structural geology. *Geosphere*, 15(2):533–547, 2019. doi: https://doi.org/10.1130/GES02039.1.

F. Wang, J. Chen, X. Dai, and H. Song. A new Dienerian (Early Triassic) brachiopod fauna from South China and implications for biotic recovery after the Permian–Triassic extinction. *Papers in Palaeontology*, 3(3):425–439, 2017. doi: https://doi.org/10.1002/spp2.1083.

B. Wernicke, G.J. Axen, and J. K. Snow. Basin and Range extensional tectonics at the latitude of Las Vegas, Nevada. *Geological Society of America Bulletin*, 100(11):1738–1757, 1988. doi: https://doi.org/10.1130/0016-7606(1988)100<1738:BARETA>2.3.CO;2.

G. Williams and T. Chapman. Strains developed in the hangingwalls of thrusts due to their slip/propagation rate—a dislocation model. *Journal of Structural Geology*, 5(6): 563–571, 1983. doi: https://doi.org/10.1016/0191-8141(83)90068-8.

B. Willis. The Mechanics of Appalachian Structure. In Powell, J. W., editor, *Thirteenth Annual Report of the United States Geological Survey to the Secretary of the Interior, 1891-1892—Part 2*, pages 217–281. U.S. Government Printing Office, 1893. doi: https://doi.org/10.3133/70039920.

G. C. Willis. The Utah thrust system—an overview. In Spangler, L.W. and Allen, C.J., editors, *Geology of Northern Utah and Vicinity*, Publication 27, pages 1–9. Utah Geological Association, 1999.

S. J. Wyld, J. W. Rogers, and P. Copeland. Metamorphic evolution of the Luning-Fencemaker fold-thrust belt, Nevada—illite crystallinity, metamorphic petrology, and 40Ar/39Ar geochronology. *Geology*, 111(1):17–38, 2003. doi: https://doi.org/10.1086/344663.

W. A. Yonkee and A. B. Weil. Tectonic evolution of the Sevier and Laramide belts within the North American Cordillera orogenic system. *Earth-Science Reviews*, 150:531–593, 2015. doi: https://doi.org/10.1016/j.earscirev.2015.08.001.

W. A. Yonkee, B. Eleogram, M. L. Wells, D. F. Stockli, S. Kelley, and D. E. Barber. Fault slip and exhumation history of the Willard Thrust Sheet, Sevier fold-thrust belt, Utah—relations to wedge propagation, hinterland uplift, and foreland basin sedimentation. *Tectonics*, 38(8):2850–2893, 2019. doi: https://doi.org/10.1029/2018TC005444.

VITA

William Joseph Michael Chandonia received a B.S. in Geology from Georgia State University in 2014. He entered into the Geology and Geophysics Program at Missouri University of Science and Technology, and received an M.S. in Geology and Geophysics in 2017. He went on for a Ph.D. under the Geology and Geophysics program at Missouri University of Science and Technology and recieved his Ph.D. in Geology and Geophysics in May 2022. While at Missouri University of Science and Technology, William was a graduate teaching assistant for many aspiring geologists and engineers in Structural Geology and Petrology, and volunteered as a student leader in the Sigma Gamma Epsilon Eta Chapter.